

SCATTERING OF ELECTROMAGNETIC RADIATION
BY DEFECTS IN CRYSTALS

by 1264

INDIRA RADHAKRISHNAN NAIR

M.Sc., Bombay University, 1962

A MASTER'S THESIS

submitted in partial fulfillment of the
requirements for the degree

MASTER OF SCIENCE

Department of Physics

KANSAS STATE UNIVERSITY

Manhattan, Kansas

1970

Approved by

C. S. Hathaway

Major Professor

LD
2668
74
1970
N34

SCATTERING OF ELECTROMAGNETIC RADIATION
BY DEFECTS IN CRYSTALS

I. INTRODUCTION	1
A. Classical Theory of the Scattering of Electromagnetic Waves	3
1. Classical Theory of Rayleigh Scattering	5
2. Classical Theory of Raman Scattering	12
B. Quantum Mechanical Theory of Rayleigh and Raman Scattering	17
1. Semiclassical Theory	17
2. Second Quantization Formalism	36
II. LATTICE DYNAMICS	38
A. Lattice Dynamics of a Perfect Crystal	38
1. The Harmonic Approximation	39
2. The Frequency Distribution Function	53
3. Simplified Interpretations of Lattice Vibrations	55
a. Raman's Theory of Lattice Dynamics	55
b. Internal and External Modes of Oscillations	56
B. Optical Modes and Electromagnetic Radiation	57
III. RAMAN EFFECT IN CRYSTALS	72
A. Born's Semiclassical Theory	74
B. Second Quantization Theory	78
C. Stimulated Raman Effect	85
D. Resonance Raman Effect	86
E. Brillouin Scattering	88
F. Second-Order Raman Effect	92
G. Selection Rules	93
IV. LATTICE DYNAMICS OF CRYSTALS WITH DEFECTS	96
A. Introduction	96
1. One-Dimensional Crystal with a Simple Defect	99
2. Three Dimensional Crystal with Defect	105
3. Defects with Internal Degrees of Freedom	115
B. Impurity-Induced Raman Scattering	118

**THIS BOOK
CONTAINS
NUMEROUS PAGES
WITH THE ORIGINAL
PRINTING BEING
SKEWED
DIFFERENTLY FROM
THE TOP OF THE
PAGE TO THE
BOTTOM.**

**THIS IS AS RECEIVED
FROM THE
CUSTOMER.**

ILLEGIBLE DOCUMENT

**THE FOLLOWING
DOCUMENT(S) IS OF
POOR LEGIBILITY IN
THE ORIGINAL**

**THIS IS THE BEST
COPY AVAILABLE**

V. COLOR CENTERS IN THE AZIDE SYSTEM AS AN EXAMPLE OF A DEFECT IN A CRYSTAL	123
A. Introduction	123
B. Electronic Spectra of U.V. Irradiated Azides	134
C. Vibrational Spectra of Pure Azides	149
D. Proposed Models for Azide Color Center Structures	153
E. Summary	156

I. INTRODUCTION

The Raman Effect in its most general aspect is the inelastic scattering of photons by any material medium, the energy lost or gained by the photons being absorbed or emitted by an elementary excitation of the medium. Since its discovery in 1925-1928 by C.V. Raman (1) in liquids and G. Landsberg and L. V. Mandelstam (2) in solid quartz, the Raman Effect has been studied in great detail in gases, liquids and solids. Though detailed investigations should lead to a better understanding of the interaction of electromagnetic radiation with matter, Raman studies have been restricted until recently to the study of the vibrational modes of molecules and solids in a manner in many respects complementary to infrared, neutron and x-ray studies. There have been numerous analyses of Raman vibrational spectra of molecules for the elucidation of their structures (3).

The availability of the laser as a source of highly monochromatic light of high intensity and well-defined polarization has given a new impetus to Raman studies. This source has opened the possibility of investigating not only clear, non-absorbing samples but also samples such as imperfect, absorbing crystals and opaque materials. The study of vibrational properties of defects with Raman and infrared techniques could lead to the elucidation of both the geometrical structure and the effective force constants associated with the defects.

The first section (Chapters I-III) of this thesis is a review of the theory of the Raman Effect. The Raman Effect is not presented with clarity or detail in any of the standard physics textbooks, graduate or undergraduate. Furthermore, no modern monographs on the subject are available. The author has synthesized much of the current literature in an effort to produce an

introduction to Raman scattering for the beginning graduate student. Classical theory of scattering of electromagnetic radiation is presented first, followed by the semiclassical quantum theory and the formalism of second quantization theory. A brief review of the dynamics of a perfect crystal lattice and of a lattice with defects, with particular attention given to the analysis of Raman spectra is presented next (Chapter III).

The second section (Chapter V) of the thesis contains a study of the electronic and Raman spectra of the pure and ultra-violet irradiated alkali metal azides (KN_3 , NaN_3 and RbN_3). The measurement of the electronic spectra of the damaged crystals is described and discussed. The unit cell analysis of the undamaged azides is followed by proposed models for the defects formed by u.v. irradiation. A point group vibrational analysis of these defect models is presented. An estimation is given of the corresponding normal mode frequencies associated with the defect using the force constants for the azide defect as determined from the infrared data of Bryant (4). Finally, the Raman spectra of the pure alkali azide crystals are described and discussed. A prediction of the Raman spectra of u.v. irradiated alkali crystals is indicated. An experimental Raman study of these defects is being initiated by the author as this thesis is being written.

A. Classical Theory of the Scattering of Electromagnetic Waves:

When electromagnetic radiation is incident on a medium it causes a change in motion of the charges in the medium. This may result in emission of electromagnetic radiation whose frequency and direction, in general, differ from that of the incident wave. This phenomenon is called scattering. A complete theory of scattering must invoke a quantum electrodynamical treatment but a fairly correct description on a macroscopic scale is given by classical electrodynamics. A brief description of the various types of scattering is presented and Rayleigh scattering is considered in detail. Most considerations in Rayleigh scattering carry over to the classical theory of Raman scattering.

Scattering is most conveniently characterized by the ratio of the amount of energy emitted by the scattering system in a given direction per unit time, to the energy flux density of incident radiation. This ratio is known as the scattering cross section. It may be easily shown that for an incident wave of unpolarized light, the cross section for the scattering by a free charge is (5)

$$d\sigma = \frac{1}{2} \left(\frac{e^2}{mc^2} \right)^2 (1 + \cos^2\theta) d\Omega$$

where θ is the angle between the directions of the incident and scattered light. This equation is derived on the assumption that the velocity v acquired by the free charge under the action of the electric field is much smaller than the velocity of light so that the magnetic force ($\propto \frac{v}{c}$) can be neglected and the electric dipole approximation holds. It also follows from the derivation that the frequency of the wave radiated by the charge, i.e. scattered by the charge, is the same as the frequency of the incident wave.

Scattering by a system of charges differs from that by a single charge. The frequency of the scattered radiation can be different from the frequency of the incident wave since there may be internal relative motions of the charges, for example, internal vibrations of the molecule. For convenience of treatment, it is usual to consider the following cases.

(A) Scattering of high-frequency waves: When the frequency of the incident wave, considered monochromatic for simplicity, is large compared with the fundamental internal frequencies of the system, the motion of the charges of the system can be considered uniform during a time interval of the order of the period of the wave. This implies the charges can be considered as essentially free and the scattering may be considered as free charge scattering to a first degree of approximation. This type of scattering is dominant in x-ray scattering and is called Thomson Scattering for historical reasons. Being primarily of the same frequency, the scattering is coherent with the incident wave.

(B) Scattering of low-frequency waves: When the scattering wave has a frequency ω small compared with the internal frequencies of the system, the scattered wave contains both the incident frequency ω_i and other frequencies of the form $\omega_s = \omega_i + \omega(\ell) n(\ell)$. Where $\omega(\ell)$ are the various characteristic frequencies of the scattering system and $n(\ell)$ are integers. The scattered wave with unchanged frequency is called the Rayleigh-scattered or coherently scattered radiation, while the scattered wave with shifted frequencies is called the Raman scattered or 'incoherently' scattered radiation. The concepts of coherent and incoherent scattering will be discussed in the framework of the quantum theory where the distinction is most easily made.

This type of scattering will be discussed in detail after a brief review of the radiation from an oscillating electric dipole and the concept of polarizability.

I. A. 1. Classical Theory of Rayleigh Scattering

Consider an oscillating electric dipole moment

$$\vec{p}(t) = \vec{p}^- e^{-i\omega t} + \vec{p}^+ e^{+i\omega t}, \quad (I.1)$$

where $\vec{p}^- = (\vec{p}^+)^*$ is an arbitrary complex amplitude. At large distances \vec{R} from the dipole the electric and magnetic fields are given by the formulae (in Gaussian units) [5,6]

$$\vec{E}(t+R/c) = \frac{1}{R^3 c^2} \left\{ (\vec{R} \times \vec{R} \times \ddot{\vec{p}}(t)) \right\}_{\text{Ret}} = \frac{\omega^2}{R^3 c^2} \left\{ (\vec{R} \times \vec{R} \times \vec{p}(t)) \right\}_{\text{Ret}} \quad (I.2a)$$

$$\vec{H}(t+R/c) = -\frac{1}{R^3 c^2} \left\{ (\vec{R} \times \ddot{\vec{p}}(t)) \right\}_{\text{Ret}} = \frac{\omega^2}{R^3 c^2} \left\{ (\vec{R} \times \vec{p}(t)) \right\}_{\text{Ret}} \quad (I.2b)$$

The magnitude of Poynting vector $\vec{S} = \frac{c}{4} \vec{E} \times \vec{H}$ can then be written as

$$S = \frac{\omega^4}{4\pi R^2 c^3} \left| \frac{\vec{R}}{R} \times \frac{\vec{R}}{R} \times \vec{p}(t) \right|^2 \quad (I.3)$$

The vector product in this expression represents the projection of $\vec{p}(t)$ on a plane perpendicular to \vec{R} . Thus if \hat{e}^1 and \hat{e}^2 are two mutually perpendicular vectors in that plane, we have

$$S = \frac{\omega^4}{4\pi R^2 c^3} \sum_{i=1,2} \sum_{\alpha,\beta=1}^3 \hat{e}_\alpha^i \hat{e}_\beta^i P_\alpha(t) P_\beta(t) \quad (I.4a)$$

This derivation due to Born (6) has the advantage that if one is interested in one linearly polarized component of the scattered radiation, for instance the component parallel to \hat{e}^1 , one has simply to omit the first

summation sign and put $i = 1$. Substituting (1) in (4) and averaging over a period of ω_1

$$S = \frac{\omega^4}{2\pi R^2 C^3} \sum_{i=1,2} \sum_{\alpha,\beta=1} e_{\alpha}^i e_{\beta}^i P_{\alpha}^{+} P_{\beta}^{-} \quad (I. 4b)$$

The general relation between an applied electric field \vec{E} and the resulting electric polarisation \vec{P} in a medium may be written in a dipole approximation in dyadic notation as

$$\vec{P} = \alpha : \vec{E} + \alpha : \vec{E} \vec{E} + \alpha : \vec{E} \vec{E} \vec{E} + \dots$$

or in component form as

$$P_i = (\alpha_{ij} E_j + \alpha_{ijk} E_j E_k + \text{higher order terms}) + \text{c.c.} \quad (I. 5)$$

The α_{ij} 's are the coefficients of linear polarizability and form a second-rank tensor, while α_{ijk} , α_{ijkl} , correspond to non-linear terms of the 2nd, 3rd... order forming tensors of increasingly higher order. Since the fields for which these non-linear effects become observable are much higher than the fields encountered in the light sources used in ordinary Raman experiments - except in the case of stimulated Raman effect experiments - one usually works in the linear approximation.

The most general expression in this linear case is

$$P_i = \alpha_{ij} E_j + \beta_{ik} E_k^* \quad (I. 6)$$

The coefficients α and β are tensors whose components are in general functions of the incident frequency and parameters of the medium. It is this induced polarization that forms the source for scattered radiation. In

general, P_j can have a frequency $\omega' \neq \omega$, the frequency of the applied field component. However, the above equation implies that all terms on the right-hand side of the equation must have the same frequency ω' as P_i on the left-hand side. Since E_j has the frequency of the applied field, ω , then E_k^* has the frequency $-\omega$. The frequency of the quantities β_{ik} must be $(\omega + \omega')$ and can be interpreted as a term which gives rise to radiation of frequency ω' due to the presence of the frequency ω . In other words, it is a term characterizing a process of stimulated emission. Though its introduction and an empirical approach to β_{ik} can be used to incorporate stimulated emission processes artificially in a classical picture, stimulated effects are usually very small and we may neglect this term. Hence $P_i = \alpha_{ij} E_j$. It can be shown that when ω differs greatly from the absorption frequencies α_{ij} is a Hermitean matrix (APPENDIX I).

Similar results hold between the magnetization \vec{M} and the magnetic field \vec{H} . Magnetic properties and the scattering processes have not been studied extensively and are neglected here. They would have to be considered for instance in the case of light scattering from a system of magnetic moments or a spin system.

Now consider the phenomenon of scattering in a dielectric medium. When light falls on a perfectly homogeneous dielectric medium, all the radiation from different volume elements of the medium will interfere destructively, except in the directions of the reflected and refracted light (8). However, consider what happens when a small spherical volume ΔV having a dielectric constant $(\epsilon + \Delta\epsilon)$ is embedded in an otherwise homogeneous, isotropic medium of dielectric constant ϵ . In the linear approximation, $\vec{D} = \epsilon\vec{E}$, so that outside the spherical volume, the electric induction is given by

$$\vec{D}_0 = \epsilon(\vec{E}) \vec{E}.$$

While inside,

$$\vec{D}_i = (\epsilon + \Delta\epsilon) \vec{E} = \epsilon \left(1 + \frac{\Delta\epsilon}{\epsilon}\right) \vec{E}.$$

Thus the presence of the small inhomogeneity has the same effect as the creation of a secondary electric intensity $\frac{\Delta\epsilon}{\epsilon} \vec{E}$ per unit volume at its center. This inhomogeneity behaves like an oscillating dipole with the frequency ω of the applied field \vec{E} and can then emit "secondary" radiation in all directions. This causes a scattering of the incident light. Thus an inhomogeneity in a medium or a "fluctuation" in a "perfect", homogeneous medium can give rise to scattering.

The electromagnetic field quantities \vec{E} , \vec{H} , \vec{D} , \vec{B} , which appear in the usual classical electrodynamics are obtained by an averaging process which may be looked upon as two operations. The first is the averaging over an element of volume physically infinitesimal but large enough to contain many molecules. This is followed by a time averaging with respect to the motion of all the particles in the medium. In the theory of scattering, one has to stop at the first averaging because the second step would annul the phenomenon of scattering. It is also clear then why there is always a certain amount, however small, of light scattered from any medium because of the statistical fluctuations of the dipole moment induced in any given volume element. The fluctuation in $\sum \vec{p}^k$ where \vec{p}^k is the induced dipole moment at the k^{th} molecule in the volume element ΔV under consideration is caused, in general, partly by the fluctuations, $\Delta n = n - \bar{n}$, in the number of molecules in ΔV and partly by fluctuations, $\Delta \vec{p}^k = \vec{p}^k - \bar{\vec{p}}^k$, in the dipole moments of the individual molecules due to

their internal motion. In calculating the scattered intensities, it is the square of these fluctuations that are involved. It can be shown that if \hat{e} denotes the unit vector in a given direction, the square of the fluctuations of the component of the dipole moment in that direction is given by (Appendix II)

$$\left| \Delta \sum_k \vec{p}^k \cdot \hat{e} \right|^2 = \bar{n} \overline{|\vec{p} \cdot \hat{e}|^2} \quad \dots \quad (I. 7)$$

where \bar{n} = average number of particles in the volume and \vec{p} = induced dipole moment per molecule.

If the molecule considered is isotropic the only fluctuation is that due to density variation. Also, the polarizability is a scalar constant so that we have $\vec{p} = a\vec{E}$, where \vec{E} is the "effective field strength" in the medium rather than that of the incident light. For gases at ordinary pressures these are almost equal and hence,

$$\left| \Delta \sum_k \vec{p}^k \cdot \hat{e} \right|^2 = \bar{n} a^2 |\vec{E} \cdot \hat{e}|^2 = \bar{n} a^2 E^2 \cos^2 \psi \quad (I. 8)$$

where ψ is the angle between the electric vector E of the incident beam and the direction of polarization we wish to examine in the scattered beam.

Substituting in Eq. (I.4), the intensity of the scattered light of polarization \hat{e} observed is given by

$$I = \frac{\omega^4}{c^4 r^2} N V a^2 E^2 \cos^2 \psi \quad (I.9a)$$

$$= \frac{\pi^2 (\mu^2 - 1)^2}{r^2 \lambda^4} \frac{V}{N} E^2 \cos^2 \psi, \quad (I.9b)$$

Since $\omega = \frac{2\pi c}{\lambda}$ and it can be shown (9, p. 87) that $a = \frac{\mu^2 - 1}{4\pi N}$, where μ is the refractive index of the gas.

For an isotropic molecule, with unpolarized light incident, say along the y-axis and observing along z, Eq. (4) shows the light scattered in a direction strictly transverse to the direction of propagation of the incident beam exhibits complete polarization even when the incident light is unpolarized. Equations (I.9a) and (I.9b) show

(1) the intensity of scattering is proportional to the square of the polarizability of the molecule.

(2) the intensity is inversely proportional to the fourth power of the wavelength if a possible dependence of the polarizability on the wavelength is neglected.

Examples of the isotropic case are single atoms, tetrahedral molecules (e.g. CH_4) or octahedral molecules (e.g. SF_6).

In a general anisotropic molecule the polarizability is a tensor and

$$\vec{p} \cdot \vec{e} = \sum_{\alpha} \sum_{\beta} a_{\alpha\beta} E_{\alpha} e_{\beta}.$$

In a gas since the orientation of the molecule is arbitrary and random we must average $a_{\alpha\beta}$ over all possible orientations. When this is done, one gets (Appendix III)

$$\left| \vec{p} \cdot \hat{e} \right|^2 = R_0 E^2 \cos^2 \psi + R E^2 \left(1 + \frac{1}{3} \cos^2 \psi \right), \quad (\text{I.10})$$

where

$$R_0 = \frac{1}{9} (\alpha_{xx} + \alpha_{yy} + \alpha_{zz})^2 = \frac{(\mu^2 - 1)^2}{16 \pi^2 N^2} \quad (\text{I.11})$$

$$R = \frac{1}{3} \left\{ (\alpha_{yy} - \alpha_{zz})^2 + (\alpha_{zz} - \alpha_{xx})^2 + (\alpha_{xx} - \alpha_{yy})^2 + 6 (|\alpha_{yz}|^2 + |\alpha_{zx}|^2 + |\alpha_{xy}|^2) \right\} \quad (\text{I.12})$$

$$= \frac{3}{5} R_0 - \frac{1}{5} (\alpha_{yy}\alpha_{zz} + \alpha_{zz}\alpha_{xx} + \alpha_{xx}\alpha_{yy})$$

In these equations (x,y,z) denote a framework fixed with respect to the molecule. Note that R vanishes if the molecule is isotropic. Thus the first term in (10) is due to fluctuations in density and the second is due to fluctuations in induced dipole moments resulting from the anisotropy. Since α_{xx} , α_{yy} , α_{zz} are all positive, then

$$R \leq \frac{3}{5} R_0. \quad (I.13)$$

The intensity of the scattered light is given by

$$I = I_0 \frac{16\pi^4}{r^2\lambda^4} NV \left\{ R_0 \cos^2 \psi + R\left(1 + \frac{1}{3} \cos^2 \psi\right) \right\} \quad (I.14a)$$

$$= I_0 \frac{16\pi^4}{r^2\lambda^4} NV \left\{ \left(R_0 + \frac{1}{3} R\right) \cos^2 \psi + R \right\}, \quad (I.14b)$$

where I_0 is the intensity of the incident light. From (13b) note that the scattered light has a "polarized" part, i.e., a part that vanishes in a direction perpendicular to the incident polarization ($\psi = \pi/2$) and an unpolarized part. The density fluctuation term contributes only to the polarized part whereas the anisotropy term contributes to both.

The nature of polarization of the scattered light is thus indicative of the anisotropy of the scattering center or molecule. We define the depolarization ratio or factors as

$$g = \frac{I_{\perp}}{I_{\parallel}} = \frac{I(\psi=\pi/2)}{I(\psi=0)} \quad (I.15)$$

I_{\perp} and I_{\parallel} are the intensities of the components of scattered light with

electric vectors perpendicular and parallel to that of the incident light.

It can be shown that, for plane polarized incident light,

$$S_p = \frac{R}{R_0 + \frac{4}{3} R} \quad (I.16)$$

and for unpolarized incident light,

$$S_n = \frac{2R}{R_0 + \frac{7}{3} R} \quad (I.17)$$

From (I.13), we find

$$S_p \leq \frac{1}{3}$$

$$S_n \leq \frac{1}{2}$$

The quantity R_0 can be obtained from the refractive index. Observations of S_p or S_n determines R and hence the optical anisotropy of a molecule. A detailed discussion of these aspects is given by Mizushima (8).

I. A. 2. Classical Theory of Raman Scattering

Raman scattering (or combinational scattering) occurs when a system has characteristic frequencies associated with it, as for instance, the vibrational frequencies of a free molecule or the lattice vibration frequencies of a crystal. The scattered light then consists of frequencies shifted from that of the incident light, in addition to the unshifted Rayleigh scattered light. This can be looked upon classically as due to a modulation of the polarizability by the characteristic vibrations.

Any complex motion of a system can be resolved into "normal mode vibrations", if we make the assumption that the displacements of the

particles from their equilibrium positions are sufficiently small so that a Taylor expansion of the potential energy in terms of this displacement may be terminated after the quadratic term (9). This approximation is called the Harmonic Approximation because the force between particles is linear in displacements as in the case of a harmonic oscillator. Each normal mode is a collective motion of the particles of the system with a characteristic frequency and with all the particles passing through their equilibrium positions in phase and at the same instant. Any actual motion of the system may then be written as a superposition of the normal modes.

The normal mode analysis applies to the motion of the nuclei in the molecule. The incident light, however, is scattered by the electrons rather than by the nuclei. As will be more evident from the quantum theoretical treatment, it is the electronic part of the polarizability rather than the ionic part that contributes predominantly to the scattering. If the first excited electronic state is sufficiently high above the ground state, we can assume that at ordinary temperatures the electronic motions at any instant are practically what they would be if the nuclei were at rest. If the frequency of the incident light is very large compared to the vibrational and rotational frequencies of the molecule - which are typically in the infrared region - and if it lies far away from any electronic absorption frequency, then we can ascribe an instantaneous polarizability to the molecule. When the molecule rotates or vibrates this polarizability will vary in time.

The polarizability being a function of the displacement of the particles, can be expressed as a function of the normal modes. Suppose $Q_1 = [Q_0 e^{i\omega_1 t} + \text{c.c.}]$ represents one such normal mode. If, for simplicity it is assumed that

the system is vibrating in that

mode alone, then

$$\alpha_{ij} = \alpha_{ij}^0 + \left. \frac{\partial \alpha_{ij}}{\partial Q_1} \right|_0 Q_1 + \left. \frac{\partial \alpha_{ij}}{\partial Q_1^*} \right|_0 Q_1^* + \frac{1}{2} \left. \frac{\partial^2 \alpha_{ij}}{\partial Q_1^2} \right|_0 Q_1 Q_1 + \frac{1}{2} \left. \frac{\partial^2 \alpha_{ij}}{\partial Q_1^{*2}} \right|_0 Q_1^* Q_1^*$$

+ higher order terms

$$= \alpha_{ij}^0 + \alpha_{ij}^1)_0 Q_0 e^{i\omega_1 t} + \alpha_{ij}^{1*})_0 Q_0^* e^{-i\omega_1 t} + \frac{1}{2} \alpha_{ij}^{11})_0 Q_0 Q_0 e^{i2\omega_1 t} \\ + \frac{1}{2} \alpha_{ij}^{11*})_0 Q_0^* Q_0^* e^{-i2\omega_1 t} + \text{higher order terms, (I.18)}$$

where $\alpha_{ij}^1)_0 \equiv \left. \frac{\partial \alpha_{ij}}{\partial Q_1} \right|_0$, $\alpha_{ij}^{1*})_0 = \left. \frac{\partial \alpha_{ij}}{\partial Q_1^*} \right|_0$, ... etc. are

polarizability derivatives evaluated at the equilibrium positions. Now, if the field of the incident radiation is

$$\vec{E} = \vec{E}_0 e^{i\omega t} \quad \text{or} \quad E_j = E_{0j} e^{i\omega t} \quad (j=1,2,3),$$

the components of the polarization induced are given by

$$P_j = \alpha_{ij} E_j \\ = \alpha_{ij}^0 E_{0j} e^{i\omega t} + \alpha_{ij}^1)_0 (Q_0 E_{0j} e^{i(\omega+\omega_1)t} + Q_0^* E_{0j} e^{i(\omega-\omega_1)t}) \\ + \frac{1}{2} \alpha_{ij}^{11})_0 (Q_0 E_{0j} e^{i(\omega+2\omega_1)t} + Q_0^* E_{0j} e^{i(\omega-2\omega_1)t}) + \text{higher} \\ \text{order terms} \quad \text{(I.19b)}$$

$$= u^0 e^{i\omega t} + u^1 e^{i(\omega+\omega_1)t} + u^{1*} e^{i(\omega-\omega_1)t} + u^2 e^{i(\omega+2\omega_1)t} \\ + u^{2*} e^{i(\omega-2\omega_1)t} + \text{higher order terms} \quad \text{(I.19c)}$$

using the notation,

$$u^0 \equiv \alpha_{ij}^0, \quad u^1 \equiv \alpha_{ij}^1)_0 Q_0, \quad u^{1*} = \alpha_{ij}^{1*})_0 Q_0^*, \text{ etc.}$$

and recalling that α_{ij} is Hermitean.

The induced polarization then gives rise to radiation at these various frequencies. The first term in Eq. (19c) gives rise to radiation at the same frequency ω as the incident radiation and represents the Rayleigh scattered light. The two succeeding terms are responsible for radiation at frequencies $\omega \pm \omega_1$ and lead to the first-order Raman scattering by the normal mode Q_1 . This yields frequencies symmetrically placed on either side of the incident frequency. The $\omega - \omega_1$ line is called the Stokes line and the $\omega + \omega_1$, the anti-Stokes line. The next pair of terms involve double the normal mode frequency in the above example of a single normal mode or the sum of two normal modes in the general case. These represent the Stokes and anti-Stokes lines of the "second-order Raman scattering." Higher order scattering is conceivable but the probability for these processes becomes increasingly small.

In the general case of n normal modes with frequencies $\{\omega_1, \dots, \omega_n\}$, Eq. (I.18) becomes

$$\begin{aligned}
 \alpha_{ij} &= \alpha_{ij}^0 + \sum_{k=1}^n \left[\left(\frac{\partial \alpha_{ij}}{\partial Q_k} \right)_0 Q_k + \left(\frac{\partial \alpha_{ij}}{\partial Q_k^*} \right)_0 Q_k^* \right] \\
 &\quad + \sum_{\ell=1}^n \sum_{m=1}^n \left[\left(\frac{\partial^2 \alpha_{ij}}{\partial Q_\ell \partial Q_m} \right)_0 Q_\ell Q_m + \left(\frac{\partial^2 \alpha_{ij}}{\partial Q_\ell^* \partial Q_m^*} \right)_0 Q_\ell^* Q_m^* \right] + \text{higher} \\
 &\hspace{15em} \text{order terms} \\
 &= \alpha_{ij}^0 + \sum_k (\alpha_{ij}^k Q_k + \alpha_{ij}^{k*} Q_k^*) + \sum_{\ell} \sum_m (\alpha_{ij}^{\ell m} Q_\ell Q_m + \alpha_{ij}^{\ell m*} Q_\ell^* Q_m^*) \\
 &\hspace{15em} + \text{higher order terms} \quad (I.20)
 \end{aligned}$$

where α_{ij}^k form the components of a mixed tensor of the third rank, covariant in indices i, j and contravariant in k and the $\alpha_{ij}^{\ell m}$ etc. form tensors of higher rank.

Since the polarizability derivatives are usually much smaller than α_{ij}^0 , the polarizability in the equilibrium position, the Raman scattered light is much less intense than the Rayleigh scattered light. Further the phases of the normal modes will, in general, vary from molecule to molecule in a gas so that the different molecules will radiate with random phases and the Raman-scattered light will thus be incoherent. Its observation will not be dependent on density fluctuations and its intensity will be proportional to the number of scattering molecules. The only difference between the calculation of the intensity of Rayleigh and Raman scattering is that in the case of the Raman scattering, one must use the corresponding induced dipole moment [for instance, the term proportional to $e^{i(\omega-\omega_k)t}$ in considering the first-order Stokes line of frequency shift ω_k] itself rather than the fluctuation $\Delta\vec{p}$. For a given ω_k , then, analogous to Eq. (4) the intensity is given by

$$I = I_0 \frac{(\omega \pm \omega_k)^4}{c^4} \frac{1}{r^2} NV \left\{ \left(R_0 + \frac{1}{3} R \right) \cos^2 \psi + R \right\} \quad (I.21)$$

where ψ is the angle between the electric vector \vec{E} of the incident field and the direction of polarization selected for observation, for instance by the setting of an analyser in the scattered beam. The equations

$$R_0 = \frac{1}{9} (\alpha_{xx}^k + \alpha_{yy}^k + \alpha_{zz}^k) \quad (I.22a)$$

and

$$R = \frac{1}{30} \left\{ (\alpha_{xx}^k - \alpha_{yy}^k) + (\alpha_{yy}^k - \alpha_{zz}^k) + (\alpha_{zz}^k - \alpha_{xx}^k) + 6(|\alpha_{yz}^k|^2 + |\alpha_{zx}^k|^2 + |\alpha_{xy}^k|^2) \right\} \quad (I.22b)$$

now involve the polarizability derivatives in place of the polarizability components in the case of the corresponding Eq. (I.14) for Rayleigh scattered intensity. While the elements α_{ij} of the polarizability tensor are always positive, the terms α_{ij}^k could be positive or negative depending upon whether the normal mode ω_k is responsible for an increase or decrease in the polarizability component α_{ij} .

The depolarization factors for Raman-scattered light are obtained as in Rayleigh scattering and are formally the same,

$$S_p = \frac{R}{R_0 + \frac{5}{3}R}, \quad S_n = \frac{2R}{R_0 + \frac{7}{3}R}. \quad (\text{I.23a,b})$$

Whereas R_0 was always positive and greater than or equal to $5/3$, R_0 can be positive, negative or zero so that we have,

$$S_p \leq \frac{3}{4}, \quad S_n \leq \frac{6}{7} \quad (\text{I.24a,b})$$

rather than the $S_p \leq \frac{1}{3}, S_n \leq \frac{1}{2}$ for Rayleigh scattering.

I. B. 1. Semiclassical Theory of Rayleigh and Raman Scattering.

In any perfectly rigorous theory of interaction of radiation with matter, the quantized radiation field should be coupled to the scattering system of nuclei and electrons and the whole treated as one quantum mechanical system. Such a theory of Raman scattering is complicated and has been developed only recently. A semiclassical theory in which the incident and scattered light fields are treated as classical electromagnetic fields while the scattering system are described quantum mechanically yields a fairly complete and accurate description of the scattered intensities and

selection rules. This theory is now described. (7)

The dipole approximation is often used in radiation problems. It is worthwhile to examine the assumptions involved and the validity of its application to the Raman scattering case.

The non-relativistic Hamiltonian for a charged particle in an electromagnetic field, in terms of the canonical variables \vec{r} and \vec{p} describing the particle and the electromagnetic potentials $\vec{A}(\vec{r}, t)$ and $\phi(\vec{r}, t)$, is

$$\begin{aligned} H &= \frac{1}{2m} \left(\vec{p} - \frac{e}{c} \vec{A} \right)^2 + e\phi \\ &= \frac{p^2}{2m} - \frac{e}{2mc} (\vec{A} \cdot \vec{p} + \vec{p} \cdot \vec{A}) + \frac{e^2}{2mc^2} A^2 + e\phi \\ &= \frac{p^2}{2m} + \frac{i\hbar e}{2mc} (\vec{A} \cdot \vec{\nabla} + \vec{\nabla} \cdot \vec{A}) + \frac{e^2}{2mc^2} A^2 + e\phi \quad (1.25) \end{aligned}$$

The Coulomb gauge, though not relativistically invariant, is used in most simple radiation problems because of its simplicity. [Ref. 11, p. 53].

The Coulomb gauge condition is $\vec{\nabla} \cdot \vec{A} = 0$. Consider $(\vec{A} \cdot \vec{\nabla} + \vec{\nabla} \cdot \vec{A})\psi$ where ψ is an arbitrary wave function

$$\begin{aligned} (\vec{A} \cdot \vec{\nabla} + \vec{\nabla} \cdot \vec{A})\psi &= \vec{A} \cdot \vec{\nabla} \psi + (\vec{\nabla} \cdot \vec{A})\psi + \vec{A} \cdot \vec{\nabla} \psi \\ &= 2\vec{A} \cdot \vec{\nabla} \psi \quad (\because \vec{\nabla} \cdot \vec{A} = 0). \end{aligned}$$

In a situation in which there is no free charge density ρ , one can choose $\phi = 0$ in the Coulomb (or Lorentz) gauge. Thus the Hamiltonian simplifies to

$$H = \frac{p^2}{2m} + \frac{i\hbar e}{mc} \vec{A} \cdot \vec{\nabla} + \frac{e^2}{2mc^2} A^2 \quad (1.26)$$

It can be shown in the quantum theory of radiation [ref. 11, p. 143] that the square of the vector potential has non-vanishing matrix elements

only for transitions in which the number of photons - quanta of the radiation field - changes by two or remains unchanged. Thus it is non-vanishing in the Raman effect but does not contribute to simple absorption or emission. In these cases, there is no approximation involved in neglecting the A^2 term.

The vector potential \vec{A} can be expanded in terms of plane waves when $\vec{J} = 0$, since it is then a solution of the homogeneous wave equation. When the wavelength of the radiation component (specified by the wave vector \vec{k}) is large compared to the dimensions of the molecular system interacting with the field and A^2 is neglected it can be shown that the electric dipole approximation is valid. In essence this means that the electric dipole moment of the system coupling with the electric field is the only important term in the interaction. [Ref. 12, p. 404]. Neglecting A^2 and the long wavelength approximation are two independent assumptions. It is conceivable that the A^2 term, though of higher order than the $\vec{A} \cdot \vec{\nabla}$ term, is not negligible a priori in the consideration of Rayleigh and Raman scattering. This point will be discussed at the end of this section. The dipole approximation is used in this section. Thus one need consider only the interaction of the electric dipole moment of the system with the electric field of the radiation.

Consider a molecular system subjected to a static uniform electric field \vec{E} . If the Hamiltonian of the system in the absence of the field is denoted by $H(0)$, the Hamiltonian in the field has the form

$$H(\vec{E}) = H(0) - \vec{M} \cdot \vec{E} \quad (I.27)$$

The operator representing the electric dipole moment of the system is denoted by \vec{M} rather than \vec{P} which was used previously. This is done to avoid confusion with the standard use of P for polarizability tensors. Thus, $\vec{M} = \sum e_{\ell} \vec{r}_{\ell}$, the sum extending over all the particles. The term H^1 is taken as the perturbation. Implicit in this is the assumption that the applied field is small in comparison with internal electric fields in the molecule of the crystal ($\sim 10^8$ volts/cm). This assumption is reasonable except in extremely high field intensities as in a pulsed laser beam, a case excluded in this treatment.

Using results of perturbation theory (12) up to the second order, the energy ϵ_{ℓ} of the state ℓ in the presence of the perturbation (H^1) is given by

$$\begin{aligned} \epsilon_{\ell}(\vec{E}) &= \epsilon_{\ell}(0) + \langle \ell | -\vec{M} \cdot \vec{E} | \ell \rangle + \sum_{r \neq \ell} \frac{\langle \ell | -\vec{M} \cdot \vec{E} | r \rangle \langle r | -\vec{M} \cdot \vec{E} | \ell \rangle}{\epsilon_{\ell}(0) - \epsilon_r(0)} \\ &= \epsilon_{\ell}(0) - \sum_{\alpha} \langle \ell | M_{\alpha} | \ell \rangle E_{\alpha} + \sum_{r \neq \ell} \sum_{\alpha \beta} \frac{\langle \ell | M_{\alpha} | r \rangle \langle r | M_{\beta} | \ell \rangle}{\epsilon_{\ell}(0) - \epsilon_r(0)} E_{\alpha} E_{\beta}. \quad (I.28) \end{aligned}$$

Noting that $\vec{M} \cdot \vec{E} = M_{\alpha} E_{\alpha}$ and that the external electric field components E_{α} can be taken outside the scalar product as long as E_{α} is independent of space coordinates, then $\epsilon_{\ell}(0)$, $\epsilon_r(0)$ and the matrix elements on the right-hand side refer to the unperturbed system.

It can be shown (Appendix IV) for a stationary state ℓ ,

$$\frac{\partial}{\partial E_{\alpha}} \epsilon_{\ell}(\vec{E}) = - \int \psi_{\alpha}^{*}(\vec{E}) M_{\alpha} \psi_{\ell}(\vec{E}) d\tau, \quad (I.29)$$

where $\psi_{\ell}(\vec{E})$ is the wave function corresponding to the energy eigenvalue $\epsilon_{\ell}(E)$. The integral on the right-hand side is the value of the electric moment of the system in state ℓ . The α^{th} component of the electric dipole

moment can thus be obtained by differentiating Eq. (I.28) with respect to E_α .

Thus,

$$\begin{aligned} \frac{\partial \epsilon_\ell(\vec{E})}{\partial E_\alpha} &= \langle \ell | M_\alpha | \ell \rangle + \sum_\beta \left\{ \frac{1}{\hbar} \sum_{r \neq \ell} \frac{\langle \ell | M_\alpha | r \rangle \langle r | M_\beta | \ell \rangle + \langle \ell | M_\beta | r \rangle \langle r | M_\alpha | \ell \rangle}{\omega_{r\ell}} \right\} E_\beta \\ &= - \int \psi_\ell^*(\vec{E}) M_\alpha \psi_\ell(\vec{E}) d\tau, \end{aligned} \quad (I.30)$$

where

$$\omega_{r\ell} \equiv \frac{1}{\hbar} [\epsilon_r(0) - \epsilon_\ell(0)]$$

is a transition frequency of the unperturbed system.

The first term in Eq. (I.30) is independent of the field and represents the permanent dipole moment of the system. The second term represents the moment induced by the applied field. The coefficient of E_β in the second term form the $\alpha\beta$ components of a second-rank tensor. This tensor is called the static polarizability.

For later calculations, the notation below is introduced.

$$P_{\alpha\beta}^{\ell\ell}(0) \equiv \frac{1}{\hbar} \sum_{r \neq \ell} \frac{\langle \ell | M_\alpha | r \rangle \langle r | M_\beta | \ell \rangle + \langle \ell | M_\beta | r \rangle \langle r | M_\alpha | \ell \rangle}{\omega_{r\ell}} \quad (I.31)$$

In this expression ℓ indicates the state to which the polarizability refers. The argument 0 indicates this is the polarizability in a static electric field i.e., a field of frequency 0. Using this notation, one can rewrite (29) and (30) as

$$\epsilon_\ell(\vec{E}) = \epsilon_\ell(0) - \sum_\alpha \langle \ell | M_\alpha | \ell \rangle E_\alpha - \frac{1}{2} \sum_{\alpha\beta} P_{\alpha\beta}^{\ell\ell}(0) E_\alpha E_\beta \quad (I.32)$$

$$\int \psi_{\ell}^*(\vec{E}) M_{\alpha} \psi_{\alpha}(\vec{E}) d\tau = \langle \ell | M_{\alpha} | \ell \rangle + \sum_{\beta} P_{\alpha\beta}^{\ell\ell}(0) E_{\beta}. \quad (I.33)$$

Consider the system in a periodic electric field of elliptic polarization given by

$$\vec{E}(t) = \vec{E}^{-} e^{-i\omega t} + \vec{E}^{+} e^{i\omega t}. \quad (I.34)$$

This is equivalent to taking the real part of a complex quantity where $\vec{E}^{-} = (\vec{E}^{+})^*$ is an arbitrary complex constant vector expression for the field. If one neglects the magnetic field which is necessarily associated with a variable electric field, the Hamiltonian of the system is given by Eq. (I.25) with the time-dependent field (I.34) in place of the static field E .

Consider the time-dependent Schrödinger equation

$$H\psi = i\hbar \frac{\partial \psi}{\partial t}$$

$$\text{i.e.,} \quad \left[H(0) - \vec{M} \cdot \vec{E}^{-} e^{-i\omega t} + \vec{M} \cdot \vec{E}^{+} e^{i\omega t} \right] \psi = i\hbar \frac{\partial \psi}{\partial t} \quad (I.35)$$

with $\psi_{\ell}(0) = \psi_{\Omega}(0) e^{-i\epsilon_{\ell}(0)t/\hbar}$ as the unperturbed wave function.

It can be shown [Ref. 12, p. 282] that the perturbed wave functions are then given by

$$\psi_{\ell}(\vec{E}) = \psi_{\ell}(0) + \left[\sum_{\mathbf{s}} (a_{\mathbf{s}}^{+} e^{i\omega t} + a_{\mathbf{s}}^{-} e^{-i\omega t}) \psi_{\mathbf{s}}(0) \right] e^{-i\epsilon_{\ell}(0)t/\hbar}, \quad (I.36)$$

where

$$a_{\mathbf{s}}^{+} = \frac{1}{\hbar} \sum_{\alpha} \frac{\langle \ell | M_{\alpha} | \ell \rangle E_{\alpha}^{\pm}}{\omega_{\mathbf{s}\ell} \pm \omega} \quad (I.37)$$

$$\omega_{\mathbf{s}\ell} = \frac{1}{\hbar} (\epsilon_{\mathbf{s}}(0) - \epsilon_{\ell}(0))$$

The above wave functions which are first-order approximations are adequate in considering the electric moment induced by the field as long as the frequency of the applied field is not too close to any of the transition frequencies $\omega_{s\ell}$ of the system. The electric dipole moment $\vec{m}(t)$ of the system is obtained by forming the expectation values:

$$\begin{aligned}\vec{m}(t) &= \int \psi_{\ell}^* \vec{M} \psi_{\ell} d\tau \\ &= \langle \ell | M_{\alpha} | \ell \rangle + e^{+i\omega t} \sum_s [\langle s | \vec{M} | \ell \rangle (a_s^-)^* + \langle \ell | \vec{M} | s \rangle a_s^+] \\ &\quad + e^{-i\omega t} \sum_s [\langle \ell | \vec{M} | s \rangle a_s^- + \langle s | \vec{M} | \ell \rangle (a_s^+)^*] \quad (I.38)\end{aligned}$$

where higher order terms are neglected.

Substituting for a_s^{\pm} from Eq. (37) and rewriting in component form yields

$$\begin{aligned}m_{\alpha}(t) &= \langle \ell | M_{\alpha} | \ell \rangle + e^{-i\omega t} \sum_s [\langle \ell | M_{\alpha} | s \rangle \left\{ \frac{1}{\hbar} \sum_{\beta} \frac{\langle s | M_{\beta} | \ell \rangle E_{\beta}^-}{\omega_{s\ell} - \omega} \right\} + \langle s | M_{\alpha} | \ell \rangle \left\{ \frac{1}{\hbar} \sum_{\beta} \frac{\langle \ell | M_{\beta} | s \rangle E_{\beta}^-}{\omega_{s\ell} + \omega} \right\}] \\ &\quad + e^{i\omega t} \sum_s [\langle s | M_{\alpha} | \ell \rangle \left\{ \frac{1}{\hbar} \sum_{\beta} \frac{\langle \ell | M_{\beta} | s \rangle E_{\beta}^+}{\omega_{s\ell} - \omega} \right\} + \langle \ell | M_{\alpha} | s \rangle \left\{ \frac{1}{\hbar} \sum_{\beta} \frac{\langle s | M_{\beta} | \ell \rangle E_{\beta}^+}{\omega_{s\ell} + \omega} \right\}]\end{aligned}$$

This equation can be written compactly as

$$m_{\alpha}(t) = \langle \ell | M_{\alpha} | \ell \rangle + \sum_{\beta} \left\{ P_{\alpha\beta}^{\ell\ell}(-\omega) E_{\beta}^- e^{-i\omega t} + P_{\alpha\beta}^{\ell\ell}(\omega) E_{\beta}^+ e^{+i\omega t} \right\}, \quad (I.39)$$

where

$$P_{\alpha\beta}^{\ell\ell}(\omega) = \frac{1}{\hbar} \sum_s \left\{ \frac{\langle \ell | M_{\alpha} | s \rangle \langle s | M_{\beta} | \ell \rangle}{\omega_{s\ell} + \omega} + \frac{\langle \ell | M_{\beta} | s \rangle \langle s | M_{\alpha} | \ell \rangle}{\omega_{s\ell} - \omega} \right\} \quad (I.40)$$

The term $s = \ell$ vanishes identically since $\omega_{s\ell} = 0$ for $s = \ell$.

$P_{\alpha\beta}^{\ell\ell}(\omega)$ is a second-rank tensor and is called the polarizability. Note here that the superscripts only denote the state and are not tensor indices. It has the following properties:

- (1) $P_{\alpha\beta}^{\lambda\lambda}(\omega) = [P_{\alpha\beta}^{\lambda\lambda}(-\omega)]^*$ which guarantees that $M(t)$ is real.
 (2) $P_{\alpha\beta}^{\lambda\lambda}(\omega) = [P_{\alpha\beta}^{\lambda\lambda}(\omega)]^*$ which is consistent with the polarizability tensor being Hermitean. (See Appendix I.)

For $\omega = 0$ the equation reduces to the equation for the static polarizability $P_{\alpha\beta}^{\lambda\lambda}(0)$ of eq. (I.31). Note also that the elements $P_{\alpha\beta}^{\lambda\lambda}(\omega)$ are independent of the arbitrary phases of the wave functions used in forming the matrix elements in the sum.

The first order wave function (I.36) and hence also the polarizability (I.39) become less accurate as ω approaches a transition frequency $\omega_{s\lambda}$. In particular it can be shown (7) that the work done by a field $\vec{E}(t)$ in a time period corresponding to the frequency ω is zero due to the Hermitean character of $P_{\alpha\beta}^{\lambda\lambda}(\omega)$. $P_{\alpha\beta}^{\lambda\lambda}(\omega)$ does not account for energy absorption. However, a molecular system can absorb energy in the neighborhood of its transition frequencies. To take this into account we must introduce an anti-Hermitean part to the polarizability tensor usually denoted by $R_{\alpha\beta}^{\lambda\lambda}(\omega)$. Removing the restriction that ω not be near any frequency $\omega_{s\lambda}$ shows the polarizability to be a general tensor, since any tensor can always be decomposed into a Hermitean and an anti-Hermitean part. Since the theory of scattering being developed here is valid only in regions where ω is not close to $\omega_{s\lambda}$, the Hermitean part of the polarizability is a sufficiently close approximation to the actual polarizability. One can describe a polarization \vec{P} , or the dipole moment per unit volume of the material medium with the help of the polarizability defined above. Maxwell's equations give a complete account of the refractive properties of the medium including dispersion, once the relation between the electric displacement vector \vec{D} and the macroscopic electric field \vec{E} in the medium is known. Implicit in the

definition of these vectors is the presence of a continuous medium. When one is considering a medium of distinctly separated molecules such as in a gas, one has only to divide the molecular moment as given by the polarizability by the average volume occupied by a molecule in order to obtain the dielectric polarization. The field acting on the system differs in general, however, from the macroscopic field [Ref. 13, Chap 12]. The difference can be ignored only if the density is very small. Otherwise, a relation must be obtained first between the macroscopic field and the field E that acts on a molecule. In the case of a crystalline solid, the whole crystal should be treated as one system. One can, however, use the polarizability theory in the above form even in this case once a relation between the electric moment of a small part of the system in a small volume element - small compared with the wavelength of the optical wave - and the macroscopic electric field is established.

Now the expression in equation (I.31), describes the electric field over a molecular system exposed to a field of elliptically polarized radiation, provided the dimension of the molecular system is small compared with the wavelength of the light wave. The radiation emitted by the induced moment represents the light scattered by the system. Thus we arrive at a description of Rayleigh scattered light by substituting for $m_{\alpha}^{+}(t)$ and $m_{\beta}^{-}(t)$ in eq. (4b),

$$\overline{S} = \frac{\omega^4}{r^2 c^4} \sum_{i=1,2} \sum_{\alpha,\beta=1}^3 \hat{e}_{\alpha}^i \hat{e}_{\beta}^i m_{\alpha}^{+} m_{\beta}^{-} \dots \quad (I.40b)$$

Since \vec{E} and \vec{H} given by (2a) and (2b) and \vec{R} form a right-handed system of orthogonal vectors., the energy flow S in Eq. (I.3) is radially outward. The total radiation is obtained by integrating $R^2 S d\Omega$ over the whole solid

angle $\Omega = 4\pi$. This gives (Appendix V)

$$\int R^2 \sin \Omega \, d\Omega = \frac{4\omega^4}{3c^3} \sum_{\alpha} m_{\alpha}^{+} m_{\alpha}^{-}. \quad (I.41)$$

From equations (1) and (38), it is seen that the following substitution holds:

$$m_{\alpha}^{+} = \sum_{\beta} P_{\alpha\beta}^{\ell\ell}(\omega) E_{\beta}^{+}, \quad m_{\alpha}^{-} = \sum_{\beta} P_{\alpha\beta}^{\ell\ell}(-\omega) E_{\beta}^{-}. \quad (I.42)$$

Since, as observed before $P_{\alpha\beta}^{\ell\ell}(\omega)$ is unambiguously defined in phase, the scattered light bears a definite phase relation with the incident light. That is, the Rayleigh scattered light is coherent with the incident light. Also since the scattering is described by the elements of the polarizability in the state ℓ of the molecular system, it is seen that the molecular system persists in a fixed quantum state and the scattering is due to the periodic deformation of the state by the electric field of the incident light.

Raman scattering, on the other hand, is associated with a quantum transition in the system. It is most easily understood in terms of quantum electrodynamics wherein the electromagnetic field is quantized. The field Eq. (I.32) may be interpreted as representing the effect of incident photons with energy $\hbar\omega$. If, as a result of scattering a photon, the molecular system goes from an initial state ℓ to a final state ℓ' , energy conservation requires that the scattered photon have energy $\omega + \Delta\omega$ so that

$$\epsilon_{\ell}(0) + \hbar\omega = \epsilon_{\ell'}(0) + \hbar(\omega + \Delta\omega) \quad (I.43)$$

With the help of this relation one can then discuss Raman scattering by treating the electromagnetic field classically.

In the semiclassical theory of Raman scattering, one considers an induced electric transition moment between two states m and ℓ of the system, given by

$$\int (\psi_m^* \vec{M} \psi_\ell + \psi_\ell^* \vec{M} \psi_m) d\tau$$

From Eqs. (I.36) and (I.37) the wave functions can be written explicitly as

$$\begin{aligned} \psi_\ell &= e^{-i\epsilon_\ell(t)/\hbar} \left\{ \psi_\ell(0) + \frac{1}{\hbar} \sum_{\beta} \sum_S \left[\frac{\langle S | M_{\beta} | L \rangle}{\omega_{S\ell} - \omega} \psi_S(0) E_{\beta}^{-} e^{-i\omega t} \right. \right. \\ &\quad \left. \left. + \frac{\langle r | M_{\beta} | \ell \rangle}{\omega_{r\ell} + \omega} \psi_r(0) E_{\beta}^{+} e^{i\omega t} \right] \right\} \\ \psi_m^* &= e^{i\epsilon_m(t)/\hbar} \left\{ \psi_m^*(0) + \frac{1}{\hbar} \sum_{\beta} \sum_S \left[\frac{\langle m | M_{\beta} | S \rangle}{\omega_{sm} - \omega} \psi_S^*(0) E_{\beta}^{+} e^{i\omega t} \right. \right. \\ &\quad \left. \left. + \frac{\langle m | M_{\beta} | S \rangle}{\omega_{sm} + \omega} \psi_S^*(0) E_{\beta}^{-} e^{-i\omega t} \right] \right\} \end{aligned}$$

Neglecting second-order terms, rearranging terms, and noting $\omega_{\ell m} = -\omega_{m\ell}$,

$$\begin{aligned} \int \left\{ \psi_m^* M_{\alpha} \psi_\ell + \psi_\ell^* M_{\alpha} \psi_m \right\} d\tau &= \langle m | M_{\alpha} | \ell \rangle e^{-i\omega_{\ell m} t} + \langle \ell | M_{\alpha} | m \rangle e^{i\omega_{\ell m} t} + \\ &\frac{1}{\hbar} \sum_{\beta} \sum_S \left[\left\{ \frac{\langle m | M_{\beta} | S \rangle \langle S | M_{\beta} | \ell \rangle}{\omega_{sm} - \omega} + \frac{\langle m | M_{\alpha} | S \rangle \langle S | M_{\beta} | \ell \rangle}{\omega_{S\ell} - \omega} \right\} E_{\beta}^{+} e^{i(\omega - \omega_{\ell m})t} \right. \\ &+ \left\{ \frac{\langle \ell | M_{\beta} | S \rangle \langle S | M_{\alpha} | m \rangle}{\omega_{S\ell} + \omega} + \frac{\langle \ell | M_{\alpha} | S \rangle \langle S | M_{\beta} | m \rangle}{\omega_{sm} + \omega} \right\} E_{\beta}^{-} e^{-i(\omega - \omega_{\ell m})t} \\ &+ \left\{ \frac{\langle \ell | M_{\beta} | S \rangle \langle S | M_{\alpha} | m \rangle}{\omega_{S\ell} - \omega} + \frac{\langle \ell | M_{\alpha} | S \rangle \langle S | M_{\beta} | m \rangle}{\omega_{sm} + \omega} \right\} E_{\beta}^{+} e^{i(\omega + \omega_{\ell m})t} \\ &\left. + \left\{ \frac{\langle m | M_{\beta} | S \rangle \langle S | M_{\alpha} | \ell \rangle}{\omega_{sm} + \omega} + \frac{\langle m | M_{\alpha} | S \rangle \langle S | M_{\beta} | \ell \rangle}{\omega_{S\ell} - \omega} \right\} E_{\beta}^{-} e^{-i(\omega - \omega_{\ell m})t} \right] \quad (I.44) \end{aligned}$$

The first two terms on the right-hand side of eq. (I.44) are independent of the electric field. They represent the dipole moment for the transition from the higher to the lower of the two states ℓ and m . The other terms describe transitions $\ell \rightarrow m$ or $m \rightarrow \ell$. From Eq. (I.43) it may be seen that the light scattered associated with the transition $\ell \rightarrow m$ must have the frequency $\omega + \omega_{\ell m}$ and hence must appear with the time factor $\exp[i(\omega + \omega_{\ell m})t]$. Similarly the terms with time dependence $\exp[i(\omega - \omega_{\ell m})t]$ describes scattering associated with the transition $m \rightarrow \ell$. Note that the two groups are transformed into one another on interchange of the indices ℓ and m . Hence we can write the electric moment describing Raman scattering with a transition $\ell \rightarrow m$ as

$$m_{\alpha}(t) = \sum_{\beta} [P_{\alpha\beta}^{\ell m}(\omega)]^* E_{\beta}^{-} e^{-i(\omega + \omega_{\ell m})t} + \sum_{\beta} P_{\alpha\beta}^{\ell m}(\omega) E_{\beta}^{+} e^{+i(\omega + \omega_{\ell m})t}, \quad (I.45)$$

where

$$P_{\alpha\beta}^{\ell m}(\omega) = \frac{1}{\hbar} \sum_S \left\{ \frac{\langle \ell | M_{\alpha} | S \rangle \langle S | M_{\beta} | m \rangle}{\omega_{S\ell} + \omega} + \frac{\langle \ell | M_{\beta} | S \rangle \langle S | M_{\alpha} | m \rangle}{\omega_{S\ell} + \omega} \right\}. \quad (I.46)$$

This is the most general form of the polarizability tensor and is called the transition polarizability from state ℓ to state m . If $m = \ell$, this reduces to the polarizability expression $P_{\alpha\beta}^{\ell\ell}(\omega)$ of (I.40). For $\omega=0$ this reduces to the static polarizability of Eq. (I.31).

Eq. (46) for the polarizability has been derived neglecting the A^2 term in the Hamiltonian. It is interesting to note that if A^2 has been included in the theory, one would have been led to the result [Ref. 12, p. 190]

$$P_{\alpha\beta}^{\ell m}(\omega) = \frac{1}{\hbar} \left[\sum_S \left\{ \frac{\langle \ell | M_{\alpha} | S \rangle \langle S | M_{\beta} | m \rangle}{\omega_{S\ell} + \omega} + \frac{\langle \ell | M_{\beta} | S \rangle \langle S | M_{\alpha} | m \rangle}{\omega_{S\ell} + \omega} \right\} + \delta_{\ell m} \right] \quad (I.47)$$

This implies that in Raman scattering, since $\ell \neq m$, there is no difference

in the final expression (46) for scattering cross section if A^2 is included in the calculation. In Rayleigh scattering, however, $\ell=m$ and this leads to a dependence of the cross-section on the angle Θ between the direction of polarization of the incident and scattered light.

Substituting from (45) into Eq. (4a) for the energy scattered per unit time into a solid angle $d\Omega$ is given by

$$R^2 \bar{S} d\Omega = \frac{(\omega + \omega_{\ell m})^4}{2\pi c^3} \sum_{i=1,2} \sum_{\alpha\beta\gamma\lambda} \hat{e}_\alpha^i \hat{e}_\beta^i [P_{\alpha\gamma}^{\ell m}(\omega)]^* P_{\beta\lambda}^{\ell m}(\omega) E_\gamma^- E_\lambda^+ d\Omega \quad (I.48)$$

and the total Raman scattering from $\ell \rightarrow m$ per unit time is

$$\begin{aligned} \int R^2 \bar{S} d\Omega &= \frac{4(\omega + \omega_{\ell m})^4}{3c^3} \sum_{\alpha} m_{\alpha}^+ m_{\alpha}^- \\ &= \frac{4(\omega + \omega_{\ell m})^4}{3c^3} \sum_{\alpha\gamma\lambda} [P_{\alpha\gamma}^{\ell m}(\omega)]^* P_{\alpha\gamma}^{\ell m}(\omega) E_\gamma^- E_\lambda^+ . \end{aligned} \quad (I.49)$$

If the interest is in the intensity only in one linearly polarized component scattered into a solid angle $d\Omega$ per unit time it is given by eq. (I.48) using the required polarization, \hat{e}_α^k , and omitting the sum over i . This is the quantity usually measured in a Raman experiment where the geometry of the set-up is fixed and a specific polarization of the Raman scattered radiation is chosen using polarization analyzer in the path of the scattered beam.

From Eqs. (I.46) and (I.49), some conclusions may be drawn about the Raman-scattered intensity. Since the frequency of the incident light enters not only in the factor $(\omega + \omega_{\ell m})^4$ but also in the denominators of all terms in the polarizability expression, the dependence of the intensity of the scattered light upon ω will in general be very complicated. However, in most cases the frequency dependence will be determined largely by the fourth power factor, especially if ω is very small compared to $\omega_{\ell m}$. On the other

hand, Placzek [Ref. 14, p. 227] has shown that if ω is very great compared to the frequencies $\omega_{\lambda m}$, the intensity of the Rayleigh scattered light will be independent of ω . The elements of polarizability $P_{\alpha\beta}^{\ell m}(\omega)$ become very small and the Raman scattered intensity approaches zero. Practically however, this would mean we are in the spectral region of hard x-rays and y-rays rather than the region of visible radiation which is the region useful for Raman spectroscopy.

Another feature that is evident from these expressions is the selection rules for the Raman process. The expression for polarizability involves terms of the type $\langle \lambda | M_{\alpha} | s \rangle$ and $\langle s | M_{\beta} | m \rangle$. These are matrix elements of the electric dipole moment involving final or initial states $|\lambda\rangle, |m\rangle$ and intermediate states $|s\rangle$. An intermediate state will contribute to the intensity only if both $\langle \lambda | M_{\alpha} | s \rangle$ and $\langle s | M_{\beta} | m \rangle$ are different from zero. The matrix elements of dipole moments between two states are those involved in absorption or emission of radiation. Thus, only those states which "combine" in absorption or emission with both the initial state λ and the final state m can serve as "intermediate" states in a Raman process. The actual position - in an energy level diagram - of the intermediate state is immaterial. It can lie above both λ and m , between them or even below both λ and m if both are excited states. The term $\langle \lambda | M_{\alpha} | m \rangle$ which determines the probability for infrared emission or absorption between the states $|\lambda\rangle$ and $|m\rangle$ does not enter the Raman intensity expressions. Thus, it is clear that the selection rules for Raman transitions are different from those for radiative transitions. A detailed consideration of selection rules will follow later.

General selection rules, and intensity and polarization relations may be derived from Eqs. (I.46) and (I.49) if the eigenstates $|\lambda\rangle, |s\rangle, |m\rangle$ are

all known. Generally these are not known and approximation methods, as in all problems in physics, must be used. A simplification of the problem due to Placzek makes it possible to derive the most important results with a good degree of accuracy in most cases. According to the adiabatic approximation (Appendix VI), the wave function of a system may be factored as follows:

$$\psi_{nv}(\vec{r}, \vec{R}) = \psi_{nv}(\vec{R}) \phi_n(\vec{r}, \vec{R}), \quad (I.50)$$

where $\phi(\vec{r}, \vec{R})$ is the wave function for the electrons moving in the field of the nuclei, which are held fixed in an arbitrary configuration \vec{R} , and n being the corresponding state label or quantum number. The eigenvalue corresponding to ϕ is $\epsilon_{en}(\vec{R})$ which is a function of \vec{R} . $\psi_{nv}(\vec{R})$ represents a wave function for the nuclei moving in the effective potential due to the electrons.

Consider a system in its lowest electronic level, with the nuclei held fixed in a configuration \vec{R} so that only the electrons move. The permanent electric moment $\vec{M}(\vec{R})$ and polarizability $P_{\alpha\beta}(\omega, \vec{R})$ are functions of \vec{R} . Then,

$$\vec{M}(\vec{R}) = \int \phi_0^*(\vec{r}, \vec{R}) \vec{M}(\vec{r}, \vec{R}) \phi_0(\vec{r}, \vec{R}) d\tau, \quad (I.51)$$

and

$$P_{\alpha\beta}(\omega, \vec{R}) = \frac{1}{\hbar} \sum_{n \neq 0} \left\{ \frac{1}{(\omega_{n0} + \omega)} \phi_0^*(\vec{r}, \vec{R}) M_\alpha(\vec{r}, \vec{R}) \phi_n(\vec{r}, \vec{R}) d\tau \phi_n^*(\vec{r}', \vec{R}) M_\beta(\vec{r}', \vec{R}) \phi_0(\vec{r}', \vec{R}) d\tau' \right. \\ \left. + \frac{1}{(\omega_{n0} - \omega)} \int \phi_0^*(\vec{r}, \vec{R}) M_\beta(\vec{r}, \vec{R}) \phi_n(\vec{r}, \vec{R}) d\tau \int \phi_n^*(\vec{r}', \vec{R}) M_\alpha(\vec{r}', \vec{R}) \phi_0(\vec{r}', \vec{R}) d\tau' \right\}, \quad (I.52)$$

where $\omega_{n0} = \frac{1}{\hbar} [\epsilon_{en}(\vec{R}^0) - \epsilon_{e0}(\vec{R}^0)]$ is the electronic transition frequency between the level n and the ground state.

At ordinary temperatures it is a good approximation to consider the molecular system as practically always in a state belonging to the lowest electronic level. Then one need calculate the polarizability only for states belonging to the lowest electronic level and the transition polarizability from similar initial states. So far the "total state" of the scattering system - that is, as defined by electronic and vibrational quantum numbers - has been considered. If, as is mostly the case one confines attention to scattering due to a change in nuclear motion alone, one need consider only $P_{\alpha\beta}^{vv'}(\omega)$ where v, v' signify vibrational states corresponding to the lowest electronic level.

According to eqn. (46),

$$\begin{aligned}
 P_{\alpha\beta}^{vv'}(\omega) &= \frac{1}{\hbar} \sum_{n''} \sum_{v''} \left\{ \frac{\langle 0v | M_{\alpha} | n''v'' \rangle \langle n''v'' | M_{\beta} | 0v' \rangle}{\omega_{n''v'', 0v'} + \omega} \right. \\
 &\quad \left. + \frac{\langle 0v | M_{\beta} | n''v'' \rangle \langle n''v'' | M_{\alpha} | 0v' \rangle}{\omega_{n''v'', 0v'} - \omega} \right\} \quad (I.53) \\
 &= \frac{1}{\hbar} \sum_{v''} \left\{ \frac{\langle 0v | M_{\alpha} | 0v'' \rangle \langle 0v'' | M_{\beta} | 0v' \rangle}{\omega_{v''v'} + \omega} + \frac{\langle 0v | M_{\beta} | 0v'' \rangle \langle 0v'' | M_{\alpha} | 0v' \rangle}{\omega_{v''v'} - \omega} \right\} \\
 &\quad + \frac{1}{\hbar} \sum_{n'' \neq 0} \left\{ \frac{\sum_{v''} \langle 0v | M_{\alpha} | n''v'' \rangle \langle n''v'' | M_{\beta} | 0v' \rangle}{\omega_{n''0} + \omega} + \frac{\sum_{v''} \langle 0v | M_{\beta} | n''v'' \rangle \langle n''v'' | M_{\alpha} | 0v' \rangle}{\omega_{n''0} - \omega} \right\}
 \end{aligned}$$

In the second equation the summation has been split into two parts corresponding to $n = 0$ and $n \neq 0$, and for the second term the approximation $\omega_{n''v'', 0v'} = \omega_{n''0}$ has been made. This is thus valid as long as the frequency is not close to anyone of frequencies $\{\omega_{n''0}\}$.

In calculating the matrix elements the whole product wave function (I.50) must be considered. But using (I.51), the first sum in (I.53) can be written as

$$\frac{1}{\hbar} \sum_{v''} \left\{ \frac{\langle v | M_{\alpha}(\vec{R}) | v'' \rangle \langle v'' | M_{\beta}(\vec{R}) | v' \rangle}{\omega_{v''v} + \omega} + \frac{\langle v | M_{\beta}(\vec{R}) | v'' \rangle \langle v'' | M_{\alpha}(\vec{R}) | v' \rangle}{\omega_{v''v} - \omega} \right\} \quad (I.54)$$

where the matrix elements are now to be formed between the nuclear states $\chi_{0v}(R)$. Thus, this term describes the behavior of the system as a purely nuclear vibrational system and is known as the ionic part of the polarizability.

The second term is easily shown to be equal to

$$\langle v | P_{\alpha\beta}(\omega, R) | v' \rangle, \quad (I.55)$$

i.e., the matrix element of $P_{\alpha\beta}(\omega, R)$ of Eq. (50) between vibrational wave functions $\psi_{0v}(R)$ and $\psi_{0v'}(R)$. This part is known as the electronic polarizability.

The contribution to the static polarizability ($v'=v, \omega=0$) by the ionic and electronic parts are roughly of equal magnitude in ionic crystals. From (50) and (54) it may be seen this means when $\omega \gg \omega_{vv}$, as is the case of light used for Raman scattering for instance, the ionic part may be omitted when considering the transition polarizability.

Thus it is a good approximation to write

$$P_{\alpha\beta}^{vv}(\omega) = \langle v | P_{\alpha\beta}(\omega, R) | v' \rangle \quad v \neq v'. \quad (I.56)$$

Using this in Eqs. (47) and (48), the angular and total Raman scattering is given by

$$I(\omega) d\Omega = \frac{(\omega + \omega_{vv})^4}{2\pi c^3} \sum_i \sum_{\alpha\beta} \sum_{\gamma\lambda} e_{\alpha}^i e_{\beta}^i \langle v' | P_{\alpha\gamma}^*(\omega, R) | v \rangle \langle v | P_{\beta\lambda}(\omega, R) | v' \rangle E_{\gamma}^- E_{\lambda}^+ d\Omega \quad (I.57)$$

$$I(\omega) = \frac{4(\omega + \omega_{VV'})^4}{3c^3} \sum_{\alpha\gamma\lambda} \langle v' | P_{\alpha\gamma}^*(\omega, R) | v \rangle \langle v | P_{\alpha\lambda}(\omega, R) | v' \rangle E_{\gamma}^{-} E_{\lambda}^{+} . \quad (I.58)$$

To obtain the experimentally observed intensities this expression must be averaged over the thermal distribution for the initial state v .

Adding eqs. (I.51) and (I.52), and putting $v' = v$, the polarizability is given by

$$\begin{aligned} P_{\alpha\beta}(\omega) = & \langle v | P_{\alpha\beta}(\omega, \vec{R}) | v \rangle \\ & + \frac{1}{h} \sum_{v''} \left\{ \frac{\langle v | M_{\alpha}(R) | v'' \rangle \langle v'' | M_{\beta}(R) | v \rangle}{\omega_{v''v} + \omega} \right. \\ & \left. + \frac{\langle v | M_{\beta}(R) | v'' \rangle \langle v'' | M_{\alpha}(R) | v \rangle}{\omega_{v''v} - \omega} \right\} \end{aligned} \quad (I.59)$$

Both electronic and ionic parts are comparable for consideration of refractive properties in the infrared region and cannot be ignored. However, in the infra-red, $\omega \ll \{\omega_{no}\}$ where the $\{\omega_{no}\}$ are the electronic transition frequencies. Hence one can put $\omega \sim 0$ in the electronic part of the polarizability. Furthermore, the displacement of R from the equilibrium value does not affect the electronic polarizability considerably, so that the first term can be written as $P_{\alpha\beta}(0, R^0)$. Note here again that $P_{\alpha\beta}^{VV'}(\omega)$ is Hermitean and to bring in effects of absorption one has to add an anti-Hermitean term.

$$I_{VV'} = \frac{(\omega_0 + \omega_{VV'})^4}{2\pi c^2} \sum_{k=1,2} \sum_{\alpha\beta} \sum_{\gamma\lambda} e_{\alpha}^k e_{\beta}^k i_{\alpha\gamma, \beta\lambda} E_{\gamma}^{-} E_{\lambda}^{+} , \quad (I.60)$$

where

$$i_{\alpha\gamma, \beta\lambda} \equiv \langle \langle v' | P_{\alpha\gamma}^* | v \rangle \langle v | P_{\beta\lambda} | v' \rangle \rangle \text{ average} . \quad (I.61)$$

Eq. (I.61) is the product of the matrix elements averaged over the thermal distribution of the initial quantum number v . The vectors \hat{e}^1 and \hat{e}^2 are mutually perpendicular unit vectors both perpendicular to the direction of scattering.

When the Raman effect of order higher than the first is considered, the frequency spectrum of the scattered radiation is continuous and the final states v' for which $i_{\alpha\gamma,\beta\lambda}$ has a non-vanishing value cover a continuous energy spectrum. Then, it is more convenient to define $i_{\alpha\gamma,\beta\lambda}$ as a function of the frequency

$$I_{\alpha\gamma,\beta\lambda}(\omega) = \sum_{\Delta\omega \rightarrow 0}^{\omega < \omega_0 + \omega_{VV}, < \omega + \Delta\omega} \sum_{v'} \langle v' | P_{\alpha\gamma}^* | v \rangle \langle v | P_{\beta\lambda} | v' \rangle. \quad (I.62)$$

If $\omega_0 \gg \omega_{VV}$, so that $\omega_0 + \omega_{VV} - \omega_0$, then

$$I(\omega)d\omega = \frac{\omega_0^4}{2\pi c^2} \sum_{i=1,2} \sum_{\alpha\gamma} \sum_{\beta\lambda} e_{\alpha}^k e_{\beta}^k i_{\alpha\gamma,\beta\lambda}(\omega) E_{\gamma}^{-} E_{\lambda}^{+} d\omega \quad (I.63)$$

gives the intensity of scattered radiation in the range $(\omega, \omega+d\omega)$.

The expression for $i_{\alpha\gamma,\beta\lambda}(\omega)$ contains the terms leading to Raman effects of first and higher orders. The next step is the expansion of the polarizability as was done in Eqs. (18,19). The first and second-order effects may be described separately. Since the interest here is only on the Raman scattering by phonons, a brief review of lattice dynamics and phonons follows before the implications of Eq. (63) are discussed for crystals. The classical lattice dynamics developed mainly by Born (7), in conjunction with the description of these lattice vibrations in the presence of a classical-non-quantized-electromagnetic field as developed by Huang (15) is the starting point for all the modern literature in Raman Effect as applied to

experiments.

The second quantization formalism in which the field is quantized is still largely of interest mainly in theoretical treatments and in experiments involving the stimulated Raman Effect which is not described at all by this classical picture. The semi-classical theory as presented above has the disadvantage that it does not describe the Raman scattering when the exciting frequency is close to an electronic frequency of the scatterer, that is, when electronic absorption processes become appreciable. The Raman Effect in this case is known as the Resonance Raman Effect. Semi-classical theories of the Resonance Raman Effect has been developed by Shorygin and co-workers [16 a,b] by including a "damping" term in the resonance denominators. The theory of Loudon using the second quantization formalism predicts some interesting properties of Resonance Raman Effect in crystals which do not arise in the semi-classical theory of Shorygin.

I. B. 2. Second Quantization Formalism

A complete description of the Raman Effect is best provided by the occupation number formalism alternatively called the method of second quantization. This formalism is based on an alternative mathematical representation of state functions which is more useful than the conventional Ψ - or wave function representation when dealing with many-body problems. A very readable and interesting account of the formalism is given by Mattuck (17).

The basic state function in the second quantization formalism is the state function $|n_1, n_2, \dots, n_i, \dots\rangle$ describing the number of particles n_i in each single particle state $\phi_i(\vec{r})$ of the many-body system. Such a state function is sufficient to describe the many-body system. Such a state

function is sufficient to describe the many-body system since the essential information is simply how many particles there are in each single particle state - or, the occupation number of the state - since the particles are indistinguishable. The main advantage of the formalism is that it enables one to deal with systems containing a variable number N of particles. This is especially useful in calculations involving intermediate states as in the Raman Effect.

The second valuable feature of the occupation number formalism is the creation and annihilation operators c_i^\dagger and c_i which create and destroy a particle in the state i . The commutation rules of these operators have built into them the symmetry properties (e.g. the Pauli exclusion principle in the case of Fermions) of Fermi and Bose systems. Using the commutation rules, the symmetrization which must be separately handled in the conventional theory, is automatically achieved. These rules are discussed in Chapter 7 of Ref. (17) and are as follows:

$$\text{Fermions:} \quad [c_\ell, c_k^\dagger]_+ \equiv c_\ell c_k^\dagger + c_k^\dagger c_\ell = \delta_{\ell k}$$

$$[c_\ell, c_k]_+ = 0 \quad [c_\ell^\dagger, c_k^\dagger]_+ = 0$$

$$\text{Bosons:} \quad [c_\ell, c_k^\dagger]_- \equiv c_\ell c_k^\dagger - c_k^\dagger c_\ell = \delta_{\ell k}$$

$$[c_\ell, c_k]_- = 0$$

$$[c_\ell^\dagger, c_k^\dagger]_- = 0$$

References (17) and (18) serve as good introduction to the techniques of second quantization. This technique will be used in discussing Raman scattering in crystals, both perfect and imperfect.

II. LATTICE DYNAMICS

A. Lattice Dynamics of a Perfect Crystal

The atoms in a crystalline solid execute small oscillations about their equilibrium positions at every temperature. At absolute zero, this is a result of the zero-point motion, and at finite temperatures a result of thermal fluctuations. In the absence of a detailed knowledge of inter-atomic forces in the solids, the problem of these oscillations is approached by expanding the potential energy of the crystal in powers of the amplitudes of these small oscillations. The hypothesis that such a potential energy for the ions exists stems from a separation of electronic and nuclear motion according to the Born-Oppenheimer adiabatic approximation (Appendix VI). In the expansion of the potential energy all terms past those quadratic in the amplitudes are neglected. This - the harmonic approximation - is the basis of almost all work in lattice dynamics. In the problems considered in the present work, the harmonic approximation is always implied.

The influence of these lattice vibrations on the thermodynamic properties of solids - especially the heat capacity - and the relation between the macroscopic elastic properties of the crystal and the atomic force constants, and similar problems have been extensively studied experimentally and theoretically. Experimental studies concentrated on the bulk properties because these were easier to measure. Earlier theoretical work on lattice dynamics very often tended to calculate thermodynamic functions, which are averaged properties, rather than the detailed frequency spectrum of the lattice. The reason for this is that singularities in the frequency spectrum are averaged out in these calculations and perturbation procedures are thus effective.

A better understanding of these singularities and the refinement of Raman instrumentation has, in recent years, made Raman spectroscopy an important method of studying the frequency spectrum and opened up a new possibility - that of studying defects in crystals. These are the aspects that will be described in detail here.

II. A. 1. The Harmonic Approximation

The theory of the ideal lattice in the harmonic approximation and the basic features of lattice dynamics will now be outlined. Ziman (19) describes both the necessary mathematical background and the theory in Chapters 1 and 2. One important theorem of Solid State Physics that is worth recalling at this stage is Bloch's Theorem [Ref. 19, p. 15] which states: "For any state function that satisfies the dynamical equation in a lattice, there exists a vector \vec{k} of the reciprocal space such that the translation by a lattice vector \vec{x} is equivalent to multiplying by the phase factor $e^{i\vec{k}\cdot\vec{x}}$. Alternatively, one can state this as follows: Translational symmetry of the crystal requires that any state function ψ of the crystal must have the form $\psi_{\vec{k}}(\vec{r}) = e^{i\vec{k}\cdot\vec{r}} U_{\vec{k}}(\vec{r})$, where $U_{\vec{k}}(\vec{r}, \vec{x}) = U_{\vec{k}}(\vec{r})$, i.e., $U_{\vec{k}}(\vec{r})$ is periodic with the periodicity of the lattice. The 'state function' here refers to the description of the state of electrons, or lattice vibrations or any other collective motion in the crystal.

All that the Bloch's theorem guarantees is that for any state function ψ there exists a vector \vec{k} . The actual values that \vec{k} can assume will be determined by the boundary conditions imposed on the problem. Most calculations do not depend critically on the choice of the boundary conditions. The most accepted boundary conditions are the Born-von Karman (or cyclic) boundary

conditions. In this scheme a crystal is considered to be infinite in extent so that surfaces, which would be imperfections, are avoided. The infinite crystal is subdivided into "macrocrystals" of $L_1 \times L_2 \times L_3 = N$ unit cells. A "macrocrystal" or "Super-cell" is thus a parallelepiped with edges $L_1 \vec{a}_1$, $L_2 \vec{a}_2$, and $L_3 \vec{a}_3$, where \vec{a}_1 , \vec{a}_2 , \vec{a}_3 are the basic lattice vectors. The cyclic boundary condition then postulates that the displacement of the k^{th} atom in the first unit cell of the macrocrystal is equal to that of the k^{th} atom in the L_1^{th} unit cell along \vec{a}_1 , L_2^{th} along \vec{a}_2 and L_3^{th} along \vec{a}_3 . This boundary condition is purely a mathematical fiction. It does not affect the results of any bulk properties of the crystal, while it simplifies the derivation of all the results in the theory of lattice dynamics that do not explicitly depend on the crystal surface. It provides a convenient way of normalizing the potential energy and kinetic energy of a crystal to a finite volume. These boundary conditions are of special relevance here because they were, for a long time, a subject of serious controversy especially in interpreting second-order Raman spectra (20), (21).

Consider a crystal composed of an infinite number of unit cells, each of which is a parallelepiped bounded by 3 non-coplanar vectors - or primitive translations, \vec{a}_1 , \vec{a}_2 and \vec{a}_3 . Each unit cell has S atoms. The ℓ^{th} unit cell is then located with reference to an arbitrary origin chosen at a lattice point by

$$\vec{r}(\ell) = \ell_1 \vec{a}_1 + \ell_2 \vec{a}_2 + \ell_3 \vec{a}_3 \quad \text{where } \ell_1, \ell_2, \ell_3 \text{ are integers.}$$

The locations of the S atoms in the unit cell are given by the vectors $\vec{r}(\mu)$ where μ distinguishes the different atoms in the unit cell so that $\mu = 0, 1, \dots, S-1$.

S-1. For convenience, choose the origin such that $\vec{r}(\mu=0) = 0$. The

position of the μ^{th} atom in the ℓ^{th} unit cell is then

$$\vec{r}_{\mu}^{(\ell)} = \vec{r}(\ell) + \vec{r}(\mu)$$

If the displacement of each atom from equilibrium position as a result of thermal fluctuation is $\vec{U}_{\mu}^{(\ell)}$, the total kinetic energy of the lattice is

$$T = \frac{1}{2} \sum_{\ell, \mu, \alpha} M_{\mu} \dot{U}_{\alpha}^{(\ell)2} \quad \dots \quad \alpha = 1, 2, 3. \quad (\text{II.1})$$

where α indicates the coordinate directions (xyz) and M_{μ} is the mass of the μ^{th} atom.

The adiabatic approximation ensures that a potential energy ϕ that is a function of the instantaneous position of all atoms can be defined. Then ϕ can be expanded in a Taylor series in powers of atomic displacements $\vec{U}_{\mu}^{(\ell)}$ from the equilibrium positions [Ref. 10, Chap. 10],

$$\phi = \phi_0 + \sum_{\ell, \mu, \alpha} \phi_{\alpha}^{(\ell)} U_{\alpha}^{(\ell)} + \frac{1}{2} \sum_{\ell, \mu, \alpha} \sum_{\ell', \mu', \alpha'} \phi_{\alpha\beta}^{(\ell, \ell'; \mu, \mu')} U_{\alpha}^{(\ell)} U_{\beta}^{(\ell')} + \text{higher order terms}, \quad (\text{II.2})$$

$\phi_0 \equiv$ static or equilibrium potential energy

$$\phi_{\alpha}^{(\ell)} = \left. \frac{\partial \phi}{\partial U_{\alpha}^{(\ell)}} \right|_0 \quad \text{is the first derivation of the potential energy evaluated in the equilibrium configuration.}$$

$$\phi_{\alpha\beta}^{(\ell, \ell'; \mu, \mu')} \equiv \left. \frac{\partial^2 \phi}{\partial U_{\alpha}^{(\ell)} \partial U_{\beta}^{(\ell')}} \right|_0$$

The static potential energy, ϕ_0 , is a constant term any may be put equal to zero by shifting the arbitrary zero of potential. The first derivative $\phi_{\alpha}^{(\ell)}$ represents the α^{th} component of the force on the μ^{th} atom in the ℓ^{th}

unit cell and must be zero in the equilibrium configuration.

This leads to a classical Hamiltonian

$$H = T + \phi = \frac{1}{2} \sum_{\ell \mu \alpha} M_{\mu} \dot{U}_{\alpha}^{(\ell)}{}^2 + \frac{1}{2} \sum_{\substack{\ell \mu \alpha \\ \ell' \mu' \beta}} \Phi_{\alpha \beta}^{(\ell \ell' \mu \mu')} U_{\alpha}^{(\ell)} U_{\beta}^{(\ell')} . \quad (\text{II.3})$$

The equations of motion of the lattice are then

$$M_{\mu} \ddot{U}_{\alpha}^{(\ell)} = \frac{-\partial \phi}{\partial U_{\alpha}^{(\ell)}} = - \sum_{\ell' \mu' \beta} \Phi_{\alpha \beta}^{(\ell \ell' \mu \mu')} U_{\beta}^{(\ell')} . \quad (\text{II.4})$$

The coefficients $\Phi_{\alpha \beta}^{(\ell \ell' \mu \mu')}$ form the components of a Cartesian tensor and so one can write the above equation in vector form as

$$M_{\mu} \ddot{\vec{U}}^{(\ell)} = - \sum_{\ell' \mu'} \Phi^{(\ell \ell' \mu \mu')} \vec{U}^{(\ell')} . \quad (\text{II.5})$$

This equation may be interpreted as follows: each term in the sum on the right is the force acting as the μ^{th} atom in the ℓ^{th} unit cell due to the displacement $\vec{U}^{(\ell')}$ of the μ'^{th} atom in the ℓ'^{th} unit cell. Thus the Φ 's are the force constants or coupling parameters.

Before discussing the solutions, consider some of the properties of the force constants. From the definition, the following properties are easily derived: (22)

a) The force constants are symmetric in their arguments

$$\Phi_{\alpha \beta}^{(\ell \ell' \mu \mu')} = \Phi_{\beta \alpha}^{(\ell' \ell \mu' \mu)} . \quad (\text{II.6})$$

b) The invariance of the force on an atom under a rigid body translation of the crystal leads to the condition

$$\sum_{\ell' \mu'} \Phi_{\alpha \beta}^{(\ell \ell' \mu \mu')} = 0 . \quad (\text{II.7})$$

c) The periodicity of the lattice requires

$$\Phi_{\alpha\beta}(\mu, \mu') = \Phi_{\alpha\beta}(\mu, \mu') = \Phi_{\alpha\beta}(\mu, \mu') \quad (\text{II.8a})$$

and

$$\Phi_{\alpha}(\mu) = \Phi_{\alpha}(\mu) \quad (\text{II.8b})$$

d) Consider an operation $[S|\vec{t}]$ of the space group of the crystal (23). S represents a proper or improper rotation about some axis and \vec{t} represents a translation of the point. $[S|\vec{t}]$ represents such a rotation followed by a translation so as to leave the crystal invariant. The effect of such an operation on an atomic position vector $\vec{r}(\mu)$

$$\begin{aligned} [S|\vec{t}] \vec{r}(\mu) &= S\vec{r}(\mu) + \vec{t} \\ &= \vec{r}(\mu'), \end{aligned}$$

where the second equation expresses explicitly that under the operation the lattice site (μ) must be taken into equivalent site (μ') . Invariance of the potential energy under such an operation leads to the law of transformation of the atomic force constants under a space group operation (24), viz.,

$$\Phi_{\alpha_1\alpha_2} \begin{bmatrix} \mu_1 & \mu_2 \\ \mu_1' & \mu_2' \end{bmatrix} = \sum_{\beta_1\beta_2} S_{\alpha_1\beta_1} S_{\alpha_2\beta_2} \Phi_{\beta_1\beta_2} \begin{bmatrix} \mu_1 & \mu_2 \\ \mu_1 & \mu_2 \end{bmatrix}, \quad (\text{II.8c})$$

where $S_{\alpha\beta}$ are the elements of the 3x3 matrix representation of the orthogonal transformation describing the operation S .

Thus, apart from a possible interchange of sublattices, the force constants $\{\Phi_{\alpha\beta}(\mu, \mu')\}$ transform as the components of a second-rank tensor.

All the above relations except (c) depend only on the existence of a potential energy and holds for perfect and imperfect lattices. Eq. (II.8c)

assumes perfect periodicity or translational symmetry of the crystal. This must thus break down in the presence of a defect in the crystal.

Since the force tensor $\Phi_{\alpha\beta}(\mu, \mu')$ depends only on the difference, one can with $h = \ell' - \ell$ write the equation of motion as

$$M_{\mu} \ddot{U}_{\mu}(\ell) = - \sum_{\ell'} \Phi_{\alpha\beta}(\mu, \mu') U_{\beta}(\ell')$$

in a manifestly translationally invariant form.

The equations of motion (II.9) form an infinite set of simultaneous linear differential equations. Bloch's theorem (18) ensures the existence of a solution with a wave vector \vec{q} of the form

$$U_{\alpha}(\ell) = \frac{1}{\sqrt{M_{\mu}}} U_{\alpha}^{(0)} \exp(-i\omega t + 2\pi i \vec{q} \cdot \vec{r}(\ell)), \quad (\text{II.10})$$

where \vec{q} is the wave vector of the wave propagating through the lattice. The symbol \vec{q} rather than \vec{k} is used for the wave vector here in accordance with the convention in solid state physics to distinguish the lattice vibration vector from that of an electron or photon. Substituting Eq. (II.10) in (II.9) and writing

$$\frac{1}{\sqrt{M_{\mu} M_{\mu'}}} \sum_{\ell} \Phi_{\alpha\beta}(\mu, \mu') \exp(-2\pi i \vec{q} \cdot \vec{r}(\ell)) \equiv D_{\alpha\beta}(\mu, \mu', \vec{q}) \quad (\text{II.11})$$

the dynamical equation reduces to

$$\sum_{\mu', \beta} D_{\alpha\beta}(\mu, \mu', \vec{q}) U_{\beta}(\mu') = \omega^2(\vec{q}) U_{\alpha}(\mu), \quad (\text{II.12})$$

that is,

$$\sum_{\mu', \beta} D_{\alpha\beta}(\mu, \mu', \vec{q}) U_{\beta}(\mu') - \omega^2 \delta_{\alpha\beta} \delta_{\mu\mu'} U_{\beta}(\mu') = 0. \quad (\text{II.13})$$

The set of equations contained in the above are eigenvalue equations whose solutions can be found by finding the roots of the equation

$$\text{Det } D_{\alpha\beta}(\vec{q}_{\mu\mu'}) U_{\beta}(\mu') - \omega^2 \delta_{\alpha\beta} \delta_{\mu\mu'} = 0. \quad (\text{II.14})$$

Thus the problem is reduced to finding the $3s$ modes of vibration of the n atoms in a unit cell. This reduction has been possible because of the structural identity of the unit cells. The equation (II.14) is of degree $3n$ in ω^2 and $3n$ solutions are obtained for each q . These solutions are denoted by $\omega_j^2(\vec{q})$, where $j = 1, 2, \dots, 3s$. It can be shown (18) that the $3n \times 3n$ matrix of the force tensor is Hermitian and hence the $\omega_j^2(\vec{q})$ have real values. This implies that $\omega_j^2(\vec{q})$ is real or pure imaginary. Since pure imaginary solutions imply exponential decay or growth in time, stability of the lattice requires that one choose $\omega_j^2(\vec{q}) > 0$, that is, the principal minors of $D_{\alpha\beta}(\vec{q}_{\mu\mu'})$ must be positive. This in turn implies additional restrictions on the force constants.

The matrix $D_{\alpha\beta}(\vec{q}_{\mu\mu'})$ is called the dynamical matrix of the crystal. For each $\omega_j(\vec{q})$, there exists an eigenvector $\hat{e}(\mu | \vec{q}_j)$ of D whose components are solutions of the dynamical equation which then becomes

$$\sum_{\mu\beta} D_{\alpha\beta}(\vec{q}_{\mu\mu'}) e_{\beta}(\mu' | \vec{q}_j) = \omega_j^2(\vec{q}) e_{\alpha}(\mu | \vec{q}_j). \quad (\text{II.15})$$

The eigenvectors are orthonormalized, so that

$$\sum_{\mu\alpha} e_{\alpha}^*(\mu | \vec{q}_j) e_{\alpha}(\mu | \vec{q}_j) = \delta_{jj'}, \quad (\text{II.16})$$

$$\sum_j e_{\beta}^*(\mu' | \vec{q}_j) e_{\alpha}(\mu | \vec{q}_j) = \delta_{\alpha\beta} \delta_{\mu\mu'}. \quad (\text{II.17})$$

The properties of the dynamical matrix and its eigenvectors and eigenvalues that are worth noting are:

- a. The eigenvalues $\omega_j^2(\vec{q})$ are positive and symmetric in q .

$$\omega_j^2(q) = \omega_j^2(-q)$$

- b. The elements $D_{\alpha\beta}$ are real only in the special case in which each atom is a center of symmetry. In most cases, $D_{\alpha\beta}$ is complex.

It is always Hermitean.

- c. The eigenvectors $e_\alpha (\vec{q} \mu | \vec{q}_j)$ are usually complex. Physically, this only means that the most general type of wave described by the e_α are elliptically polarized. Real e_α would correspond to the case of plane polarized elastic waves (24).

- d. The $D_{\alpha\beta}(\vec{q})$ are continuous functions of \vec{q} .

Instead of involving the Bloch Theorem at the outset one could have proceeded according to the 'normal mode' technique commonly used in molecular spectroscopy [10], [3]. That is, recognizing that the kinetic and potential energies T and V of the problem is quadratic one can find a transformation which simultaneously diagonalizes the kinetic and potential energy matrices. The coordinates in which this diagonalization is achieved are called the normal coordinates. These coordinates $Q(\vec{q}_j)$ are given by

$$Q(\vec{q}_j) = \frac{1}{\sqrt{N}} \sum_{\mu} e_\alpha (\mu | \vec{q}_j) U_\alpha (\mu) e^{-2\pi i \vec{q} \cdot \vec{r}(\mu)} \quad (\text{II.18})$$

$$= \frac{1}{\sqrt{N}} \sum_{\mu} e (\mu | \vec{q}_j) \cdot \vec{U} (\mu) e^{-2\pi i \vec{q} \cdot \vec{r}(\mu)}. \quad (\text{II.19})$$

In terms of the normal coordinates, the Hamiltonian for the lattice becomes

$$H = \frac{1}{2} \sum_{\vec{q}, j} \dot{Q}^* (\vec{q}_j) \dot{Q} (\vec{q}_j) + \omega_j^2(q) Q^* (\vec{q}_j) Q (\vec{q}_j) \quad (\text{II.20})$$

and the equations of motion of the coordinate, obtained by substituting for $U_\alpha(\vec{r}_\mu)$ in terms of the normal coordinates in the dynamical equation, is

$$Q(\vec{q}_j) + \omega_j^2(\vec{q}) Q(\vec{q}_j) = 0. \quad (\text{II.21})$$

Each normal coordinate therefore is a simple periodic function involving only one of the frequencies $\omega_j(\vec{q})$, that is, each normal mode describes an independent mode of vibration of the crystal with only one frequency. Every atom in each mode vibrates with the same frequency and with the same phase, and there are as many normal modes ($3sN$) as there are number of degrees of freedom of the crystal. The general motion of the crystal as a whole is a superposition of the normal mode motions each weighted by the coefficients $e_\alpha(\mu | \vec{q}_j) \exp(2\pi i \vec{q} \cdot \vec{r}(\mu))$, i.e., by the appropriate polarisation and phase factors.

The relation expressed by the equations

$$\omega_j = \omega_j(\vec{q}) \quad j = 1, 2, \dots, 3s. \quad (\text{II.22})$$

is called the DISPERSION RELATION for the lattice. A closed expression for the function $\omega_j(\vec{q})$ can be obtained only for special simple models of the crystal. For a given \vec{q} , the $3s$ functions ω_j are called "the branches j of the dispersion curve".

Of the $3s$ solutions, for each \vec{q} , it can be shown that [22] three and only three go to zero as \vec{q} goes to zero. The corresponding modes are called acoustic modes. On close examination (12,18) it may be shown that for

these modes the characteristic condition is

$$\frac{\vec{e}(\mu | 0_j)}{\sqrt{M_\mu}} = \frac{\vec{e}(\mu' | 0_j)}{\sqrt{M_{\mu'}}} = \vec{U}(\mu | 0_j) = \vec{U}(\mu' | 0_j).$$

That is, all s particles in each unit cell move parallel and with equal amplitudes, as is characteristic of the displacements in an elastic continuum upon which a sound wave is impressed. This analogy is responsible for the name of these modes.

The remaining (3s-3) modes whose frequencies do not vanish at $\vec{q} = 0$ are called optical modes. This nomenclature arises from the following fact: In an ionic lattice of the NaCl type the two ions in each unit cell are out of phase with each other by 180° in these modes at $\vec{q} = 0$. Their center-of-mass remains fixed. Since the two ions are of opposite sign, a net fluctuating dipole moment for the crystal is introduced by these modes of vibration. This dipole moment can interact with an external electromagnetic field and give rise to optical phenomena. The name is misleading because, both acoustic and optical modes are capable of interacting with electromagnetic radiation, though, as will be seen, the first-order interactions of a crystal with radiation of optical wavelengths are predominantly by means of the optical modes. Also, an optical mode need not always possess a dipole moment, e.g., in homopolar crystals.

The three acoustic modes and 3s-3 optical modes differ from each other in the nature of their polarization. In general, a constant frequency surface of a crystal, drawn in q -space [19] can be quite complicated. It is customary to classify the modes formally into longitudinal and transverse acoustic and optical modes, though the actual polarization vector in an

anisotropic crystal can be very complicated and bears no simple parallel or perpendicular type of relationship to the \vec{q} vector.

Before discussing the nature of the dispersion relations, consider the quantum-mechanical treatment of the problem. It is more convenient to express the complex normal coordinates $\{Q(\vec{q}_j)\}$ in terms of real coordinates q 's (distinguished from the wave vector \vec{q}) as defined by

$$Q(\vec{q}_j) = \frac{1}{\sqrt{2}} \left\{ q_1(\vec{q}_j) + i q_2(\vec{q}_j) \right\} \quad (\text{II.23})$$

where the $q(\vec{q}_j)$ are real.

The Hamiltonian can then be written as

$$H = \frac{1}{2} \sum_{q>0} \sum_j \sum_{\lambda=1,2} \left[\dot{q}_\lambda^2(\vec{q}_j) + \omega_j^2(\vec{q}) q_\lambda^2(\vec{q}_j) \right] . \quad (\text{II.24})$$

With the equivalence

$$\dot{q}(\vec{q}_j) \equiv p(\vec{q}_j) \Rightarrow -i\hbar \frac{\partial}{\partial q(\vec{q}_j)} \quad (\text{II.25})$$

the Schrodinger equation for the vibrating crystal is

$$\frac{1}{2} \sum_{\vec{q},j} \left\{ -\hbar^2 \frac{\partial^2}{\partial q^2(\vec{q}_j)} + \omega_j^2(\vec{q}) q^2(\vec{q}_j) \right\} \Psi = E\Psi \quad (\text{II.26})$$

The total wave function Ψ describing the vibrational states of the crystal can be written as a simple product of "single particle" wave functions, i.e.,

$$\Psi = \prod_{q,j} \left\{ \psi_{n_j}(\vec{q}) [q(\vec{q}_j)] \right\} ,$$

where $n_j(\vec{q})$ describes the state of the "oscillator" (\vec{q}_j) . Each $\psi_{n_j}(\vec{q})$ satisfies an equation of the harmonic oscillator type, viz.,

$$\left\{ \frac{-\hbar^2}{2} \frac{\partial^2}{\partial \rho^2(\vec{q})} + \frac{1}{2} \omega_j^2(\vec{q}) \rho^2(\vec{q}) \right\} \psi_{n_j}(\vec{q}) = E_{n_j}(\vec{q}) \psi_{n_j}(\vec{q}) \quad (\text{II.27})$$

whose solutions are

$$\psi_n(\rho) = \left\{ \frac{\alpha}{\sqrt{\pi} 2^n n!} \right\}^{1/2} \exp\left(-\frac{1}{2} \alpha^2 \rho^2\right) H_n(\alpha \rho), \quad (\text{II.28})$$

where $\alpha_j^2(\vec{q}) = \frac{\omega_j(\vec{q})}{\hbar}$ and $H_n(x)$ is the n^{th} Hermite polynomial. The associated energy levels are

$$E_{n_j}(\vec{q}) = \left(n_j(\vec{q}) + \frac{1}{2}\right) \omega_j(\vec{q}) \quad , \quad n_j(q) = 0, 1, 2, \dots (\text{II.29})$$

The total energy of the crystal is then

$$E = \sum_q \sum_{n_j} E_{n_j}(\vec{q}) \quad . \quad (\text{II.30})$$

Instead of regarding a lattice vibration of wavenumber $|\vec{q}|$ as one fictitious harmonic oscillator having quantized energy $E_{n_j}(\vec{q})$, the lattice vibration may be regarded as a set of quanta each having energy $\omega_j(\vec{q})$ together with a ground state of energy $\frac{1}{2} \omega_j(\vec{q})$. These quanta are called phonons, in analogy to photons. They behave very much like particles in a quantum mechanical sense. [16]. Phonons, as a long-range collective property of the ions of the crystal interacting through an electron gas, have been discussed extensively by Pines. [26].

The problem of the monatomic and diatomic linear lattice is discussed in detail by Kittel [11] and Ziman [16]. The important results are discussed below.

For a monatomic linear lattice, with only nearest neighbour interaction by central forces of strength $\phi_{\alpha\beta}(\ell, \ell+1) = \alpha$, the dispersion relation is

$$\omega(a) = 2\pi\sqrt{\frac{\alpha}{M}} \sin\left(\frac{qa}{2}\right), \quad (\text{II.31})$$

where M is the mass of the atoms and a is the nearest-neighbour distance.

For a diatomic linear chain, the corresponding dispersion relations are

$$\omega_{\pm}^2 = 4\pi^2\alpha \left[\left(\frac{1}{M_1} + \frac{1}{M_2} \right) \pm \sqrt{\left\{ \left(\frac{1}{M_1} + \frac{1}{M_2} \right)^2 - \frac{4 \sin^2 qa}{M_1 M_2} \right\}} \right], \quad (\text{II.32})$$

the plus sign indicating the optical and the minus sign the acoustic branch.

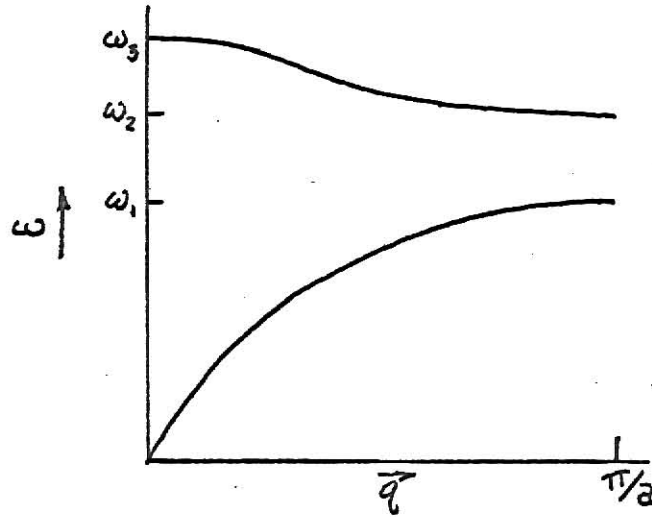


Fig. 1. Dispersion curve for diatomic lattice

The dispersion curve for the diatomic lattice is shown in the figure 1. This figure illustrates the following features.

- a. One sees that ω is always a periodic function of q with a period $\frac{2\pi}{a}$, where a is the lattice spacing. Thus all one needs to consider is a region $-\frac{\pi}{a} \leq q \leq \frac{\pi}{a}$ of the q -space. This region is called the Brillouin zone.

Any value of q outside the Brillouin zone simply repeats precisely the same motion. This is just a restatement of Bloch's Theorem.

The significance of \vec{q} may be observed easily. The cyclic boundary conditions for a 3-dimensional macrocrystal of dimensions $L_1\vec{a}_1, L_2\vec{a}_2, L_3\vec{a}_3$ in the 3 lattice directions are:

$$\psi(\vec{r}) = \psi(\vec{r} + L_1\vec{a}_1) = \psi(\vec{r} + L_2\vec{a}_2) = \psi(\vec{r} + L_3\vec{a}_3) \quad (\text{II.33})$$

for any state function ψ , of the crystal. For a Bloch state of wave vector \vec{q} this implies

$$e^{i\vec{q} \cdot L_1\vec{a}_1} = e^{i\vec{q} \cdot L_2\vec{a}_2} = e^{i\vec{q} \cdot L_3\vec{a}_3} = 1, \quad (\text{II.34})$$

which in turn means that \vec{q} is of the form

$$\begin{aligned} \vec{q} &= q_1\vec{b}_1 + q_2\vec{b}_2 + q_3\vec{b}_3, \\ &= \frac{2\pi m_1}{L_1} \vec{b}_1 + \frac{2\pi m_2}{L_2} \vec{b}_2 + \frac{2\pi m_3}{L_3} \vec{b}_3. \end{aligned} \quad (\text{II.35})$$

Thus, \vec{q} is a vector in the reciprocal lattice and there are $L_1 \times L_2 \times L_3 = N$ allowed values of \vec{q} in one reciprocal cell i.e., in one Brillouin zone.

This result can be stated as: There are as many allowed wave vectors in a Brillouin zone as there are unit cells in the block of crystal. As one Brillouin zone is typically of dimensions 1\AA^{-1} , while $N \sim 10^{24}$ in 1 cm^3 of a crystal, the values of q for lattice vibrations are very closely spaced and form a quasi-continuum.

b. For small (aq), i.e., wavelengths large compared to the lattice constant, ω is proportional to q for the acoustic vibrations. The chain of atoms behaves like a heavy elastic string. This also implies that in this region the wave velocity $\frac{\partial \omega}{\partial q}$ is a constant and there is no dispersion of the

wave in the lattice while at higher q , $\frac{d\omega}{dq}$ is a function of q . From the nature of the optical branch one sees that very often in a first crude approximation, the optical branch can be represented by a horizontal straight line, ignoring dispersion effects.

c. Energy gap: All dispersion curves show a cut-off frequency [for instance, ω_3 in Fig. (1)]. There are no normal modes of the lattice corresponding to frequencies above this value. Physically, this is to be expected as, the massive ions of the lattice cannot vibrate above a certain frequency determined by the force constants and the masses of the ions. There can also be a frequency "gap" between the upper limit (ω_1) of the acoustic branch and lower limit (ω_2) of the optical branch in which there are no normal mode frequencies. Conversely, if one tries to propagate waves of frequency in the region of the gap or above cut-off, these waves are rapidly damped in space on moving through the crystal. The detailed analytic picture of this phenomenon is discussed beautifully by Brillouin [27]. In a real crystal inequivalent directions have different dispersion curves. Here it may not possess a general frequency gap as the gaps for different directions may be different. A maximum cut-off value can always be found.

II. A. 2 The Frequency Distribution Function

Another function of the lattice vibrations that play an important role in interpreting Raman spectra is the frequency distribution function $g(\omega)d\omega$ [also called the "lattice spectrum"] defined as the number of allowed frequencies in the range $(\omega, \omega+d\omega)$. This function has a direct effect on the cross-section of phonon processes. The complexity and anisotropy of the dispersion curves makes it difficult to obtain analytic expressions for $g(\omega)$ even in the simplest cases (18) and one has to use simplified models or resort

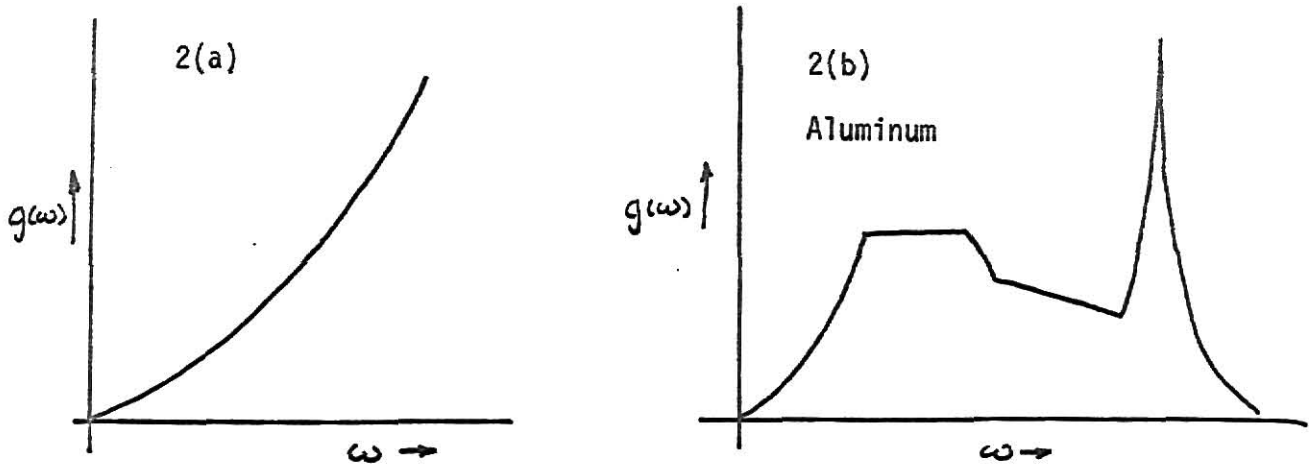
to piecing together experimentally obtained information to construct the function. The Debye spectrum [16, p 43], defined by

$$g(\omega) d\omega = 3sN \frac{3\omega^2}{\omega_D^3} d\omega \quad 0 < \omega < \omega_D \quad (\text{II.35})$$

$$= 0 \quad \omega > \omega_D \quad (\text{II.36})$$

formed the basis of most calculations until very recently. It is a crude approximation to the frequency distribution in the acoustic modes of primitive lattices.

The figure 2(a) shows a Debye spectrum and 2(b) a true lattice spectrum.



Though, formally, a solution of Eq. (II.22) should yield $g(\omega)$, it is usually obtained by solving the equation numerically for a closely spaced net of values of \vec{q} and finding how many values of ω_q fall into each range of \vec{q} . This analysis, is aided by a theorem due to Van Hove [28][22] and its extension due to Phillips [29]. Van Hove's work develops a general property of frequency distribution functions from group-theoretical and topological considerations. The theorem enables all the slope discontinuities which occur in the density-of-states function to be located and to be decided.

This approach of mapping the density of states is called critical point analysis and is of importance in interpreting second-order Raman spectra.

The main result of Van Hove's work was to show that the distribution function for a three-dimensional crystal always has a minimum number of critical points. A critical point is a point at which there is an analytic singularity in the frequency distribution $g(\omega)$ of a crystal. Van Hove's theorem was derived from the observation that the saddle points of the dispersion relation $\omega(q)$ (i.e., points where $g_{\text{rad } q} \omega = 0$) produce singularities in $g(\omega)$ [27], together with Morse's theorem [31] according to which the periodicity of the crystal implies the existence of a minimum number of saddle points for ω .

If all critical points could be located, an interpolation scheme might give a good approximation to $g(\omega)$. Phillips has shown that by analyzing the matrix elements of $\nabla_q \omega^2$ by group theory one can find all the critical points that must occur because of symmetry including possible degeneracies. A very good approximation to the frequency spectrum can be obtained using this approach. It is found then that most of the singularities in the phonon spectra occur at points of high symmetry in the Brillouin Zone. The remaining critical points can occur at lines or planes of high symmetry.

II. A. 3. Simplified Interpretations of Lattice Vibrations

a. Raman's theory of lattice vibrations:

Raman [21] formulated a theory of lattice dynamics different from the one discussed here objecting to the Born-von Karman boundary condition. In this theory, the condition that in all normal modes of oscillation of a crystal, the ratio of the corresponding displacements of every pair of

equivalent atoms situated along any one principal axis of the Bravais lattice should be the same, together with the requirement that all displacements in a physically realisable normal mode should be real, leads to the result that there can be at the most only $(24s-3)$ normal modes when pure translations are excluded. These are merely the normal modes of the group consisting of the $8s$ atoms located in a cell, the edges of which are found by choosing twice the primitive translation along each axis. Symmetry can cause degeneracy of the modes.

Raman's analysis, has no physical basis and was rejected. Lately however, it has been shown [32] that a critical point analysis of second-order Raman spectra is equivalent to the "supercell analysis" of Raman. This, however, is only a fortuitous coincidence and though Raman's analysis can be used to pick out modes most prominent in second-order Raman scattering, it has no standing as a theory with a physical basis.

b. Internal and External modes of Oscillation.

The $3s-3$ optical modes are very often classified as internal and external modes. This distinction is not a clear-cut one. It depends on the possibility of a division of the s nonequivalent atoms in the unit cell into p groups such that the forces between one group and the other are comparatively weak, whereas the forces that exist between the members of any one group are quite strong. As a simple example consider a unit cell of a crystal such as NH_4NO_3 . The NH_4^+ ion and NO_3^- ion each forms a strongly bound group while the ionic binding between the two ions is weak in comparison. Thus the oscillations involving a movement of the p groups - two in the present example - relative to each other will exhibit low frequencies in general and are termed "external vibrations". The others, involving the relative movements

of the individual members in each of the groups, will generally exhibit higher frequencies and are called internal vibrations. The internal vibrations of the NO_3^- ion for instance may have nearly the same frequency for different nitrates since it is only slightly affected by the presence of the other ions in the crystal. The frequencies of the internal oscillations of groups of the same type but occupying inequivalent positions in the crystal lattice also may be slightly different. The external modes are classified as rotational and translational depending on whether the relative movements of the groups are of a translatory or rotatory type. In complicated crystals, where a full and detailed analysis is difficult, this classification is of great help.

B. Optical Modes and Electromagnetic Radiation

The optical vibrations of long wavelength are, as will be seen, of special importance in considering the Raman Effect in crystals. In general, an electromagnetic wave interacts only with lattice vibrations of comparable wavevector and will be strongly affected only if its frequency is near that of the lattice vibrations. Lattice vibration frequencies range from 0 to 10^{13} sec^{-1} . Light waves of similar frequency have a wavelength greater than

$$c \times 10^{-13} \sim 0.003 \text{ cm} \gg 10^{-8} \text{ cm},$$

the order of the lattice constant in a typical case. Thus the lattice vibrations which can interact with light in a first-order process are very long waves with practically vanishing wave vector, $|\vec{k}| \sim 10^{-5}$ times the size of the Brillouin zone. The strength of the interaction of course depends on the electric moments associated with the particular lattice vibration.

The optical modes are most often represented by Einstein models or suppressed in macroscopic analyses which are mainly aimed at establishing a theory of elasticity based on lattice vibrations. The acoustic modes are of primary importance in these analyses. There are three important features of optical vibrations of relevance here. Since only one of the standard textbooks contain any discussion of these details [30], it is dealt with at some length here. The features of importance are:

- (1) The $3(s-1)$ optical modes in a crystal with s nonequivalent atoms per primitive cell can be classified approximately into one longitudinal and two transverse branches.
- (2) The limiting frequency ω_ℓ of the longitudinal branch as $\vec{k} \rightarrow 0$ is appreciably higher than the limiting frequency ω_t of the transverse branches. The approximate theoretical relation between these frequencies is the famous Lyddane - Sachs - Teller relation

$$\frac{\omega_t^2}{t} = \frac{\epsilon_0}{\epsilon} \omega_\ell^2 \quad , \quad (\text{II.37})$$

where ϵ_0 is the static dielectric constant and ϵ is the square of the optical refractive index.

- (3) The coupling between electromagnetic radiation (or photons) and lattice vibrations (or phonons) is particularly marked for long wavelength transverse optical phonons, and there results a forbidden frequency gap between ω_t and ω_ℓ in which a thick crystal does not transmit energy. This is equivalent to the statement that the crystal has a strong optical reflection band in the region of the frequency gap between ω_t and ω_ℓ . These points can be shown using classical electromagnetic theory and the theory of lattice vibrations. The

consequent description is a beautiful illustration of the effects of interaction of two systems. It also serves as reminder, especially to a student, of the fact that all theory - usually based on isolated physical systems - consists at best, only of refined approximations. The following discussion is based on an extremely lucid article by K. Huang [15].

Before proceeding to the mathematical details it is advisable to discuss the physics involved in the treatment. Lattice vibrations and their interaction with electromagnetic radiation may be treated using the standard methods of electrostatics rather than the complete set of Maxwell's equations. Such a procedure is equivalent to assuming an unretarded interaction between the charges in the lattice. This treatment yields reasonable results because retardation becomes important only in the case of lattice vibrations of wavelength of the order of $2\pi c/\omega_0 = 10^{-3}$ cm where ω_0 is the approximate limiting optical frequency of the optical branch at $\vec{k} = 0$. A shorter wave will have a phase velocity so small compared with c , the velocity of light, that retardation can be ignored. As these long waves form only a minute fraction of the vibrational modes of the lattice - as is evident from the density of states - the major part of the lattice vibrational spectrum can be calculated without considering the retardation. For vibrations of long wavelength, retardation is important. The theory of Huang is an attempt to obtain macroscopic equations which completely describe this type of lattice behavior in the presence of electromagnetic radiation by treating only the long wavelength (small k) region of lattice vibrations using the complete set of Maxwell's equations. Note also that for these long wavelengths, the crystal essentially behaves as a continuum, that is, dispersive effects are

small and the frequencies of these vibrations are essentially those of the optical mode at $k = 0$. This is also evident from a typical dispersion curve of the optical branch. As an example a diatomic, cubic crystal is considered to avoid phenomena due to optical anisotropy e.g., birefringence. The electrostatic approximation:

To describe the long optical vibrations of an ionic crystal, one needs a parameter specifying relative displacement between positive and negative ions. For an elastic - acoustic - vibration, the effective inertial mass for a unit volume is the density; for the optical type of motion, the corresponding mass is the reduced mass of the positive and negative ions, $\bar{M} = \frac{M_+ M_-}{M_+ + M_-}$, divided by the volume of a unit cell. It has been found that the most convenient parameter to use is the displacement of the positive ions relative to the negative ions multiplied by the square root of this effective mass per unit volume, denoted by \vec{W} . This parameter is easily chosen in the case of ionic crystals. For molecular crystals, however, the optical modes will include also the internal modes of the molecule and the treatment of the problem will be considerably different. Huang defines two phenomenological equations whose interpretation becomes apparent as the theory is developed. These equations are

$$\ddot{\vec{W}} = b_{11} \dot{\vec{W}} + b_{12} \vec{E}, \quad (\text{II.38})$$

$$\ddot{\vec{P}} = b_{21} \dot{\vec{W}} + b_{22} \vec{E}, \quad (\text{II.39})$$

where \vec{P} and \vec{E} are the dielectric polarization and electric field, respectively.

The conditions under which the equations are valid are:

- (a) \vec{W} , \vec{P} and \vec{E} vary negligibly over a unit cell
- (b) \vec{W} , \vec{P} and \vec{E} vary negligibly within time intervals of the order of the

periods of electronic motion (that is, the inverse of electronic transition frequencies.)

(c) Anharmonic forces and non-linear effects are ignored.

Condition (a) is equivalent to the long wavelength approximation and eliminates the necessity of consideration of space derivatives of \vec{W} , \vec{P} and \vec{E} . Condition (b) ensures the validity of the adiabatic approximation. Thus no electronic coordinates appear in the equations (II.38,39) though electronic polarization is necessarily included in \vec{P} . Condition (c) is equivalent to the harmonic approximation; i.e., the assumption of a Hooke-type of law leading to the linearity of the equations. Since optical isotropy is assumed, the coefficients are all scalar quantities.

This leads to two important results which are derived clearly in Ref. [7], p. 82-87.

(i) $b_{12} = b_{21}$. Using this result, the b-coefficients can be expressed in terms of experimentally measurable quantities viz., $b_{11} = \omega_0^2$; $b_{12} = b_{21} = (\epsilon_0 - \epsilon)^{1/2} \omega^2$; $b_{22} = (\epsilon - 1) \omega_0^2$, where ω_0 is the lattice infra-red "dispersion" frequency,

(ii) The lattice equations [39,40] considered in conjunction with the Maxwell's equations for an electrostatic situation in the absence of free charges,

$$\vec{\nabla} \cdot (\vec{E} + 4\pi\vec{P}) = 0 \quad (\text{II.40})$$

$$\text{and} \quad \vec{\nabla} \times \vec{E} = 0 \quad (\text{II.41})$$

yields solutions of two distinct types.

The first type is solenoidal, i.e.,

$$\vec{W} = \vec{W}_t(\vec{r}) e^{-i\omega_t t} \text{ with } \vec{\nabla} \cdot \vec{W}_t = 0 \text{ and } \omega_t^2 = -b_{11} = -\omega_0^2. \quad (\text{II.42})$$

For this type of solution, the electric field \vec{E} vanishes identically, i.e., $\vec{E}_t = 0$.

The second type is irrotational, i.e.,

$$\vec{W} = W(\vec{r})e^{-i\omega_\ell t} \text{ with } \vec{\nabla} \times \vec{W}_\ell = 0 \quad \text{and} \quad \omega_\ell^2 = -b_{11} + \frac{4\pi b_{12}b_{21}}{1+4\pi b_{22}}. \quad (\text{II.43})$$

In this case, the macroscopic field E accompanying the displacement \vec{w}_ℓ is related to the dielectric polarization by

$$\vec{E}_\ell = \frac{-b_{21}}{1+4\pi b_{22}} \vec{W}_\ell = \frac{-(\epsilon_0 - \epsilon_\infty)^{1/2}}{\epsilon_\infty} \vec{W}_\ell. \quad (\text{II.44})$$

Transverse and longitudinal plane waves can then be considered as special cases of the solenoidal and irrotational functions $\vec{W}_t(\vec{r})$ and $\vec{W}_\ell(\vec{r})$ respectively. Any arbitrary lattice vibration of the optical type can be represented as linear superpositions of such plane waves of different wave numbers and directions of propagation. All the transverse waves of long wavelength then vibrate with the frequency ω_t and longitudinal with ω_ℓ . It can be shown rigorously [33]

$$\frac{\omega_\ell}{\omega_t} = \left[\frac{\epsilon_0}{\epsilon_\infty} \right]^{1/2}. \quad (\text{II.45})$$

Thus since $\epsilon_0 > \epsilon_\infty$, the longitudinal vibrations have greater frequency. This is a consequence of the fact that for a transverse vibration \vec{E} vanishes everywhere and the vibrational frequency is solely determined by the local elastic restoring force. In the longitudinal case, there is an electric field term which contributes to the restoring force in addition to the elastic term. In a non-ionic crystal such as diamond the motion is solely determined by elastic forces and the transverse and longitudinal vibrations

thus become degenerate ($\omega_l = \omega_t$) at $k = 0$.

In numerous problems, for instance, if one attempts to build a macroscopic theory of Raman scattering by plasmons, it becomes necessary to consider the case where the charge density - at least locally - is non-zero. Then with $\vec{\nabla} \cdot \vec{D} = \rho$ and following the same procedure as before, one finds the transverse vibrations unaffected by the presence of free charges. Also the local electric field is only dependent on the amplitudes of longitudinal vibrations and is given by

$$\vec{E} = -\omega_l \left[4\pi \left(\frac{1}{\epsilon_\infty} - \frac{1}{\epsilon_0} \right) \right]^{1/2} \vec{W}_l + \frac{1}{\epsilon_\infty} \vec{E}_{\text{vac}}, \quad (\text{II.4})$$

where \vec{E}_{vac} is the coulomb field

$$E_{\text{vac}}(\vec{r}, t) = - \vec{\nabla} \int \frac{\rho(\vec{r}', t)}{|\vec{r} - \vec{r}'|} d\vec{r}'$$

that would be produced in vacuum by the charge density $\rho(\vec{r}', t)$.

Eq. (II.46) gives the local field in a crystal. This is the expression to be used instead of the applied field \vec{E}_{vac} in considering phenomena involving electric fields in a crystal.

Retardation Effect and Modification of Lattice Vibrations in the Presence of an Electromagnetic Field.

Consider first a physical system composed of the crystal and the radiation field. The dynamical equation of this system and its solutions no longer concern lattice vibrations alone. The complete system of equations required are the dynamical equations of the lattice (II.38,39) together with Maxwell's equations. In the absence of the lattice Maxwell's equations alone would lead to light waves in vacuum, which we may consider as vibrational

modes of the radiation field - all modes being transverse, with two modes to each wave number. These two modes correspond to the two possible polarizations for each wave number.

Again if there were no interactions between the lattice and the radiation field, the vibrational modes (for a given wave number) of the combined system would simply be the two pure radiation modes and the three lattice modes (remembering that only optical vibrations of a diatomic lattice are being considered) calculated in the unretarded case. When the two fields interact it is to be expected that these modes would be mixed to a certain extent so that the terms "light wave" and "lattice wave" (or photon and phonon) are no longer unambiguously applicable. However, the total number of modes, which are essentially the number of degrees of freedom of the system, should be the same.

The set of equations to be considered now are, (assuming no free charges or currents)

$$\vec{\nabla} \cdot (\vec{E} + 4\pi\vec{P}) = 0, \quad (\text{II.47})$$

$$\vec{\nabla} \cdot \vec{H} = 0, \quad (\text{II.48})$$

$$\vec{\nabla} \times \vec{E} = -\frac{1}{c} \frac{\partial \vec{H}}{\partial t}, \quad (\text{II.49})$$

$$\vec{\nabla} \times \vec{H} = \frac{1}{c} \frac{\partial}{\partial t} (\vec{E} + 4\pi\vec{P}), \quad (\text{II.50})$$

together with
$$\ddot{\vec{W}} = b_{11} \vec{W} + b_{12} \vec{E}, \quad (\text{II.38})$$

$$\ddot{\vec{P}} = b_{21} \vec{W} + b_{22} \vec{E}. \quad (\text{II.39})$$

When the trial solutions

$$\left. \begin{aligned} \vec{W} &= \vec{W}_0 \\ \vec{P} &= \vec{P}_0 \\ \vec{E} &= \vec{E}_0 \\ \vec{H} &= \vec{H}_0 \end{aligned} \right\} \times e^{i(\vec{k} \cdot \vec{r} - \omega t)} \quad (\text{II.51})$$

are substituted the following are obtained:

$$-\omega^2 \vec{W} = b_{11} \vec{W} + b_{12} \vec{E}, \quad (\text{II.52})$$

$$\vec{P} = b_{12} \vec{W} + b_{22} \vec{E}, \quad (\text{II.53})$$

$$\vec{k} \cdot (\vec{E} + 4\pi \vec{P}) = 0, \quad (\text{II.54})$$

$$\vec{k} \cdot \vec{H} = 0, \quad (\text{II.55})$$

$$\vec{k} \times \vec{E} = \frac{\omega}{c} \vec{H}, \quad \text{and} \quad (\text{II.56})$$

$$\vec{k} \times \vec{H} = -\frac{\omega}{c} (\vec{E} + 4\pi \vec{P}). \quad (\text{II.57})$$

It may be noticed immediately that no solution exists in which $\vec{E} = 0$ since this would lead to the trivial case

$$\vec{E} = \vec{H} = \vec{P} = \vec{W} = 0.$$

$$\therefore \vec{E} \neq 0 \Rightarrow \vec{W} = \frac{b_{12} \vec{E}}{-b_{11} - \omega^2}, \quad \text{and} \quad (\text{II.58})$$

$$\therefore \vec{P} = \frac{b_{12} b_{21}}{-b_{11} - \omega^2} + b_{22} \vec{E}. \quad (\text{II.59})$$

Eq. (II. 8) can now be written using (II.13) as

$$\therefore \vec{k} \cdot \vec{E} \left\{ 1 + 4\pi b_{22} + \frac{4\pi b_{12}b_{21}}{-b_{11}-\omega^2} \right\} = 0. \quad (\text{II.60})$$

This implies two possibilities :

$$(i) \quad 1 + 4\pi b_{22} + \frac{4\pi b_{12}b_{21}}{-b_{11}-\omega^2} = 0, \quad (\text{II.61})$$

$$\vec{E} + 4\pi\vec{P} = 0, \quad (\text{II.62})$$

$$(ii) \quad \vec{k} \cdot \vec{E} = 0, \quad (\text{II.63})$$

$$\vec{E} \perp \vec{k}. \quad (\text{II.64})$$

Case (i). Owing to Eqs. (II.16), (II.11) reduces to

$$\vec{k} \times \vec{H} = 0, \quad \vec{H} = 0 \quad \text{or} \quad \vec{H} \parallel \vec{k}. \quad (\text{II.65})$$

But Eq. (II. 9) implies $\vec{H} = 0$ or $\vec{H} \perp \vec{k}$. These two conditions can be satisfied only if $\vec{H} = 0$. Eq. (II.10) becomes

$$\vec{k} \times \vec{E} = 0, \quad \text{i.e., } \vec{E} \text{ is parallel to } \vec{k}. \quad (\text{II.66})$$

So this case yields

$$\vec{H} \parallel \vec{P} \parallel \vec{E} \parallel \vec{k}. \quad (\text{II.67})$$

The frequency is given in this case by

$$\omega^2 = -b_{11} + \frac{4\pi b_{12}b_{21}}{1+4\pi b_{22}}. \quad (\text{II.68})$$

Note that this frequency is equal to the ω_p in the unretarded case. These

solutions are thus longitudinal vibrations, the same as in the unretarded case with one mode corresponding to each wave number. Since $\vec{H} = 0$, the radiation field takes no part in these vibrations. That is to say, these represent the pure longitudinal optic vibrations of the crystal in absence of the radiation field.

$$\text{Case (ii)} \quad \vec{E} \perp \vec{k} \quad (\text{II.64})$$

Then Eq. (II.9) shows that \vec{k} , \vec{E} and \vec{H} form a right-handed orthogonal system of vectors. With

$$|k\vec{E}| = \frac{\omega}{c} |\vec{H}| \quad (\text{II.69})$$

(II.11) reduces to

$$kH = \frac{\omega}{c} (E + 4\pi P). \quad (\text{II.70})$$

which with the help of (II.13) and (II.23) becomes

$$\left(\frac{ck}{\omega}\right)^2 E = \left\{ 1 + 4\pi b_{22} + \frac{4\pi b_{12}b_{21}}{-b_{11}-\omega^2} \right\} E. \quad (\text{II.71})$$

$E \neq 0$ implies

$$\left(\frac{ck}{\omega}\right)^2 = 1 + 4\pi b_{22} + \frac{4\pi b_{12}b_{21}}{-b_{11}-\omega^2} \quad (\text{II.72})$$

$$= \epsilon_{\infty} + \frac{\epsilon_0 + \epsilon_{\infty}}{\omega_0^2 - \omega^2} \quad (\text{II.73})$$

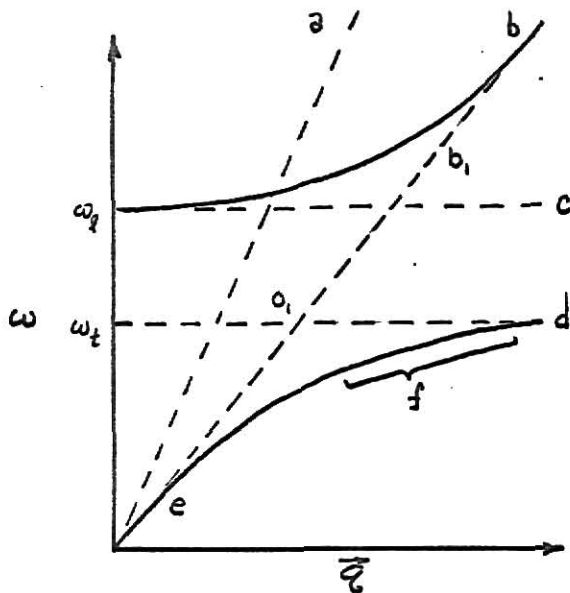
Once \vec{E} is chosen, \vec{W} , \vec{P} and \vec{H} are completely determined by (II.58,59) and (56). The solutions are all transverse since

$$\vec{k}, (\vec{W} \parallel \vec{P} \parallel \vec{E}), \vec{H}$$

are mutually perpendicular. The transverse condition $\vec{k} \perp \vec{E}$ implies that

implies that for every \vec{k} there are two independent choices of \vec{E}_0 . Moreover from (II.73) one sees that there are two frequencies for a given \vec{k} . Thus four independent transverse vibrational modes, corresponding to two frequencies (each doubly degenerate) exist for each \vec{k} .

The five vibrational modes have thus been obtained in the long wavelength approximation. Fig. 3 below shows the dispersion curves of pure lattice vibrations and electromagnetic waves as well as the dispersion curves of the interacting system.



- a. light in vacuum
- b. optical transverse waves with dispersion
- b₁. light wave without dispersion
- c. pure longitudinal lattice vibrations
- d. pure transverse lattice vibrations
- e. transverse optical waves
- f. "lattice vibration part" of the optical waves.

Fig. 3: Long wavelength lattice vibrations in the presence of electromagnetic radiation

The term "optical waves" is used for the "mixed" waves. The general principle that when two vibrating systems are coupled, their mutual perturbation is strongest and hence their modes mix most when the frequencies are equal, while in the case of very different frequencies, the coupled modes are essentially like the original oscillation of one system with a very small admixture of the other, is clearly illustrated here. The original lattice dispersion curves are C (longitudinal) and d (transverse, doubly degenerate),

while b_1 represents the "dispersion" curve for light in the crystal if the crystal were to behave as a purely refractive, dispersionless medium. One sees that the interaction is strongest where these dispersion curves are closest. Of course, there is no interaction with the longitudinal curve C. The intersection point O corresponds to resonance between the two fields. As one moves away from O, the actual solutions (solid lines) approach the solutions (dotted lines) for the non-interacting case. Physically, the reason is clear. On the high frequency side of the resonance point, the frequency of the light becomes so high that the ions cannot take part in the vibrations appreciably and hence solutions corresponding to fixed ions (i.e., $\vec{W} = 0$, or $\vec{P} = \frac{\epsilon_\infty - 1}{4\pi} \vec{E}$, so that medium is purely refractive) provide a good approximation. Here, the lower branch represents essentially pure lattice vibrations with phase velocities very small compared to $\frac{C}{\epsilon_\infty}$ so that retardation effects are negligible and the electrostatic approximation is good.

A consideration of energy density as done in detail by Huang [33] gives the relative proportion of mechanical to radiative energy in the optical waves. The result is shown in Fig. 4.

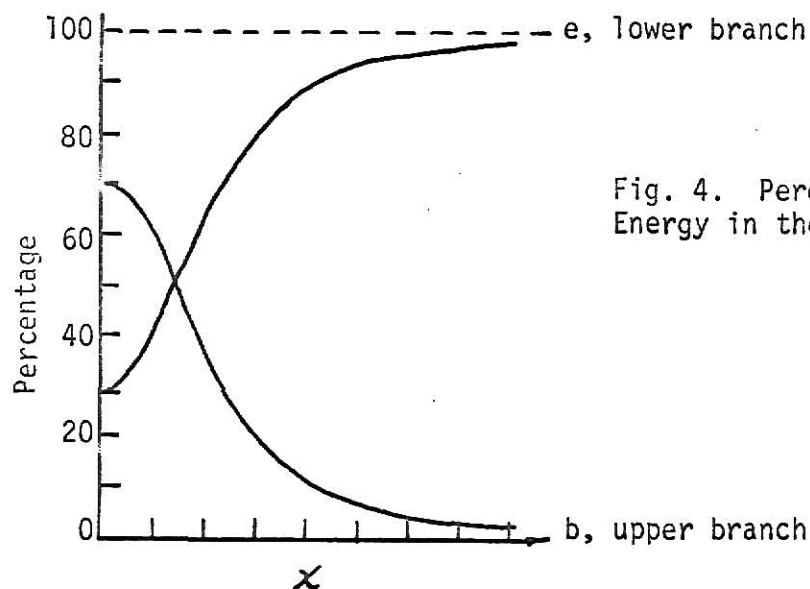


Fig. 4. Percentage Mechanical Energy in the Transverse Modes.

Towards the right of the resonance point, the lower branch approaches pure lattice oscillations which the upper branch tends to pure radiation energy. This picture thus leads to the usual, and to a beginner, terrifying statements [for instance Ref. (22c)] that "the lower branch is "photon-like" at low \vec{k} and "phonon-like" at high \vec{k} with frequency ω_y , while the upper branch is phonon-like at low \vec{k} with frequency ω_t and photon-like at high \vec{k} ." The actual dispersion curves for the optical waves are repeated in Fig. (5) for the sake of clarity. The frequency region between ω_t and ω_ℓ is a "forbidden" band of high reflectivity.

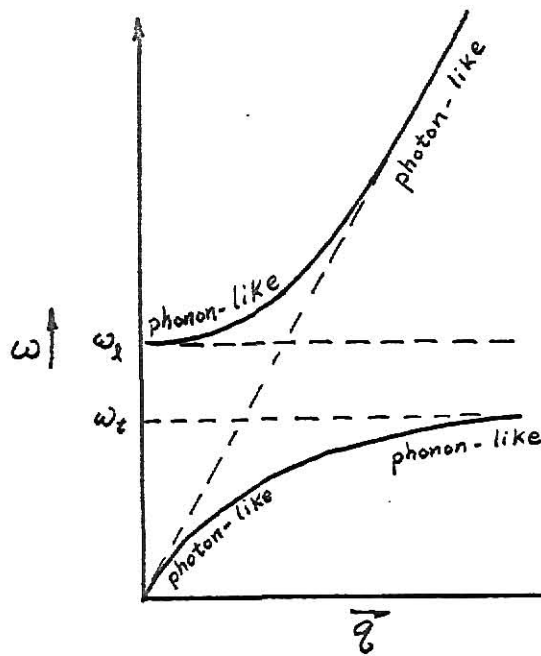


Fig. 5. Actual dispersion curves at low q in the presence of electromagnetic radiation.

This description of long-wavelength optic vibrations is meant as an introduction to the relevant sections 2.1-2.3 of (22c) which describes the dispersion curves for uniaxial and biaxial crystals in detail. Hence, these details are not repeated here.

It is necessary to distinguish between those lattice vibrations which give rise to an electric dipole moment in the lattice and those which do not. Since an electric dipole moment can interact with radiation in absorption, the first type of vibrations are said to be "infra-red active", and show up as absorption peaks in an infra red spectrum of the crystal. For an infra red inactive phonon, the restoring forces are mainly the mechanical forces which are short-range, and hence do not have dispersive effects on long wavelength phonons. Infra-red active phonons, on the other hand, produce long-range electric fields in the lattice. This distinction becomes important in considering the Raman effect due to phonons.

III. RAMAN EFFECT IN CRYSTALS

Though the Raman Effect was discovered in the crystals [2] quartz and calcite almost simultaneously with the discovery in liquids, the detailed theory as discussed in Chapters II and III was developed mainly for molecular scattering in gases and liquids. The Raman analysis became primarily a tool for the determination of molecular structures. Embedding the molecule of interest in a crystal only increased the complexity of the problem due to the coupling between molecules in the solid state. Also, in crystals, the intensity of the Raman Effect is small. In many ionic crystals and in fact in all crystals in which every atom is at a centre of inversion as in the case of NaCl, KCl, etc., the first order Raman Effect is forbidden by crystal symmetry. The second-order effect is feeble and needed very long exposures with the earlier photographic techniques of detection.

Born [20] was the first to present a semi-classical theory for scattering from crystals based on the general theory of Chapter I, Sec. B. The mathematical details of present-day theories which require a knowledge of many-body techniques for their understanding, are clearly illustrated in the works of Loudon [34],[35] and Birman [36]. These theoretical treatments are not reproduced here. Only the results which have direct bearing on experimental analysis are discussed.

First-order Raman scattering is described by the first-order term in the Taylor expansion of the induced electric moment of the crystal in terms of normal coordinates, i.e., in terms of phonon modes - both optic and acoustic. Only the scattering due to optic phonons will be considered here. The phonon wave vector can take on any value in the Brillouin zone, the

maximum being $\frac{\pi}{d}$, where d is the "lattice constant" for the direction considered. This maximum is typically of the order of $3 \times 10^8 \text{ cm}^{-1}$. Incident light of wavenumber about $2 \times 10^4 \text{ cm}^{-1}$ (or wavelength 5,000 Å) has a wave vector k in the crystal given by $|\vec{k}| = \frac{n\omega}{c} = 2\pi n \frac{\nu}{c} = 2\pi \times n \times \frac{1}{\lambda} = 2\pi \times \text{refractive index} \times \text{wavenumber}$. Usually, in a Raman scattering experiment the light scattered through 90° is observed so that the Rayleigh - scattered background is a minimum. If \vec{k}_i and \vec{k}_s denote the wave-vectors of the incident and scattered photons and \vec{q} that of the phonon, wave vector conservation implies

$$\vec{k}_i = \vec{k}_s + \vec{q} . \quad (\text{III.1})$$

Since $|\vec{q}|$ is typically of the order of $100\text{-}1500 \text{ cm}^{-1}$ while $|\vec{k}| \approx 2 \times 10^4 \text{ cm}^{-1}$ we can put $|\vec{k}_i| \approx |\vec{k}_s|$. The transverse geometry gives $\vec{k}_i \perp \vec{k}_s$. This leads to $q \approx \sqrt{2} \times 2 \times 10^5 \text{ cm}^{-1}$, which is small compared to $\frac{\pi}{d} (\sim 3 \times 10^8 \text{ cm}^{-1})$. Thus phonons of importance in the first order Raman Effect have large wavelengths, or, equivalently, wave-vectors $|\vec{q}|$ small in magnitude compared to the size of the Brillouin zone. This smallness of $|\vec{q}|$ leads to great simplification in the theory. All theories assume $|\vec{q}| \approx 0$ for the first-order Raman effect and this is often misleadingly called the " $\vec{q} = 0$ (or $\vec{k} = 0$) selection rule".

In crystals which have centre of inversion symmetry, any one phonon cannot be simultaneously Raman and infra-red active. But in crystals which do not have a centre of inversion symmetry, phonons can be both Raman- and infra-red active. As discussed before, an infra-red inactive phonon is not strongly dispersed, i.e., the optical branch is "flat" near and at $q = 0$. Hence all such phonons of small wave-vector have the same frequency as the $q = 0$ phonons. In this case, the Raman frequency shift measures the phonon frequencies at $q = 0$ and no variation in the Raman shift is produced by

variation of scattering angle or of the orientation of the light beams with respect to the crystal axis. However, for infra-red-active phonons, the accompanying long-range electric fields gives rise to strong dispersion. This leads to Raman frequencies different from the $\vec{q} = 0$ values, and to a variation of the frequency with the direction of \vec{q} in non-cubic crystals. These variations are described in detail by Loudon [35a,c].

A description of important features and results of the various theoretical approaches is now presented.

1. Born's Semiclassical Theory

Born's polarizability theory of Raman scattering [20] by crystals is just an extension of the general semiclassical theory of Chapter III. The intensity of Raman scattering per unit solid angle due to a transition from a vibrational state v to another state v' is given by Eq. (I.57).

$$I = \frac{\omega_0^4}{2\pi c^2} \sum_{k=1,2} \sum_{\alpha\beta} \sum_{\gamma\lambda} e_{\alpha}^k e_{\beta}^k i_{\alpha\gamma,\beta\lambda} E_{\gamma}^{-} E_{\lambda}^{+} \quad (\text{III.2})$$

where $i_{\alpha\gamma,\beta\lambda}$ denotes the product of the matrix elements of the electronic polarizability:

$$i_{\alpha\gamma,\beta\lambda} = \left\{ \langle v' | P_{\alpha\gamma}^{*} | v \rangle \langle v | P_{\beta\lambda} | v' \rangle \right\}_{\text{Average}} \quad (\text{III.3})$$

If the frequency spectrum of the scattered radiation is continuous as in the case of second or higher order scattering, the state v' for which $i_{\alpha\gamma,\beta\lambda}$ has a non-vanishing value cover a continuous energy spectrum. It is then convenient to introduce $i_{\alpha\gamma,\beta\lambda}$ as a function of frequency

$$i_{\alpha\gamma,\beta\lambda}(\omega) = \lim_{\Delta\omega \rightarrow 0} \sum_v^{\omega < \omega_0 + \omega} \sum_{v'}^{\omega < \omega + \Delta\omega} \left\{ \langle v' | P_{\alpha\gamma}^{*} | v \rangle \langle v | P_{\beta\lambda} | v' \rangle \right\}_{\text{Av.}} \quad (\text{III.4})$$

The problem thus is reduced to the calculation of the quantity $i_{\alpha\gamma,\lambda}^{(\omega)}$.

Here, to conform to the convention that has become rather permanent in literature, for the case of crystals, one writes $P_{\rho\sigma} = \alpha_{\rho\sigma}$ so that

$$i_{\rho\sigma,\mu\nu} = \left\{ [\alpha_{\rho\sigma}]_{VV'}, [\alpha_{\mu\nu}^*]_{VV'} \right\}_{Av}. \quad (\text{III.5})$$

for all vibrational transitions $v \rightarrow v'$. If now, ϵ_v be the energy in the state v then multiplying by the Boltzmann factor, the thermal average is

$$\langle i_{\rho\sigma,\mu\nu} \rangle = \frac{\sum_v [i_{\rho\sigma,\mu\nu}]_{VV'} e^{-\epsilon_v/kT}}{\sum_v e^{-\epsilon_v/kT}} \quad (\text{III.6})$$

The summation being taken over the initial state v .

The polarizability is now expanded in a Taylor series in the atomic displacements $U_{\beta\mu}^{(L)}$ as

$$\alpha_{\rho\sigma} = \alpha_{\rho\sigma}^{(0)} + \alpha_{\rho\sigma}^{(1)} + \alpha_{\rho\sigma}^{(2)} + \dots, \quad (\text{III.7})$$

where $\alpha_{\rho\sigma}^{(0)} = \text{constant}$

$$\alpha_{\rho\sigma}^{(1)} = \sum_{\beta} \sum_{\mu} \left(\frac{\partial \alpha_{\rho\sigma}}{\partial U_{\beta\mu}^{(L)}} \right)_0 U_{\beta\mu}^{(L)} \equiv \sum_{\beta} \sum_{\mu} \alpha_{\rho\sigma}^{\beta}{}_{\mu}^{(L)} U_{\beta\mu}^{(L)} \quad (\text{III.8})$$

$$\begin{aligned} \alpha_{\rho\sigma}^{(2)} &= \sum_{\beta\gamma} \sum_{\mu} \sum_{\mu'} \left(\frac{\partial^2 \alpha_{\rho\sigma}}{\partial U_{\beta\mu}^{(L)} \partial U_{\gamma\mu'}^{(L)}} \right)_0 U_{\beta\mu}^{(L)} U_{\gamma\mu'}^{(L)} \equiv \sum_{\beta\gamma} \sum_{\mu\mu'} \alpha_{\rho\sigma}^{\beta\gamma}{}_{\mu\mu'}^{(L,L')} U_{\beta\mu}^{(L)} U_{\gamma\mu'}^{(L')}. \end{aligned} \quad (\text{III.9})$$

All these quantities are symmetric in ρ, σ but not in the other indices.

This expansion can be written in terms of the normal coordinates $Q(\vec{q}_j)$. Both the expansion in terms of normal coordinates and the displacements are derived here since even in present day literature one finds authors resorting

to either expression depending on the context. In terms of normal coordinates

$$\alpha_{\rho\sigma}^{(1)} = \sum_{\beta} \sum_{\mu \ell} \alpha_{\rho\sigma}^{\beta}(\mu) U_{\beta}^{(\ell)}(\mu) \quad (\text{III.10a})$$

$$= \frac{1}{\sqrt{N}} \sum_{\mathbf{q}} \sum_{\mathbf{j}} \sum_{\beta} \sum_{\mu \ell} \alpha_{\rho\sigma}^{\beta}(\mu) \exp(2\pi i \vec{r}(\ell) \cdot \vec{q}) Q(\vec{q})_{\mathbf{j}} e_{\beta}(\mu | \vec{q}) \quad (\text{III.10b})$$

expressing $U_{\beta}^{(\ell)}(\mu)$ in terms of the normal coordinates. Note that $\alpha_{\rho\sigma}^{\beta}(\mu)$ has been written as $\alpha_{\rho\sigma}^{\beta}(\mu)$, independent of the cell index ℓ . (See Born [20]). Recalling that, because of the translational invariance of the lattice,

$$\sum_{\ell} e^{2\pi i \vec{q} \cdot \vec{r}(\ell)} = \delta(\vec{q}) \quad \text{then}$$

$$\alpha_{\rho\sigma}^{(1)} = \frac{1}{\sqrt{N}} \sum_{\mathbf{j}} \sum_{\beta} \sum_{\mu} \alpha_{\rho\sigma}^{\beta}(\mu) e_{\beta}(\mu | \vec{0}) Q(\vec{0})_{\mathbf{j}}. \quad (\text{III.11})$$

It is worth noting at this point that the $q = 0$ selection rule has come in as a result of translational invariance, where as in usual theories, one has to bring it in as an approximation. The first-order Raman effect in a crystal is thus due to the $q = 0$ optical mode, where each of the s simple lattices corresponding to the s points of the base moves like a rigid system. The first-order Raman-spectrum is thus a line spectrum of not more than $3s-3$ lines, ie. it is analogous to the Raman Effect of a molecule of s particles with a fixed orientation in space (translations allowed, rotations excluded.)

The equation for the thermal average of the products of the two first-order transition matrix elements is derived by Born [7, p. 210] in the form reproduced below:

$\left\{ \langle v A(q) v' \rangle \langle v' B(q) v \rangle \right\}_{Av}$	$\omega_{vv'}$
$A_j B_j \begin{cases} c_j e^{-\beta_j} \\ c_j \end{cases}$	ω_j
	$-\omega_j$

where $c_j \equiv \frac{h/2\omega_j}{1 - e^{-h\omega_j/kT}}$, $\beta_j \equiv h\omega_j/kT$.

From the results and equation (III.6) it is easy to see that the Stokes line ($-\omega_j$) and anti-Stokes line (ω_j) should bear an intensity ratio $\frac{I_{\text{antistokes}}}{I_{\text{stokes}}} \sim e^{-\beta_j}$ according to this theory.

Note here that $\alpha_{\rho\sigma}^\mu$ the polarizability tensor for the first-order scattering is a third-rank tensor. As remarked before it is covariant in indices ρ, σ and contravariant in μ . Since it is of rank 3, the transformation equations for $\alpha_{\rho\sigma}^\mu$ when a new set of axes are related to the old by the unitary transformation is

$$\alpha_{\rho\sigma}^\mu = (A)_{\beta\rho} (A)_{\gamma\sigma} (A^{-1})_{\mu\nu} \alpha_{\beta\gamma}^\nu \quad (\text{III.7})$$

If A is now restricted to be a symmetry operation of the crystal, all crystal properties, in particular the polarizability should be invariant under A , so that

$$\alpha_{\rho\sigma}^\mu = A_{\beta\rho} A_{\gamma\sigma} (A^{-1})_{\mu\nu} \alpha_{\beta\gamma}^\nu. \quad (\text{III.8})$$

Choose A to be the inversion transformation defined by $(A)_{\beta\rho} = -\delta_{\beta\rho}$.

Then, under the inversion,

$$\alpha_{\rho\sigma}^\mu = (-\delta_{\beta\rho})(-\delta_{\gamma\sigma})(-\delta_{\mu\nu}) \alpha_{\beta\gamma}^\nu \quad (\text{III.9})$$

$$= -\alpha_{\rho\sigma}^{\mu},$$

since an inversion operation is its own inverse. Thus $\alpha_{\rho\sigma}^{\mu}$ is zero in any crystal in which every atom or ion possesses a centre of inversion symmetry. Thus in alkali halides, and other crystals possessing this property, there is no first-order Raman effect.

For the second-order Raman effect, one has analogous to the first-order case,

$$\alpha_{\rho\sigma}^{(2)} = \frac{1}{N} \sum_q \sum_{JJ'} \sum_l \sum_{\mu\mu'} \sum_{\beta\gamma} \alpha_{\rho\sigma}^{\beta\gamma}(\mu\mu', l) e^{2\pi i \vec{r}(l) \cdot \vec{q}} e_{\beta}(\mu | \vec{q}_J) e_{\gamma}(\mu' | \vec{q}_{J'}). \quad (\text{III.10})$$

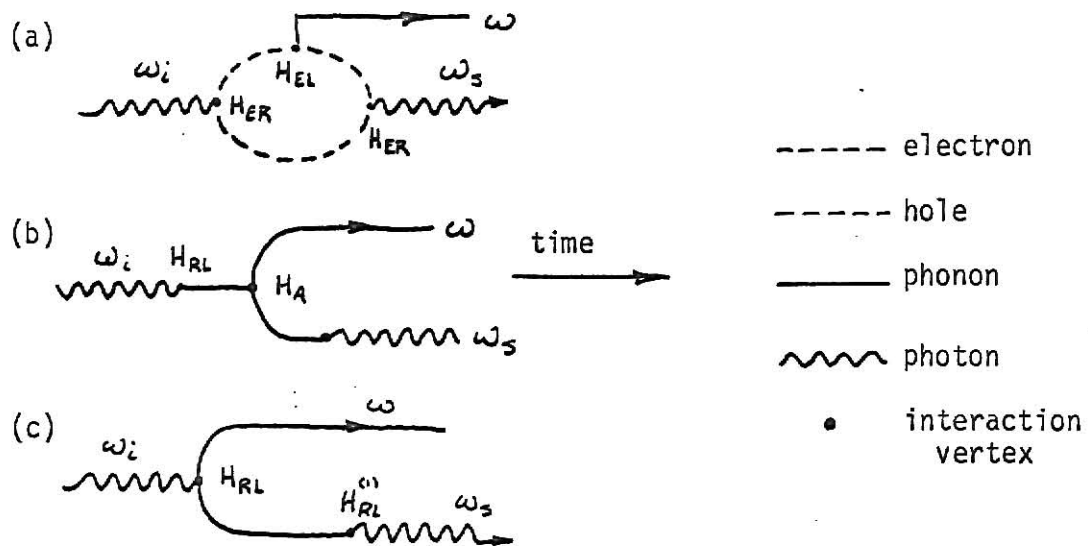
Following detailed considerations of the matrix elements involved Born (19) has shown that the observable second-order spectrum should consist of $9s^2$ superimposed continuous bands, each having a different maximum point, so that a general continuum with a number of peaks is observed. In the light of van Hove's theorem the different maxima in the second-order spectrum must be indicative of the singularities in the frequency distribution function.

B. Second Quantization Theory

1. First Order Raman Effect

The more modern theoretical approaches use the compact notation and concise language of second quantization. The Raman scattering process consists of three real transitions: (1) the absorption of the incident photon ω_i , (2) the emission or absorption of phonons, and (3) the emission of the scattered photon ω_s . The first-order Raman process may be represented in an interaction diagram or a "Feynman diagram", see Ref. [17], the initial state with only the photon ω_i present occurs at the left of each diagram, and the final state with the photon ω_s and a phonon ω occurs on the right.

Various alternative processes can be envisaged to connect the final and initial stages, depending on the relative strengths of the interactions. Three of the possible intermediate processes as shown by Loudon (3) are:



The three interacting systems here are the radiation field, (R), the electron system (E) of the crystal and the phonon system or the lattice vibrations (L). H_{ER} , H_{EL} , H_{RL} denote the interactions between these systems taken two at a time. Since Raman scattering by phonons changes only the vibrational state of the crystal while the electronic state is unchanged, it might seem at first that a radiation lattice interaction without the intermediary of electrons, is responsible for the scattering. However, a look at the diagrams shows that (b) and (c) involve interaction vertices where two or more phonon lines meet. This implies that phonon-phonon interaction, i.e., anharmonic effects described by a Hamiltonian H_A must be important for these processes to be strong. These processes have a small probability of occurrence since at ordinary temperatures in most crystals, anharmonicity is only a small perturbation. Also, these diagrams require the existence of a dipole moment associated with lattice vibrations that can

interact with the radiation. This implies that these processes cannot take place in a homopolar crystal such as diamond and at least for these crystals the process shown in (a), that is, scattering via intermediate excitation of electrons is the main possibility.

The three real transitions are thus connected by virtual electronic transitions, ω_i and ω_s being assumed to be too small to cause real inter-band electronic transitions. In such cases, time-ordering of the processes is not possible [17, p. 140], ie., the three real transitions can occur in any time order, giving six possible sequences of the process.

Thus the complete Hamiltonian for the problem is

$$H = H_R + H_L + H_E + H_{ER} + H_{EL} = H_0 + H_1,$$

where $H_0 = H_R + H_L + H_E$ is the sum of the radiation, phonon and electric Hamiltonian in the absence of interaction and $H_1 = H_{ER} + H_{EL}$ is the sum of electron-radiation and electron-lattice Hamiltonian. The radiation-lattice term being small is neglected. All theoretical work on the Raman effect also assumes that the crystal is in the electronic ground state before and after the scattering process. The theories differ in the description of the intermediate "virtual" transitions. In the theory of Loudon [35a], for instance, the electronic virtual interaction state is assumed to be a free electron-hole pair, while Birman [36] assumes exciton states, that is, electron-hole pairs bound by Coulomb interaction, to be the intermediate states.

The general form of the Hamiltonian may be written in second quantization notation as

$$H_0 = \sum_k \hbar\omega_k a_k^\dagger a_k + \sum_q \hbar\omega_q b_q^\dagger b_q + \sum_n \hbar\omega_n c_n^\dagger c_n \quad (\text{III.11})$$

$$\begin{aligned}
H_I &= H_{ER} + H_{EL} \\
&= \sum_{nn', k} \eta_{nn'}^{nn'} (a_k^\dagger + a_{-k}) (c_n^\dagger c_n + c_n^\dagger, c_n) + \\
&\quad + \sum_{mm', q} \beta_q^{mm'} (b_q^\dagger + b_q) (c_m^\dagger c_m + c_m^\dagger, c_m),
\end{aligned} \tag{III-12}$$

where a's are photon creation and destruction operators, the b's similar phonon operators and the c's are Fermion operators which create or destroy electrons. The coupling constants η and β depend respectively on the strength of interactions H_{ER} and H_{EL} . Their forms depend on the interaction mechanisms used in the theory.

The general procedure followed in many body theory would be to perform a suitable canonical transformation [17, Chap. 8] so that the interaction term is eliminated in the lowest order. The remaining Hamiltonian can be transformed using creation-destruction operators. Raman scattering can then be calculated using first order time-dependent perturbation theory, taking the appropriate higher order terms in the transformed, perturbing Hamiltonian (35). Such a procedure allows calculations in cases where H_{EL} is larger than H_{ER} . However, this method would be so laborious that it is better to risk the loss of generality by examining physically the relative order of magnitude of these terms, to determine which Hamiltonian would be a first order perturbation. The excitation of a phonon produces a displacement of the atoms in the lattice and this perturbs the periodic potential acting on the electrons. This is the main source of electron-lattice interaction energy H_{EL} in almost all cases. Birman [36] has shown that the corresponding Hamiltonian is typically 100 times smaller than H_{ER} . Thus H_{ER} should be treated in a first-order perturbation and H_{EL} in a higher order. All theoretical work so far,

including the work of Birman, however, treats them both in the same order. The term described above is the only source of interaction in most homopolar crystals. However, it is conceivable that in ionic crystals, for instance CaF_2 , a Fröhlich type of electron-lattice interaction may be relevant [17, Chap. 15]. Birman has shown for CdS, and GaAs that $\left(\frac{H_{\text{EL}}^{(d)}}{H_{\text{EL}}^{(f)}} \right) \sim 1$, where $H_{\text{EL}}^{(d)}$ is the first type of electron lattice interaction calculated from deformed potential and $H_{\text{EL}}^{(f)}$ is the Fröhlich type of term.

As experimental results which could conclusively establish one picture as a more accurate description than another are very meagre, the choice of a model remains a matter of personal opinion. Measurements of Raman scattered intensity made with great precisions are necessary for a final judgement. The detailed theory as formulated by Loudon is described in Ref. [35a]. A sketchy description of this theory is given here with the sole idea of facilitating the introduction of the Raman Tensor.

Suppose the crystal is in its electronic ground state at time $t = 0$ when the photons are incident. The probability that at time t , one photon ω_i has been destroyed, and a photon ω_s and phonon ω_0 have been created is, from time-dependent perturbation theory, [12, Chap. XVII].

$$W(t) = \sum_{\vec{q}, \vec{k}_s} |\langle n_i - 1, n_s + 1; n_0 + 1; 0 | e^{-iHt/\hbar} | n_i, n_s; n_0; 0 \rangle|^2 \quad (\text{III.13})$$

H is the total Hamiltonian; n_i , n_s and n_0 are the numbers of incident photons, scattered photons and optic phonons, respectively. The final zero in the bra and ket indicates the electronic ground state. The wave vectors \vec{k}_s and \vec{q} denote the scattered photon and phonon, respectively. In the summation over k_s , the direction of the scattered photon is restricted to lie within a small solid angle determined by the geometry of the detector.

If one considers only spontaneous Raman scattering ($n_s=0$), then

$$W^0(t) \sim \sum_{\vec{q}, \vec{k}_s} \sum_{a,b} \left| \frac{\langle n_i-1, 1; n_0+1; 0 | H_I | a \rangle \langle a | H_I | b \rangle \langle b | H_I | n_i, 0; n_0; 0 \rangle^2}{(\omega_a - \omega_i)(\omega_b - \omega_i)} \right| \times \delta(\omega_i - \omega_0 - \omega_s), \quad (\text{III.14})$$

where a and b run over complete sets of intermediate states. In the first two of the H_I matrix elements the H_{ER} part contributes; in the third matrix element, H_{EL} and H_{ER} both contribute. The superscript 0 on the W indicates the fact that only scattering by optic phonons are considered. The main source of electron-lattice interaction is the deformed-potential interaction. It is the only source in most cases as has already been mentioned (al, p. 214-217). Loudon [35a] has used the method of Whitfield [37] in which electron-lattice interaction is arrived at by expanding the perturbed periodic potential in a Taylor series in the components of the atomic displacement. Loudon uses the matrix elements of H_{EL} between two states as derived by Whitfield, i.e.,

$$\langle \alpha | H_{EL} | \beta \rangle = \varepsilon_{\alpha\beta}^{ij} \bar{S}_{ij}, \quad (\text{III.15})$$

where $\varepsilon_{\alpha\beta}^{ij}$ is the matrix element of the deformation potential and S_{ij} is a strain component $\frac{\partial U_i}{\partial R_j}$. The detailed properties of these operators are not important here.

The Hamiltonian H_{ER} is described in detail by Heitler [11] and is given by

$$H_{ER} = \frac{e}{m} \sum_j \sum_k \left(\frac{2\pi\hbar}{nV\omega_k} \right)^{1/2} \left\{ a_k e^{i\vec{k}_0 \cdot \vec{r}_j} + a_k^\dagger e^{-i\vec{k}_0 \cdot \vec{r}_j} \right\} \vec{\varepsilon}_k \cdot \vec{p}_j, \quad (\text{III.16})$$

where a_k and a_k^\dagger are the destruction and creation operators for a photon of wave vector \vec{k} and energy $\hbar\omega_k$; \vec{p}_j and \vec{r}_j are the momentum and position vectors of electron j , n is the dielectric constant (ϵ_∞), V the crystal volume and

ϵ_k the unit polarization vector of photon k .

When these interaction Hamiltonians are substituted into (III.14), the scattering probability $W(t)$ as a function of time becomes

$$W(t) = \frac{4\pi^2 T e^4}{n^2 a^2 M N} \sum_{\vec{q}, \vec{k}_2} \frac{n_1(n_0+1)}{\omega_1 \omega_0 \omega_2} \left| \epsilon_{0q}^i R_{12}^i(-\omega_1, \omega_2, \omega_0) \right|^2 \times \frac{(2\pi)^3}{V} \delta(\vec{k}_1 - \vec{q} - \vec{k}_2) \delta(\omega_1 - \omega_0 - \omega_2), \quad (\text{III.17})$$

where $\hat{\epsilon}_{sq}$ is a unit vector depending on the direction of \vec{q} . See Peierls [38] for details.

The term $R_{12}^i(-\omega_1, \omega_2, \omega_0)$ is of interest here. It is given by

$$R_{12}^i(-\omega_1, \omega_2, \omega_0) = \frac{1}{V} \sum_{\alpha, \beta} \left\{ \frac{p_{0\beta}^2 p_{\beta\alpha}^1 \Xi_{\alpha 0}^i}{(\omega_\beta + \omega_0 - \omega_1)(\omega_\alpha + \omega_0)} + \frac{p_{0\beta}^1 p_{\beta\alpha}^2 \Xi_{\alpha 0}^i}{(\omega_\beta + \omega_0 + \omega_2)(\omega_\alpha + \omega_0)} \right. \\ \left. + \frac{p_{0\beta}^2 \Xi_{\beta\alpha}^i p_{\alpha 0}^1}{(\omega_\beta + \omega_0 - \omega_1)(\omega_\alpha - \omega_1)} + \frac{p_{0\beta}^1 \Xi_{\beta\alpha}^i p_{\alpha 0}^2}{(\omega_\beta + \omega_0 + \omega_2)(\omega_\alpha + \omega_2)} \right. \\ \left. + \frac{\Xi_{0\beta}^i p_{\beta\alpha}^2 p_{\alpha 0}^1}{(\omega_\beta + \omega_2 - \omega_1)(\omega_\alpha - \omega_1)} + \frac{\Xi_{0\beta}^1 p_{\beta\alpha}^i p_{\alpha 0}^2}{(\omega_\beta + \omega_2 - \omega_1)(\omega_\alpha + \omega_2)} \right\}. \quad (\text{III.18})$$

$p_{\beta\alpha}^{1,2}$ represents the matrix element $\langle \alpha | p^{1,2} | \beta \rangle$, the superscripts indicating that the components are to be taken in the directions of polarization of the photons ω_1 and ω_2 . The six terms arise from the six types of scattering processes. R_{12}^i is called the Raman tensor, its subscripts indicate the photon polarization directions, and superscript the phonon polarization. The signs attached to the frequencies as the arguments of R are such that a negative (positive) frequency corresponds to destruction (creation) of the appropriate photon or phonon.

The symmetry of the Raman tensor is worth considering in detail. It is analogous to the $\alpha_{\rho\sigma}^\mu$ in the semiclassical theory. However, while $\alpha_{\rho\sigma}^\mu$ is symmetric in ρ and σ , R_{12}^i need not be symmetric in 1 and 2. Instead,

the Raman tensor has the following properties

$$(a) \quad R_{12}^i(-\omega_1, \omega_2, \omega_0) = R_{21}^i(\omega_2, \omega_1, \omega_0),$$

showing there is no significance in the order in which the photon variables are written.

(b) $R_{12}^i(-\omega_1, \omega_2, \omega_0) = R_{12}^i(\omega_1, -\omega_2, -\omega_0)$ for $\omega_1 = \omega_0 + \omega_2$, and (a) and (b) together lead to

$$(c) \quad R_{12}^i(-\omega_1, \omega_2, \omega_0) = R_{21}^i(-\omega_1 + \omega_0, \omega_2 - \omega_0, -\omega_0).$$

This shows that the Raman scattering is in general not symmetric with respect to interchange of polarization of incident and scattered photons. However when ω_0 is small compared to $\omega_\alpha - \omega_1$ and $\omega_\alpha - \omega_1$ for all α , as is the case except in Resonance Raman Effect, the dominant term in the Raman tensor is symmetric in the photon polarizations.

The above symmetry properties hold independently of the crystal structure. Crystal symmetry introduces further simplifications which will be discussed in the section on selection rules.

C. Stimulated Raman Effect

Instead of the expression for the first-order process, the probability for a s-phonon process can be written as

$$P_s \propto \frac{n_1(n_2+1)}{s!} \sum_s | \langle s | H_{ER} | s \rangle \langle s | \frac{1}{H_0 - E_0} H_{EL}^S | s-1 \rangle \langle s-1 | \frac{1}{H_0 - E_0} H_{EL}^{S-1} | s-2 \rangle \dots \\ \times \dots \times \langle s | \frac{1}{H_0 - E_0} H_{ER} | 0 \rangle |^2, \quad (III.19)$$

where the matrix elements of a_k in H_{ER} between the initial and final photon-states i and f , the first containing n_1 and the second n_2 photons have already

been calculated. The states $|s-r\rangle$ are products of electronic and vibrational states, the (s-r) label indicating the number of phonons created with respect to the ground state. In this s-phonon process, only the final and initial vertices involve photon processes.

The factor $n_1 n_2$, depending on the number n_2 of the photons in the final state of frequency ω_2 shows that, in addition to the spontaneous Raman effect, which depends on the initial number n_1 of photons, there will also be a stimulated Raman Effect if the geometry of the experiment is such that n_2 is non-zero. This dependence on the product of occupation numbers also shows that this is a non-linear process. This stimulated effect-also called the Raman Laser Effect - was experimentally observed by Woodbury [39] and is discussed in [40]. It will not be discussed here.

D. Resonance Raman Effect-Spontaneous and Stimulated:

The Raman tensor and hence the scattering efficiency contains terms which either diverge or become relatively large when the frequency of the exciting radiation is equal to an allowed optical transition frequency of the scattering material. This predicted increase in intensity known as the resonance Raman effect is familiar in Raman scattering from liquids.

The exciting frequency being close to a transition frequency of the scattering substance may lead to a significant absorption of the radiation. The scattered radiation being close to this may also be attenuated. These factors offset the increased scattering efficiency to some extent.

Two types of resonance scattering have been treated theoretically by Loudon [41]. These are scattering by lattice vibrations or phonons and the electronic Raman effect, i.e., Raman scattering by electronic states of

impurity atoms in crystals. Electronic Raman scattering has been observed in only a few experiments, originally by Hougen and Singh [42a] and more recently by Koenigstein [42b]. Resonance Raman scattering by phonons has been observed only in Raman experiments in crystals with defects, in particular the color centre work of Worlock and Porto [43]. A reflection geometry experiment was used by Russell [44] on the first-order Raman line of silicon in which the exciting frequency was in the region of absorption due to indirect electronic transitions.

The area of resonance Raman scattering from crystals is thus new and unexplored. The conclusions from Loudon's theory are interesting and await experimental verification. According to this theory for scattering by electronic levels, the Raman intensity achieves its maximum value when the exciting frequency is sufficiently close to resonance for virtually all the exciting light to be observed or scattered in the crystal. Further increase in absorption coefficient does not produce any change in the scattered intensity. For scattering by lattice vibrations the exciting frequency is usually chosen to be smaller than the energy gap so that absorption of the exciting beam is negligible. The Raman efficiency increases steeply as the exciting frequency approaches the absorption edge. When the exciting frequency is increased until it is above the absorption edge, the Raman efficiency falls sharply to a small frequency independent value. The largest scattering therefore occurs when the exciting frequency lies just below the absorption edge. These conclusions apply to spontaneous and stimulated Raman scattering and as noted before, they await experimental verification. The experimental results are also likely to be complicated as one might have fluorescence transitions due to electronic excitation in addition to Raman scattering.

E. Brillouin Scattering:

So far, only Raman scattering from optic vibrations of crystal has been discussed. Acoustic lattice vibrations can also give rise to first-order Raman scattering. Brillouin [45] predicted this phenomenon on the basis that thermal elastic waves in solids can be looked upon as inhomogeneities in a medium and give rise to scattering. The scattered light intensity would be a function of the scattering angle due to crystal anisotropy. This type of scattering is called Brillouin scattering. Brillouin shifts are very small, of the order of 2 or 3 cm^{-1} for many crystals. Due to the smallness of the phonon frequency, the stokes and antistokes lines have almost the same intensity for a given branch. Measurements of Brillouin spectra have generally been used to check measurements of already known elastic constants. Very little work has been done in this field owing to the difficulty in detecting the shifted lines, which are extremely close to the exciting line.

Selection Rules and Symmetry of Raman Scattered Light.

For a given value of the wave-vector \vec{q} , the different branches of the dispersion curve correspond to different normal modes of the crystal, i.e., different symmetries of vibration of the atoms in the unit cell. Each mode is characterized by an irreducible representation of the space group of the crystal lattice. Hence, the selection rules for Raman-active phonons can be determined by standard group-theoretical methods.

For first-order Raman scattering by a perfect crystal under non-resonance conditions, the $\vec{q} = 0$ rule holds, provided the phonons are not infra-red active as well. For these phonons, the $\vec{q} = 0$ rule must be supplemented by the condition that only modes that transform as a second-rank tensor under the

point-group operations of the space group will be Raman active. Alternatively, one can state this as "a phonon can be first-order Raman active if and only if its irreducible representation is the same as one of the irreducible representations which occur in the reduction of the polarizability tensor", which is the usual statement found in text-books on molecular spectroscopy. For example, see Wilson, Decius & Cross [46] and Heine [47]. The irreducible representations by which the components of the polarizability tensor transform listed by Wilson et. al., and for the set of 32 crystal point groups.

At this point, it is advisable to examine critically the nature of the Raman tensor, $R_{\rho\sigma}^{\mu}$ or, equivalently the polarizability derivative tensor, $\alpha_{\rho\sigma}^{\mu} \equiv \frac{\partial \alpha_{\rho\sigma}}{\partial Q_{\mu}}$. Thus $\alpha_{\rho\sigma}^{\mu}$ is truly a third-rank tensor and in fact, it is this property that leads to the conclusion that no first-order Raman scattering can occur in alkali halide crystals, or any crystal in which every atom or ion possesses a center of inversion symmetry. However, in the $q = 0$ limit and within the harmonic approximation, the normal modes $\{Q_{\mu}\}$ are linearly independent of each other and each Q_{μ} transforms according to an irreducible representation of the point group. Thus the third rank tensor $\alpha_{\rho\sigma}^{\mu}$ can be written or decomposed into the tensors $\{\frac{\partial \alpha_{\rho\sigma}}{\partial Q_{\mu}}\}$, one for each Q_{μ} . These tensors transform as second-rank tensors. This leads to the erroneous statement often found in literature that the Raman tensor is a second-rank symmetric tensor. It would be more appropriate to say that in the harmonic approximation and infinite wavelength limit, and when the exciting frequency is far removed from all absorption frequencies of the crystal, the Raman tensor can be broken up into symmetric second-rank tensors, each transforming according to an irreducible representation of the point group operations of the space-group of the crystal. The point group analysis can then be used. Mathieu [48]

has listed the Raman-active vibrational symmetries for the different crystal classes. Many examples are worked out in detail by Bhagavantam and Venkatarayndu [49].

Loudon [35c] has collected the results of various authors into a complete table of Raman tensors for the crystal symmetry classes. The table gives both the symmetry of the Raman active vibrations and the dependence of the Raman-scattered radiation on the polarizations of the incident and scattered light. Thus by observing the polarization dependence of a Raman line, one can infer the symmetry of the lattice vibration responsible for the scattering. In crystals which do not have a center of inversion among the elements of the point group, only even-parity vibrations (usually subscripted by g) can be Raman active and only odd-parity (u) vibrations can be infra-red active. This fact leads to the complementary nature of Raman data and infra-red absorption measurements.

The axes (x,y,z) which form the basis for Loudon's representation of the Raman tensor are the crystal principal axes (x_1, x_2, x_3) defined for all crystals by Nye [50]. Very often, however, crystals have natural growth faces which are not any of the principal planes in the Nye system, such as NaNO_3 , CaCO_3 or the tetragonal phosphates. For purposes of experiment, it would be advantageous to use the perfect growth faces as reference planes. In these instances, then it is useful to obtain a transformation matrix between the Nye system of axes and a convenient system of laboratory axes based on the experimental set-up and the positioning of the natural faces of the crystal.

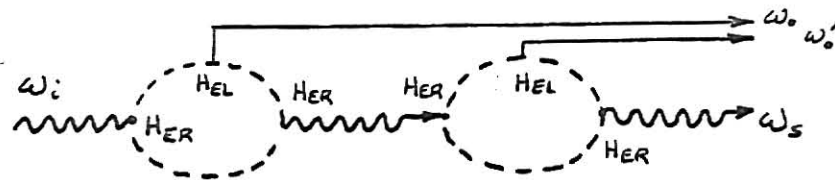
The interpretation of first-order Raman spectra due to phonons which are also infra-red active requires the realization that for this type of vibration, the accompanying long-range electric fields leads to a lifting of some of

the degeneracy of the optical phonon branches. Experimentally, this type of scattering was regarded as "anomalous" until its features were explained by Poulet [51]. The main differences are an increase in the number of first order Raman peaks from that expected by the group-theoretical analysis due to the lifting of the degeneracy, and an angular dependence of the Raman-scattered intensity in some uniaxial crystals. The details are given by Loudon [35], p. 445.

F. SECOND-ORDER RAMAN EFFECT

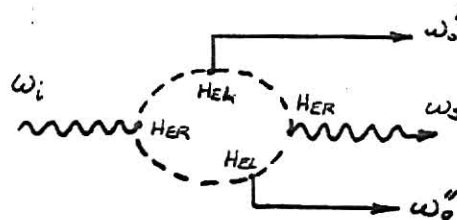
The second-order Raman Effect is a two-phonon process, i.e., a process in which two phonons participate. They may both be created (giving a Stokes component in the scattered light), both destroyed (anti-Stokes component) or one created and one destroyed (one Stokes and one anti-Stokes component).

A second-order scattering can give rise to a line or a continuous spectrum, depending on the nature of the process involved. The line spectrum occurs when a second order process is the result of two successive first-order Raman scattering processes as shown in figure below.



The two phonons involved should then individually satisfy first-order Raman selection rules and this type of spectrum gives no information in addition to that provided by the first-order spectrum. Hence, one usually analyzes only the continuous second-order spectrum.

The continuous spectrum is due to a scattering process in which the light interacts with a pair of phonons in a single event, as in the figure below.



There is now no restriction on the phonon wave vectors to lie in any particular part of the Brillouin zone since all that conservation of momentum now demands is that the sum of the wave vectors of the two phonons should balance the change in wave vector of the scattered photon. Since the photon wave vectors are small compared to the Brillouin zone this effectively leads to the fact that the wave vectors of the two phonons involved should be equal and opposite. The continuous frequency distribution of the scattered photons is thus proportional to a weighted density of lattice vibration states in which two phonons of equal and opposite wave vector are present. The weighting arises from the dependence of the interactions involved on frequency and wave vector. The second-order continuous spectrum, being a single event, possesses a scattering efficiency which is independent of the crystal size. The line spectrum, however, being due to two successive first-order scatterings, depends on crystal volume, it being assumed in both cases, that the crystal is transparent to all the photon frequencies involved. This distinction leads to the possibility of resolving the second-order line and continuous spectra in cases where the continuum has sharp features or where the lines are broad.

G. Theory and Selection Rules

The formal theory of second-order Raman scattering using the polarizability expansion was developed by Born and Bradburn [20] who applied their results to NaCl. A treatment using second-quantisation formalism has been developed by Birman [36]. However, these treatments are outside the scope of this thesis. Moreover, experimental analysis of second-order Raman spectra is based on critical-point analysis schemes rather than on any theory.

In the section on lattice dynamics, the critical point approach has been briefly discussed. Since the structure of the second-order spectrum involves both the frequency dependence of the interaction mechanisms and that of the phonon density of states, it is natural to expect sharp discontinuities in the spectrum corresponding to critical points provided the corresponding Raman process is not forbidden by selection rules. Moreover, since the interactions involved are very unlikely to have a frequency dependence with sharp discontinuities (again, assuming one is not near any resonance frequency), it is to be expected that all discontinuities in the second-order spectrum correspond to critical points of the density of states.

It is thus important to have selection rules at particular \vec{q} -vectors for the pairs of phonon branches which can contribute to second-order Raman effect. The relevant group-theoretical description is found in Bhagavantam [49]. If the two phonons involved belong to the same branch, the two-phonon state is called an 'overtone' while if they belong to different branches, it is called a "combination". For combination states, the Raman transition is allowed if the kronecker product of the irreducible representations of the two phonons contains irreducible representations in common with the polarizability tensor. For overtone states, the symmetrized kronecker square of the irreducible representation must be formed to determine the selection rule. The various general rules that follow are discussed in detail by Loudon [35c] and Bhagavantam [49, p. 89].

Some general selection rules for first and second-order Raman Effect may be stated as follows:

- a. All modes classified under the totally symmetric classes are always Raman-active.

- b. If a center of inversion is one of the elements in the group, all normal modes symmetric with respect to it are Raman active and all modes anti-symmetric with respect to it are infrared active.
- c. The first overtone of every normal mode is Raman active irrespective of whether the fundamental itself is active or not.
- d. All Raman active normal modes combine with each one of the modes coming under the totally symmetric class to give Raman active combination tones. The combination of an inactive mode with a totally symmetric one is also inactive.

IV. LATTICE DYNAMICS OF CRYSTALS WITH DEFECTS

A. Introduction

So far, a perfect lattice possessing perfect translational symmetry and infinite in extent has been assumed in deriving the properties of lattice vibrations. The interest in this work, however, is mainly on Raman scattering as modified by the presence of a defect in the lattice. A brief review of the defect problem in lattice dynamics is now given. Typical defects or imperfections in a solid are vacancies, interstitial and substitutional impurities, disorder, dislocations, and stacking faults. In addition surfaces must always be present in a finite crystal and constitute a fault. Even a low concentration of these impurities may have striking effects on the macroscopic properties as is well-known from semiconductor physics. Only substitutional point impurities are treated here, with a brief reference to a "molecular group" defect or a defect with internal degrees of freedom. The treatment is based directly on the extensive work of Maradudin and co-workers [51,52,53].

The earliest theoretical work on point defects was done in Russia by I.M. Lifshitz [54] in a series of papers still relatively unavailable in English, so that most of it was repeated by Montroll and co-workers [55,56]. Experimental work was non-existent then, and the theoretical work aimed mainly at determination of the modification in the frequencies, the associated displacements in the normal modes of a crystal, and the effect of these modifications on the thermodynamic functions of the crystal. Because of computational difficulties the first calculations were carried out for artificial crystal models, and dealt with time-independent properties.

The possibility of being able to observe the defect properties directly rather than by their effects on thermodynamic properties, using the Mössbauer Effect was pointed out by Visscher [57]. For the first time the dynamics of the defect in a lattice was brought to the attention of experimentalists. Though the direct Mössbauer measurement has not yet been performed due to difficulties in measurement, an increasing amount of work has been done in infra-red spectroscopy and neutron spectroscopy [58,59,60]. Raman spectroscopy has been applied to the problem only recently [43], but seems to have a very promising future in the understanding of defect lattice dynamics.

The main reason for the lack of interest of experimentalists in the problem seems to be, as Krumhans [61] has pointed out that in early theoretical works "the subject became something of a theater in which to display mathematical virtuosity, at the expense of the underlying physical simplicity of things." The review articles [51,52,53], however, treat the mathematics very clearly.

When defects are introduced into crystal lattices their effects on the normal mode frequencies of the lattice are of two kinds: the individual frequency levels inside the bands of allowed frequencies are shifted by small amounts, and a small number of frequencies which normally lie near the band edges emerge out of the allowed bands into the gaps of forbidden frequencies. The normal modes associated with these frequencies are the features of interest here.

The recent theoretical and experimental work on lattice vibrations has had two primary aims. One is the study of the new effects such as localized and resonance modes which are directly the results of the presence of defects [58,59]. The second type of study is the use of impurity atoms

as probes, generally through the relaxation of selection rules, for studying dynamical properties of the essentially perfect host crystal.

Before using Green's function methods to obtain the actual solution, consider the physical picture. In a crude picture, the defect mass M' can be looked at as being coupled by a force constant α' to the rigid lattice so that it would tend to vibrate at a frequency ω_0 , where

$$\omega_0^2 = 4\pi \frac{2\alpha'}{M'} . \quad (\text{IV.1})$$

The cut-off frequency for the monatomic lattice is $\omega_m = 2\pi \frac{\alpha}{M}$. If $\omega_0 > \omega_m$, the vibrational frequency characteristic of the defect is higher than that which can propagate via phonons through the crystal. It must therefore possess nonpropagating modes that are (exponentially) damped in space. This is analogous to the exponential attenuation suffered by microwaves in wave guides at frequencies below cut-off. The corresponding mode is called a localized mode and though the picture above is crude, it may be observed that localized modes will occur under the appropriate conditions for a light impurity ($M' < M$) or one coupled to its surroundings more strongly than a host atom ($\alpha' > \alpha$).

In reality there are additional complications due to the vibrations of the surrounding lattice. In non-Bravais lattices which possess both optical and acoustic branches, the localized modes may occur at frequencies in the frequency gap of the host crystal or above the maximum of the optical branch. Also, the impurity may have internal structure, that is, it may be a molecule or ion with its own characteristic frequencies that would tend to fall outside the phonon band frequencies. These internal vibrations would become localized, nonpropagating modes once the ion is in the crystal.

Suppose, on the other hand, that ω_0 is within the band of allowed frequencies. The excited impurity atom oscillating at ω_0 can then lose energy by exciting phonons of the same frequency. This will cause damping - in time - of the oscillation. If somehow the impurity is coupled only weakly to the system or if the density of phonon states at frequencies near ω_0 is small, the damping will be weak and the impurity will oscillate for a long time independent of the surroundings. It will thus have a frequency spectrum centered at some ω_r , shifted from ω_0 because of the dynamical response of the lattice. It will possess a width Γ_r which is a measure of the density of phonon states. Such a mode is called a resonance mode or a virtual localized mode. As far as the impurity is concerned, the state is quite similar to a localized mode. If $\Gamma_r \ll \omega_r$, both behave as a simple Einstein oscillator.

The simplest kind of resonance occurs for a heavy impurity $M' > M$ or one weakly coupled to its surroundings. At low frequencies there are only acoustical phonons and these have a density of states proportional to ω^2 . This dependence is sufficient to guarantee that, if the resonance occurs at low enough frequency, it will be narrow.

1. One-Dimensional Crystal with Defect

To examine the behavior of the localized modes, consider a monatomic linear chain (39). For the perfect chain with force constants α and atoms of mass M , the equations of motion assuming nearest neighbor interactions are

$$M\ddot{x}_n = \alpha(x_{n+1} - x_n) - \alpha(x_n - x_{n-1}), \quad n = \frac{N}{2} + 1, \dots, \frac{N}{2}. \quad (\text{IV.2})$$

Substituting $x_n = U_n e^{i\omega t}$, the time independent equations are

$$M\omega^2 U_n + \alpha [U_{n+1} - 2U_n + U_{n-1}] = 0 \quad (\text{IV.3})$$

which could alternatively be written in matrix notation as

$$\mathcal{L} U = 0, \quad (\text{IV.4})$$

where

$$U \text{ is a column vector } \begin{pmatrix} U_1 \\ U_2 \\ \vdots \\ U_N \end{pmatrix}$$

and \mathcal{L} is a $N \times N$ determinant defined by

$$(\mathcal{L})_{mn} = M\omega^2 \delta_{mn} - \alpha \{ \delta_{m,n-1} - 2\delta_{mn} + \delta_{m,n+1} \}. \quad (\text{IV.5})$$

The condition for non-trivial solution is then

$$\det \{ \mathcal{L} \} = 0 \quad (\text{IV.6})$$

which leads, with the cyclic boundary condition $U_n = U_{n+N}$, to the solution

$$U_n(s) = e^{2\pi i s n / N}, \quad (\text{IV.7})$$

and the dispersion relation

$$\omega_s^2 = \omega_L^2 \left[\sin^2 \frac{\pi s}{N} \right], \quad (\text{IV.8})$$

where $\omega_L = 2\pi \sqrt{\frac{\alpha}{M}}$ and $s = -\frac{N}{2} + 1, \dots, \frac{N}{2}$ numbers the normal modes.

When the crystal is perturbed by defects, some force constants and masses are different from the others. Then the coefficients of certain u 's are different and the equation which shows the effect of these local changes is

$$\sum_n \mathcal{L}_{mn} U_n = \sum_k (\delta \mathcal{L})_{mk} U_k, \quad (\text{IV.9})$$

where $(\delta \mathcal{L})$ is the matrix characterizing the defects. Its rank equals the number of degrees of freedom affected by the introduction of the defects. If the defects are few and localized this is a small number.

The most convenient way to solve the above equation is through the use of Green's functions [62, 63]. The Green's function G_{mn} is defined by the equation

$$\mathcal{L} G = 1, \quad (\text{IV.10a})$$

or

$$\sum_k \mathcal{L}_{mk} G_{kn} = \delta_{mn}, \quad (\text{IV.10b})$$

i.e., G is the matrix inverse to \mathcal{L} .

Eq. (IV.9) can be solved in terms of G as

$$U_n = \sum_k G_n(\delta L)_{nk} U_k \quad (\text{IV.11})$$

The unknown displacements $\{U_n\}$ appear on both sides of this equation. and hence, Eq. (IV.11) can hardly be called a solution. However, it does express the displacement of any atom in the chain in terms of the few atoms directly affected by the introduction of the defects since $(\delta L)_{mn}$ is zero except for these atoms.

Eq. (IV.11) may be written as

$$\sum_k U_k (\delta_{nk} - G_n (\delta L)_{nk}) = 0 \quad (\text{IV.12})$$

or in matrix form,

$$(I - G \delta L) U = 0. \quad (\text{IV.13})$$

The condition for non-trivial solution of these equations is

$$\det \{ I - G\delta L \} = 0 . \quad (\text{IV.14})$$

This yields the frequencies of the perturbed normal modes.

For an application of the above, one needs to find the Green's function first. For this, recall that the Kronecker delta can be expanded as

$$\delta_{mn} = \frac{1}{N} \sum_{s=-\frac{N}{2}+1}^{\frac{N}{2}} e^{2\pi i s(m-n)/N} . \quad (\text{IV.15})$$

Now G_{mn} can also be expanded in a Fourier series as

$$G_{mn} = \frac{1}{N} \sum_{s=-\frac{N}{2}+1}^{\frac{N}{2}} f_s e^{2\pi i s(m-n)/N} . \quad (\text{IV.16})$$

Substituting from (IV.12) and (IV.13) into (IV-76) and using (IV-2), the Green's function is obtained as

$$G_{mn} = \frac{1}{N} \sum_{s=-\frac{N}{2}+1}^{\frac{N}{2}} \frac{e^{2\pi i s(m-n)/N}}{M\omega^2 - 2\alpha + 2\alpha \cos \frac{2\pi s}{N}} . \quad (\text{IV.17})$$

Replacing s by $-s$ it can be easily shown that

$$G_{mn} = G_{nm} \quad (\text{IV.18})$$

and depends only on the difference $|m-n|$. Thus the Green's function can be written as a function of a single index $G_\ell = G_{-\ell}$.

Maradudin [64] has shown that G_ℓ can be expressed as

$$G_\ell = \frac{1}{2\alpha \sin \phi} \left[\cot \frac{N\phi}{2} \cos \ell\phi + \sin |\ell|\phi \right], \quad (\text{IV.19})$$

where

$$\phi = 2 \sin^{-1} \frac{\omega}{\omega^2} = \cos^{-1} \left\{ 1 - \frac{M\omega^2}{2\alpha} \right\} . \quad (\text{IV.20})$$

Now consider the application of these results to a substitutional isotope defect at $n = 0$. For simplicity, assume that the force constant is unchanged. Only those modes of the chain that are symmetric (i.e., $U_n = U_{-n}$) are affected by the presence of the defect because for antisymmetric modes ($U_n = -U_{-n}$) the origin is a node and hence not affected by a mass change at the origin.

The elements of L are given by

$$(\delta L)_{mn} = \epsilon M \omega^2 \delta_{m0} \delta_{n0}, \quad (\text{IV.21})$$

where ϵ is the mass defect parameter defined previously and Eq. (IV.17) becomes

$$U_n = \epsilon M \omega^2 G_{n0} U_0. \quad (\text{IV.22})$$

The vibration of the defect can be determined by setting $n = 0$ in (IV.20), yielding

$$1 = \epsilon M \omega^2 G_0. \quad (\text{IV.23})$$

Substituting for G_0 from (IV.19) and (20), the values of ϕ which when substituted into (20) give the perturbed normal mode frequencies are the roots of

$$\epsilon \tan(\phi/2) = \tan \frac{N\phi}{2}. \quad (\text{IV.24})$$

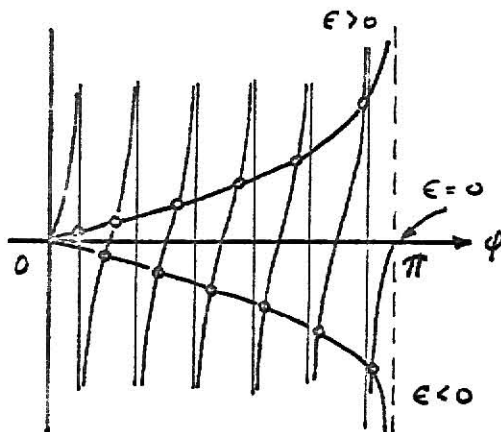


Fig. 6. The graphical solution of Eq. (IV.24) for the case $N=12$.

The right-hand side of eq. (24) is plotted against the left in the above figure for $N = 12$. In the absence of any defect the allowed values of Φ are given by the intersection of $\tan N\phi/2$ with the horizontal axis since for a perfect lattice $\phi_s^{(0)} = \frac{2\pi s}{N}$. When $\epsilon < 0$, corresponding to a heavy impurity, the allowed values of Φ are lowered relative to the unperturbed values. On the other hand, for $\epsilon > 0$, i.e., in the case of a light impurity, the allowed values of ϕ 's are above the unperturbed values.

Solving (2b) by successive approximations starting from $\phi_s = \phi_s^{(0)}$, to a first approximation,

$$\phi_s \approx \frac{2\pi s}{N} + \frac{2}{N} \tan^{-1}(\epsilon \tan \frac{\pi s}{N}) \quad (\text{IV.25})$$

and hence

$$\omega_s \approx \omega_L \left| \sin \frac{\pi s}{N} \right| + \frac{\omega_L}{N} \left[\left(\cos \frac{\pi s}{N} \right) \tan^{-1}(\epsilon \tan \frac{s}{N}) \right] \quad (\text{IV.26})$$

The fig. 6 also shows that when $\epsilon > 0$, there is one less solution than when $\phi = 0$. This "missing" mode corresponds to a complex value ϕ and has a frequency $> \omega_L$, the cut-off frequency of the monatomic lattice. Setting $\phi = \pi + iZ$ in eq. (22) one obtains, as N becomes large,

$$Z = \ln \frac{1+\epsilon}{1-\epsilon}. \quad (\text{IV.27})$$

This solution corresponds to a frequency

$$\omega_0^2 = \frac{\omega_L^2}{1-\epsilon^2} > \omega_L^2. \quad (\text{IV.28})$$

The time-independent amplitude of vibration U_n of the n^{th} atom corresponding to this mode, recalling that $U_r(s) \propto e^{in\phi_s}$, is

$$U_n \propto (-1)^n \left(\frac{1-\epsilon}{1+\epsilon} \right)^{|n|}. \quad (\text{IV.29})$$

The displacements are wavelike in the cases described by (25), i.e., when ω is in the allowed frequency region. These wave-like solutions are called "in-band modes". The last mode Eq. (29) however decays in space exponentially as n increases, i.e., as one moves away from the impurity atom. This is a localized mode as described to previously

An examination of the exact expression for the amplitudes of the two types of modes (for detailed derivation, [51, p. 433-434]) brings out another difference between them in addition to their spatial dependence. The expressions are

$$U_n(s) = \left(\frac{2}{MN}\right)^{1/2} \frac{1}{(1+\epsilon^2 \tan^2 \frac{\phi_s}{2})^{1/2}} \times [\cos n\phi_s + \epsilon \tan \frac{\phi_s}{2} \sin |n| \phi_s], \quad 0 < \phi_s < \pi \quad (\text{IV.30})$$

$$U_n(s) = (-1)^n \left(\frac{2}{M}\right)^{1/2} \left(\frac{\epsilon}{1-\epsilon^2}\right)^{1/2} \left(\frac{1-\epsilon}{1+\epsilon}\right)^{|n|}, \quad \begin{matrix} 0 < \epsilon < 1 \\ \omega = \omega_0 > \omega_L \end{matrix} \quad (\text{IV.31})$$

The amplitude of the wave-like, in-band mode is of $O(N^{-1/2})$, where N is the number of atoms, (in three dimensions, the number of unit cells in the crystal), while the amplitude of a localized mode is of $O(1)$. The frequency shift, too, is of $O(N^{-1})$ for resonance modes while it is independent of the dimensions of the lattice for a true localized mode. Thus, in calculations involving amplitudes or functions of frequencies, the change brought about by the presence of a defect in the allowed band of the perfect crystal is much less dramatic than that due to a localized mode.

2. Three Dimensional Crystal with Defects

Though the theory of the one-dimensional crystal illustrates the occurrence of local modes, the realistic three-dimensional problem is worth considering to illustrate the technique actually employed in defect problems. While it is

true one never has a crystal containing only a single impurity, in many physical situations where the impurity concentration is small one can obtain a good approximation for the effects of the impurity by multiplying the effect produced by a single impurity by the number of impurities. This approach has been used successfully in infra-red absorption studies of defects with concentrations not exceeding 10^{18} cm^{-3} . It is reasonable to neglect the interactions between true impurity centers. Once the concentration exceeds that for which interactions can be neglected, the defect is no longer an "impurity" but an integral part of the host crystal itself. In such cases the system is referred to as a mixed crystal, such (Si+Ge) systems.

The equations of motion of the host crystal (II.9) may be written as

$$\mathcal{L} \mathcal{U} = 0 \quad (\text{IV.32a})$$

where \mathcal{L} is now a $3sN \times 3sN$ matrix whose rows and columns are labelled by the triple index $(\lambda\mu\alpha)$ and whose $(\lambda\mu\alpha; \lambda'\mu'\beta)$ element is given by

$$\left\{ M_K \omega^2 \delta_{\lambda\lambda'} \delta_{\mu\mu'} \delta_{\alpha\beta} - \phi_{\alpha\beta}^{(0)}(\lambda\lambda', \mu\mu') \right\}, \quad (\text{IV.32b})$$

where the $\phi_{\alpha\mu}^{(0)}$ are the elements of the force constant tensor for the unperturbed crystal. The matrix \mathcal{U} is a column vector whose $3sN$ elements are the amplitudes $\{U_{\alpha}(\lambda_{\mu})\}$.

For later developments, it is useful to note here that the equation of motion may also be written as

$$(\mathcal{M}_0 \omega^2 - \mathcal{L}) = 0 \quad (\text{IV.32c})$$

where \mathcal{M}_0 is a diagonal matrix whose elements are the masses at the individual lattice points. Dividing the element of each row and column of this matrix by the square root of the mass appearing in the corresponding diagonal element,

the corresponding secular equation may be written as

$$|M_0| |\Pi\omega^2 - D_0| = 0 \quad (\text{IV.32d})$$

where D_0 is the dynamical matrix of the pure lattice.

When a substitutional impurity is introduced, the time-independent equations of motion can be written as

$$\sum_{\ell, \mu, \beta} \left\{ M_{\ell\mu} \omega^2 \delta_{\ell\ell'} \delta_{\mu\mu'} \delta_{\alpha\beta} - \Phi_{\alpha\beta} \left(\begin{smallmatrix} \ell\ell' \\ \mu\mu' \end{smallmatrix} \right) U_{\beta} \left(\begin{smallmatrix} \ell \\ \mu' \end{smallmatrix} \right) \right\} = 0, \quad (\text{IV.33a})$$

where $M_{\ell\mu}$ is the mass of the atom at the site $\left(\begin{smallmatrix} \ell \\ \mu \end{smallmatrix} \right)$ while $\Phi_{\alpha\beta}$ now represents the force constants of the perturbed crystal. The secular equation corresponding to (IV.32c) may be written analogous to eq (IV.32d) as

$$|M| |\Pi\omega^2 - D| = 0 \quad (\text{IV.34})$$

Eq. (1) can be written more compactly as

$$(L - \delta L) U = 0, \quad (\text{IV.35})$$

where

$$\begin{aligned} \delta L_{\alpha\beta} \left(\begin{smallmatrix} \ell\mu \\ \ell'\mu' \end{smallmatrix} \right) &= -\omega^2 (M_{\ell\mu} - M_{\mu}) \delta_{\ell\ell'} \delta_{\mu\mu'} \delta_{\alpha\beta} \\ &\quad + \left\{ \Phi_{\alpha\beta} \left(\begin{smallmatrix} \ell\ell' \\ \mu\mu' \end{smallmatrix} \right) - \Phi_{\alpha\beta}^{(0)} \left(\begin{smallmatrix} \ell\ell' \\ \mu\mu' \end{smallmatrix} \right) \right\} \\ &= -\omega^2 \Delta M_{\ell\mu} \delta_{\ell\ell'} \delta_{\mu\mu'} \delta_{\alpha\beta} + \Delta \Phi_{\alpha\beta} \left(\begin{smallmatrix} \ell\mu \\ \ell'\mu' \end{smallmatrix} \right) \end{aligned} \quad (\text{IV.36})$$

Thus L has non-vanishing elements only if the site $\left(\begin{smallmatrix} \ell \\ \mu \end{smallmatrix} \right)$ or $\left(\begin{smallmatrix} \ell' \\ \mu' \end{smallmatrix} \right)$ or both are the impurity site itself and the sites of atoms with which the impurity interacts directly. It is therefore, a matrix which has non-vanishing elements only in a $3n \times 3n$ block where n is the number of lattice sites including the impurity site, directly affected by the introduction of the

impurity atom. If the impurity is a highly localized imperfection, n is a small number.

Because the potential energy of interaction is not generally known, the elements of $\Delta\Phi$ are unknown and they must be determined by comparing the predictions of the theory with the results of experiments based on some physical property affected by the presence of defects in the crystal. The form of $\Delta\Phi$ used must be consistent with those general invariance and symmetry conditions (II.6,7,8) which apply to the imperfect crystal.

The conditions (II.6,7,8a,b) based only on the quadratic nature of the potential energy expansion continue to hold. However, the presence of an impurity atom distinguishes one lattice site from all the others. The crystal is no longer taken into itself by a displacement through one of the translation vectors of the crystal. In other words, the crystal has lost translational symmetry. This means $\Delta\Phi_{\alpha\beta}(\ell\ell';\ell'\mu')$ depends on both ℓ and ℓ' and not merely on the difference. These observations lead to three general conditions on the force constants, viz.,

$$(i) \Delta\Phi_{\alpha\beta}(\ell\ell';\ell'\mu') = \Delta\Phi_{\alpha\beta}(\ell'\mu';\ell\ell'), \quad (IV.37a)$$

$$(ii) \sum_{\ell\mu} \Delta\Phi_{\alpha\beta}(\ell\ell';\ell'\mu') = 0, \quad (IV.37b)$$

$$(iii) \sum_{\ell'\mu'} \Delta\Phi_{\alpha\beta}(\ell\ell';\ell'\mu') r_{\gamma\mu}^{(\ell')} = \sum_{\ell'\mu'} \Delta\Phi_{\alpha\gamma}(\ell\ell';\ell'\mu') r_{\beta\mu}^{(\ell')}. \quad (IV.37c)$$

Because of the loss of translational symmetry, only some set of symmetry operations which must be of the form $[S|\vec{0}]$ still take the crystal into itself. These operations are necessarily point group operations about the impurity site. The order of this group may be equal to or smaller than the order of the point group of operations which when applied at the impurity site take the perfect

crystal into itself. The law of transformation of the elements $\{\Delta\Phi_{\alpha\beta}(\mu; \ell'\mu')\}$ can therefore be written as

$$\Delta\Phi_{\alpha_1\alpha_2}(L_1M_1; L_2M_2) = \sum_{\beta_1\beta_2} S_{\alpha_1\beta_1} S_{\alpha_2\beta_2} \Delta\Phi_{\beta_1\beta_2}(\ell_1\mu_1; \ell_2\mu_2), \quad (\text{IV.37d})$$

where (LM) is the lattice site into which $(\ell\mu)$ is taken by a proper or improper rotation described by S, applied at the impurity site, which takes the crystal into itself. The equations (IV.37) are general, and must not be violated in any calculation of an impurity induced property.

To solve the equations of motion, the usual technique is to introduce the Green's function matrix defined by

$$G_{\alpha\beta}(\mu; \ell'\mu'; \omega^2) \equiv L_{\alpha\beta}^{-1}(\mu; \ell'\mu'; \omega^2)$$

Using the eigenfunction expansion technique as described for instance by Jackson [65] p. 89, one can expand the Green's function for the impurity problem in terms of the normal coordinates of the host crystal, which are the eigenfunctions of the homogeneous equations corresponding to eq. (IV.35). This then gives

$$G_{\alpha\beta}(\mu; \ell'\mu'; \omega^2) = \frac{1}{N(M_\mu M_{\mu'})^{1/2}} \sum_{\vec{q}j} \frac{W_\alpha(\mu | \vec{q}j) W_\beta^*(\mu' | \vec{q}j)}{\omega^2 - \omega_j^2(\vec{q})} \times \exp[i\vec{q} \cdot \vec{r}(\mu) - \vec{r}(\mu')] , \quad (\text{IV.38})$$

where $\omega_j(\vec{q})$ is the frequency of the normal mode of the perfect crystal described by the wave-vector \vec{q} and phonon branch index j. $\vec{W}(\mu | \vec{q}j)$ is related to the polarization vector $\hat{e}(\mu | \vec{q}j)$ of by a phase factor,

$$\vec{W}(\mu | \vec{q}j) \equiv \vec{e}(\mu | \vec{q}j) e^{-i\vec{q} \cdot \vec{r}(\mu)} . \quad (\text{IV.39})$$

The sum over \vec{q} in (5) is taken over the first Brillouin zone for the crystal. Using the transformation properties of $\omega_j(\vec{q})$ and $W(\mu|\vec{q}j)$, the Green's function (5) may be shown to satisfy the same boundary conditions as the displacements $U_\alpha(\mu)$ (i.e., cyclic boundary conditions). Also, G has the same transformation as $\Phi^{(0)}$.

Using Green's function, Eq. (IV.35) can be written as

$$u = G(\delta L)u. \quad (\text{IV.40})$$

By suitably labelling rows and columns, since δL has only a few non-vanishing elements, it may be partitioned as:

$$\delta L = \left(\begin{array}{c|c} \delta L & 0 \\ \hline 0 & 0 \end{array} \right) \quad (\text{IV.41a})$$

The matrix G and column vector u may also be compatibly partitioned as

$$G = \left(\begin{array}{c|c} g & G_{12} \\ \hline G_{21} & G_{22} \end{array} \right), \quad u = \begin{pmatrix} u_1 \\ u_2 \end{pmatrix}. \quad (\text{IV.41b})$$

So that δL and g are $3n \times 3n$ matrices, $G_{12} = G_{21}^T$ is a $3n \times (3_S N - 3n)$ matrix, and G_{22} is of order $(3_S N - 3n) \times (3_S N - 3n)$. The column u_1 has as elements the $3n$ displacement components of the impurity atom and the atoms with which it directly interacts.

Substituting (8a) and (8b) into (7) the following equations are obtained:

$$u_1 = g \delta L u_1, \quad (\text{IV.42})$$

$$u_2 = G_{21} \delta L u_2. \quad (\text{IV.43})$$

Thus the displacements of the atoms in the space of δL are obtained from the solution of a set of $3n$ homogeneous equations in the $3n$ unknown displacement

components of these atoms.

The condition that (9) have a non-trivial solution is

$$\Delta(\omega^2) \equiv |\mathbb{I} - g\delta\mathbb{U}| = 0. \quad (\text{IV.44})$$

The roots of this equation are the frequencies of those normal modes of the crystal which are perturbed by the introduction of the impurity. This equation shows that not all modes are perturbed by the presence of the impurity. Since the determinant of a product of two matrices is the product of their individual determinants,

$$|\mathbb{U} - \delta\mathbb{U}| = |\mathbb{U}| |\mathbb{I} - \mathbb{G}\delta\mathbb{U}|. \quad (\text{IV.45})$$

Therefore,

$$\Delta(\omega^2) = |\mathbb{I} - \mathbb{G}\delta\mathbb{U}| = \frac{|\mathbb{U} - \delta\mathbb{U}|}{|\mathbb{U}|}, \quad (\text{IV.46})$$

$$= \frac{|\mathbb{M}^{\frac{1}{2}} (\omega^2 \mathbb{I} - \mathbb{D}) \mathbb{M}^{\frac{1}{2}}|}{|\mathbb{M}_0^{\frac{1}{2}} (\omega^2 \mathbb{I} - \mathbb{D}_0) \mathbb{M}_0^{\frac{1}{2}}|}, \quad (\text{IV.47})$$

$$= \left| \frac{\mathbb{M}}{\mathbb{M}_0} \right| \prod_s \frac{\omega^2 - \omega_s^2}{\omega^2 - \omega_{0s}^2}, \quad (\text{IV.48})$$

where (48) follows from (47) due to the fact that the square of the frequencies of the lattice are eigenvalues of the dynamical matrix. The normal mode frequencies of the unperturbed crystal have been denoted by ω_{0s} .

Eq. (48) shows that only those modes of the crystal which are perturbed by the introduction of the defect contribute zeros to the determinant $|\Delta(\omega^2)|$. The factors in the product on the right-hand side of (48) which correspond to the unperturbed normal modes cancel. This shows that not all of the modes are perturbed.

To proceed with the equations of motion, the elements of the dynamical

matrix for the perturbed crystal are given by

$$D_{\alpha\beta}(\ell\ell') = \frac{\Phi_{\alpha\beta}(\ell\ell')}{(M_{\ell\mu} M_{\ell'\mu'})^{1/2}} \quad (IV.49)$$

Because the modes of the perturbed crystal can no longer be labelled by a wave vector \vec{q} and branch index j (translational invariance and Bloch's theorem being no longer applicable), the modes are usually labelled simply by an index r running from 1 to $3sN$. The eigenvalue equations for the perturbed crystal are then

$$\sum_{\ell\mu\beta} D_{\alpha\beta}(\ell\ell') B_{\beta}^{(\ell')}(\ell') = \omega_r^2 B_{\alpha}^{(r)}(\ell) \quad (IV.50)$$

The matrix D is still real and symmetric so that $\{B_{\alpha}^{(r)}(\ell)\}$ may be chosen to be real, and orthonormal. Then

$$\sum_{\ell\mu\beta} B_{\alpha}^{(r)}(\ell) B_{\alpha}^{(r')}(\ell) = \delta_{rr'} \quad (IV.51)$$

$$\sum_r B_{\alpha}^{(r)}(\ell) B_{\beta}^{(r)}(\ell') = \delta_{\ell\ell'} \delta_{\mu\mu'} \delta_{\alpha\beta} \quad (IV.52)$$

The reduced amplitudes $\{u_{\alpha}^{(r)}(\ell)\}$ defined by

$$u_{\alpha}^{(r)}(\ell) = \frac{B_{\alpha}^{(r)}(\ell)}{(M_{\ell\mu})^{1/2}} \quad (IV.53)$$

are the displacement amplitudes of the perturbed crystal vibrating in the r^{th} normal mode.

For those modes of the crystal which do not feel the presence of the impurity atom, the conditions

$$(\delta u) u = 0 \quad (IV.54a)$$

$$u u = 0 \quad (IV.54b)$$

must be simultaneously satisfied for the amplitudes of the atoms vibrating in each mode of this type. The atomic displacements in these modes are thus approximate superpositions of the amplitudes of the unperturbed crystal which satisfy the additional condition (54a). Therefore, the displacement amplitudes given by the solutions of equations (42) and (43) are only for the modes perturbed by the introduction of the impurity into the crystal, whose frequencies are given by eq. (44). The normalization condition for both kinds of modes however is given by Eq. (16) which in terms of U_α becomes

$$\sum_{\ell\mu\alpha} M_{\ell\mu} U_\alpha^{(s)}(\ell)_\mu U_\alpha^{(s')}(\ell)_\mu = \delta_{ss'} \quad (\text{IV.55})$$

However, for those modes which are affected by the introduction of the impurity atom, the normalization condition for the vector $\vec{u}_1^{(s)}$ can be rewritten as a normalization condition for $\vec{U}_1^{(s)}$ in the space of δL .

The spatial dependence of the solutions $\vec{U}^{(s)}$ of (42) and (43) is determined essentially by the dependence of $G_{\alpha\beta}(\ell\mu; \ell'\mu'; \omega^2)$ on the separation between unit cells ℓ and ℓ' . This dependence is different if the perturbed frequency ω_s lies in one of the bands of frequencies allowed to the normal modes of the perfect crystal than when it does not.

Because the elements of the determinant $\Delta(\omega^2)$ whose zeros are the frequencies of the perturbed normal modes are linear combinations of the elements of the Green's function matrix (eq., see eq. (45) and because the Green's function (35) has poles at the unperturbed normal mode frequencies (i.e., $G \rightarrow \infty$ as $\omega \rightarrow \omega_{0s}$), there is in general at least one solution of the equation $\Delta(\omega^2) = 0$ between any two unperturbed frequencies.

It can be shown, as in the linear case, that the displacement amplitudes decay faster than exponentially with increasing distance from the impurity

atom, i.e., the modes are localized. It is also found, in general, that in a three-dimensional crystal localized modes do not occur for arbitrarily small difference between the mass and force constants associated with the impurity atom and the one it replaces. An isotopic impurity, i.e., an impurity which differs from the atom it replaces only in its mass, does not give rise to a high frequency localized mode unless its mass is lighter than that of the atom it replaces by a critical amount which depends on the frequency spectrum of the host crystal [64]. Critical impurity masses also exist for the occurrence of localized modes in a gap in the frequency spectrum of a crystal, and there are critical values of the perturbed force constants which must be exceeded in order that localized modes occur. The mathematical derivation of these conditions are very involved.

It must be noted that though the partitioning gives rise to the matrix $\mathcal{G}\delta\mathcal{L}$ which is smaller in dimension than $\mathcal{G}\delta\mathcal{L}$, even $\mathcal{G}\delta\mathcal{L}$ can be quite formidable in order. In the case of an isotopic impurity in a cubic Bravais crystal with nearest neighbor interaction, $\mathcal{G}\delta\mathcal{L}$ is a 3×3 matrix, proportional to the unit matrix, and the determination of the eigenvectors and eigenvalues is easy. However, if the defect has mass and interactions with nearest neighbors different from the host lattice, the order of $\mathcal{G}\delta\mathcal{L}$ increases considerably. If z is the number of neighbors with which the impurity interacts then $\mathcal{G}\delta\mathcal{L}$ is of order $3(z+1) \times 3(z+1)$ so that in the case of a simple cubic, body-centered cubic or face-centered cubic crystal, $\mathcal{G}\delta\mathcal{L}$ becomes a 21×21 , 27×27 and 39×39 matrix, respectively. In such cases the eigenvalue problem becomes difficult to solve and a systematic approach using group theory becomes essential.

3. Defects with Internal degrees of Freedom:

So far, it has been implicitly assumed that the introduction of the defect did not change the number of degrees of freedom associated with the pure lattice. One could conceivably introduce defects, for instant, as in the experiment where NO_2^- was substituted for Cl^- in KCl [66], where new degrees of freedom are added to the crystal. The generalization of the theory for this case was first worked out by Wagner [67] and is applicable to the case of molecular impurity centers and of interstitial atoms. The main result of the mathematical derivation is that if any of the natural frequencies $\{\omega_k\}$ of the molecular system lie in the band of allowed frequencies for the lattice, the corresponding lattice modes are strongly perturbed - as is to be expected physically from the resonance type of situation.

The use of symmetry and group theory in lattice dynamical defect problems:

For certain derivations, it is convenient to generalize Eq. (IV.42) as a general eigenvalue equation so that

$$\mathfrak{g} d\mathfrak{l} \Psi^{(s)} = \lambda_s \Psi^{(s)}. \quad (\text{IV.56})$$

The eigenvalue λ_s is now a function of ω^2 and comparing (IV.56) and (IV.42) one sees that the determination of the perturbed normal mode frequencies is equivalent to solving the set of equations

$$\lambda_s(\omega^2) = 1, \quad (s = 1, 2, \dots, 3n). \quad (\text{IV.57})$$

Now although \mathfrak{g} and $d\mathfrak{l}$ are separately symmetric in the indices (l, μ, α) and (l', μ', β) , the product $\mathfrak{g} d\mathfrak{l}$ in general need not be symmetric. This leads to

the result that $\psi^{(s)}$ and $\tilde{\psi}^{(s)}$ are not orthogonal vectors. One then has to introduce a set of left-hand eigenvectors $\{\tilde{\zeta}_\alpha^{(s)}(\mathbf{R}_\mu)\}$ such that

$$(\tilde{\zeta}^{(s)})_{\alpha} g_{\mu} d\mu = \lambda_s (\tilde{\zeta}^{(s)})_{\alpha}, \quad (\text{IV.58})$$

where $\zeta^{(s)}$ and $\psi^{(s)}$ have the same eigenvalue λ_s .

It can be shown [52] that $\zeta^{(s)}$ and $\psi^{(s)}$ can be chosen to satisfy the following orthonormality and closure conditions:

$$\sum_{\mathbf{R}_\mu \alpha} \zeta_\alpha^{(s)}(\mathbf{R}_\mu) \psi_\alpha^{(s')}(\mathbf{R}_\mu) = \delta_{ss'}, \quad (\text{IV.59})$$

$$\sum_s \zeta_\alpha^{(s)}(\mathbf{R}_\mu) \psi_\beta^{(s)}(\mathbf{R}'_{\mu'}) = \delta_{\mathbf{R}\mathbf{R}'} \delta_{\mu\mu'} \delta_{\alpha\beta}. \quad (\text{IV.60})$$

This implies that the $(1 \times 3n)$ column matrix $\{\psi^{(s)}\}$ and the $(3n \times 1)$ row matrix $\{\tilde{\zeta}^{(s)}\}$ are inverses of each other.

The inverse matrix $(\Pi - g\delta\mathcal{D})^{-1}$ is required for application to the theory of impurity induced infra-red absorption and Raman scattering. Using the above conditions it can be shown that the left and right hand inverse of this matrix $(\Pi - g\delta\mathcal{D})$ is given by

$$(\Pi - g\delta\mathcal{D})_{\mathbf{R}_\mu \alpha; \mathbf{R}'_{\mu'} \beta}^{-1} = \sum_s \frac{\psi_\alpha^{(s)}(\mathbf{R}_\mu) \tilde{\zeta}_\beta^{(s)}(\mathbf{R}'_{\mu'})}{(1 - \lambda_s)}. \quad (\text{IV.61})$$

It is therefore useful to be able to determine the eigenvalues and eigenvectors of δ .

Despite the fact that the perturbed crystal no longer has translational symmetry the reduced Green's function matrix g in the space of $\delta\mathcal{D}$ transforms in the same way as the complete Green's function matrix G , provided the operations are applied at the lattice site occupied by the impurity atom. That is, g has the symmetry defined by $[S|0]$, where $[S|\vec{\tau}]$ is the space group

of the original crystal. The matrix \mathcal{S} transforms according to some set of symmetry operations (R) depending on the symmetry of the defect. The defect can have a higher symmetry than the host crystal as when the site of the defect still possess the symmetry of the full rotation group (S) of the space group of the host crystal, while the surrounding atoms no longer possess such symmetry. Alternatively, the defect may have lower symmetry, as in the example of a defect introduced substitutionally into a simple cubic crystal with different force constant along x- than along y- and z- directions. The symmetry group \mathcal{V} of the perturbed crystal at the defect site is the intersection of the groups (S) and (R). This group determines the structure of the matrix $A \equiv \mathcal{G}\mathcal{S}\mathcal{Q}$. Often, this matrix is further simplified by special simplifications in the form of \mathcal{S} . For example, it may be assumed that only central force interactions exist between the atoms of the lattice.

Because only the coordinates of the defect atom and the atoms with which it directly interacts appear in the matrix A , it is convenient to picture the defect atom and the atoms with which it interacts as comprising an n-atomic molecule, separated from the rest of the crystal. The conventional techniques of normal mode analysis molecular spectroscopy [3] (also described in detail by Maradudin [52]) then can be followed.

Briefly, the procedure is as follows: One first finds the representation, $\{\Gamma(S)\}$ of the group \mathcal{V} in the basis given by the vector $\{\vec{r}_\alpha(l_\mu)\}$, where $\{\vec{r}_\alpha(l_\mu)\}$ is the displacement of the impurity when all the other atoms are not displaced. This representation is called the total representation. It is then reduced into the irreducible sets $\{\Gamma^{(\sigma)}(S)\}$. With the matrices $\{\Gamma^{(\sigma)}(S)\}$, One can determine the forms of the eigenvectors which transform according to the different irreducible representations contained in the total representation.

B. Impurity-Induced Raman Scattering by Crystals:

Though the first experiment proposed for the study of impurities involved the Mössbauer effect and the first experimental evidence of local modes involved infra-red absorption and neutron scattering, there has been tremendous interest in recent years in the Raman effect as an experimental technique for the investigation of the vibrational properties of crystals containing defects or impurities. This interest has been mainly due to the availability of lasers as excitation sources. At the same time, it is now possible with the aid of high speed computers to determine numerically, on the basis of realistic models, the eigenvalues and eigen functions of impure crystal thus facilitating detailed analysis of their Raman spectra. The first Raman spectra of crystals containing substitutional impurities was obtained by Stekhanov and Eliashberg [69], for KCl crystals doped with Li^+ , Br^- and I^- .

In this section, the modifications in the Raman spectrum of a crystal caused by the introduction of impurities are outlined. The development is drawn mainly from the articles by Maradudin et al., [53], [68].

A crystal loses its translational invariance when an impurity is introduced. Recalling the development of the theory of Raman effect in crystals, it is evident that this implies the $\vec{q} = 0$ selection rule no longer holds for the imperfect crystal. In other words, the phonons involved in Raman scattering may lie anywhere in the Brillouin zone for this case. Thus there are two types of effects caused by the introduction of the impurity.

(a) Impurities make it possible to induce first-order Raman scattering processes with a continuous spectrum in crystals in which, in the absence of impurities, none are possible.

(b) The line spectrum in those crystals in which a first-order Raman

effect exists in the absence of defects, may be replaced by a continuous spectrum, which reflects the singularities in the frequency spectrum of the perfect host crystal, as well as resonance or localized modes if impurities are present and possess the appropriate symmetry.

The theory is based on the method of Born developed in Sec IB. According to eq. (I.63) the intensity of Raman scattering per unit solid angle is given by

$$I(\omega) = \frac{\omega_0^4}{2\pi c^3} \sum_{\alpha\beta, \gamma\lambda} e_\alpha e_\beta i_{\alpha\gamma, \beta\lambda}^{(\Omega)} E_\gamma^- E_\lambda^+, \quad (\text{IV.62})$$

where Ω denotes the phonon frequency involved in the scattering. In the case of discrete states, as has already been mentioned

$$i_{\alpha\gamma, \beta\lambda}^{(\Omega)} = \sum_{mn} [\exp(-\beta E_m)/Z] \langle m | P_{\beta\lambda} | n \rangle \langle n | P_{\alpha\gamma}^* | m \rangle \times \delta(\Omega - \frac{1}{\hbar}(E_m - E_n)) \quad (\text{IV.63})$$

or, equivalently, in integral form,

$$i_{\alpha\gamma, \beta\lambda}^{(\Omega)} = \frac{1}{2\pi} \int_{-\infty}^{\infty} dt e^{-i\Omega t} \langle P_{\beta\lambda}(t) P_{\alpha\gamma}^*(0) \rangle. \quad (\text{IV.64})$$

In considering first-order scattering one is interested only in the term $\sum_{\ell\mu\sigma} P_{\alpha\beta}^\sigma(\ell_\mu) U_\sigma(\ell_\mu)$ in the expansion of the polarizability $P_{\alpha\beta}$ in terms of atomic displacements U_σ . Then the intensity of light scattered by the one-phonon (first-order Raman) process is governed by the function

$$i_{\alpha\gamma, \beta\lambda}^{(\Omega)} = \sum_{\substack{\ell\mu\sigma \\ \ell'\mu'\rho}} P_{\alpha\gamma}^\sigma(\ell_\mu) P_{\beta\lambda}^\rho(\ell'_\mu) I_{\sigma\rho}(\ell_\mu, \ell'_\mu; \omega), \quad (\text{IV.65})$$

where

$$I_{\sigma\rho}(\ell_\mu, \ell'_\mu; \omega) \equiv \frac{1}{2\pi} \int_{-\infty}^{\infty} dt e^{-i\omega t} \langle U_\sigma(\ell_\mu; t) U_\rho(\ell'_\mu; 0) \rangle$$

with $\langle \rangle$ denoting the displacement correlation function [See Maradudin [53b]].

The components of the ionic displacements can be expressed [(53b) p. 287] in terms of phonon creation and annihilation operations b_s^\dagger and b_s for the perturbed crystal, as

$$U_{\alpha}^{(\ell)} = \left(\frac{\hbar}{2M_{\ell\mu}} \right)^{1/2} \sum_s \frac{B_{\alpha}^{(s)}(\ell)}{(\omega_s)^{1/2}} (b_s + b_s^\dagger), \quad (\text{IV.66})$$

where $B_{\alpha}^{(s)}(\ell)$ are the normal coordinates of the perturbed crystal given by eq. (IV.50).

The Heisenberg representations of b_s^\dagger and b_s are given by

$$\begin{aligned} b_s(t) &= e^{iHt/\hbar} b_s e^{-iHt/\hbar} = b_s e^{-i\omega_s t}, \\ b_s^\dagger(t) &= e^{iHt/\hbar} b_s^\dagger e^{-iHt/\hbar} = b_s^\dagger e^{i\omega_s t}, \end{aligned} \quad (\text{IV.67})$$

where H is the Hamiltonian for the perturbed crystal. For a canonical distribution the time thermal averages of their products are given by

$$\begin{aligned} \langle b_s^\dagger b_{s'} \rangle &= \delta_{ss'} n_s; \quad \langle b_s b_{s'}^\dagger \rangle = \delta_{ss'} \{n_s + 1\} \\ \langle b_s b_{s'} \rangle &= \langle b_s^\dagger b_{s'}^\dagger \rangle = 0, \end{aligned} \quad (\text{IV.68})$$

where n_s is the Bose distribution function

$$n_s = n(\omega_s) = \left\{ \exp\left(\frac{\hbar\omega_s}{kT}\right) - 1 \right\}^{-1}. \quad (\text{IV.69})$$

If the ionic displacement is replaced by the expansion and use is made of the properties of the creation and annihilation operators, one gets, after a considerable amount of work

$$\begin{aligned} I_{\sigma\rho}(\ell\mu, \ell'\mu'; \omega) &= \left(\frac{\hbar n(\omega)}{(M_{\ell\mu} M_{\ell'\mu'})} \right)^{1/2} \left(\sinh \omega \right) \sum_s B_{\sigma}^{(s)}(\ell)_{\mu} B_{\rho}^{(s)}(\ell')_{\mu'} \delta(\omega^2 - \omega_s^2) \\ &= \frac{\hbar n(\omega)}{(M_{\ell\mu} M_{\ell'\mu'})}^{1/2} \sinh \omega \, I_m U_{\sigma\rho}(\ell\mu, \ell'\mu'; \omega^2 - i0). \end{aligned} \quad (\text{IV.70})$$

Here, the notation $f(\omega^2 - i0)$ stands for $\lim_{\epsilon \rightarrow 0} f(\omega^2 - i\epsilon)$, while $U_{\mu\nu}$ is the Green's function matrix for the perturbed crystal, i.e., the elements of $\mathcal{U} = (\mathbb{U} - \epsilon \mathbb{U})^{-1}$. It is given by

$$U_{\sigma\rho}(\ell_\mu, \ell'_\mu; \omega^2) = \frac{1}{(M_{\ell_\mu} M_{\ell'_\mu})}^{1/2} \sum_S \frac{B_\sigma^{(S)}(\ell_\mu) B_\sigma^{(S)}(\ell'_\mu)}{\omega^2 - \omega_S^2}. \quad (\text{IV.71})$$

Now, $i_{\alpha\gamma, \beta\lambda}$ can be written as

$$i_{\alpha\gamma, \beta\lambda}(\omega) = \left(\frac{\hbar n(\omega)}{\pi} \right) \left(\sin h \omega \right) \sum_{\substack{\ell_\mu \sigma \\ \ell'_\mu \sigma}} P_{\alpha\gamma}^\sigma(\ell_\mu) P_{\beta\lambda}^\sigma(\ell'_\mu) I_m U_{\sigma\rho}(\ell_\mu, \ell'_\mu; \omega^2 - i0). \quad (\text{IV.72})$$

This result is general and relevant for any crystal containing defects. Its actual evaluation, however, requires explicit knowledge of the electronic wave functions (for the evaluation of $P_{\alpha\gamma}^\sigma$) as well as the vibrational eigenfrequencies and eigenfunctions of the perturbed crystal. Therefore, some approximation based on a model is necessary before one can proceed further.

Maradudin et. al [68] have applied this theory to the case of a rocksalt structure, assuming the impurity interacts only with its six nearest neighbors. The impurity is still at a center of inversion but the neighbors no longer possess this symmetry and for these, the coefficients $P_{\alpha\gamma}^\sigma(\ell_\mu)$ no longer vanish, unlike the case of the pure cubic crystal. Application of group theory helps in the reduction of this third order tensor. If an impurity induced first-order spectrum with its polarization dependence can be observed experimentally, the values of the elements of the tensor can be inferred.

One advantage possessed by first-order Raman scattering experiments in comparison with infrared lattice vibration absorption experiments is that they can give information about the symmetry properties of the vibration modes responsible for the scattering. For instance in the case of scattering

by H^- impurities in KCl (), it was found that only modes of A_{1g} symmetry contribute to $i_{xx,xx} + 2 i_{xx,yy}$, only E_g modes contribute to $i_{xx,xx} - i_{xx,yy}$ and only F_{2g} modes contribute to $i_{xy,xy}$. Therefore, modes of definite symmetry in a perturbed crystal can be studied with suitable experimental arrangements - viz., particular crystal orientations and polarization of incident and scattered light.

In the case of crystals which display a first-order Raman spectrum in the absence of impurities, the principal effect of introducing impurities into the crystal is to replace the line spectrum by a continuous spectrum, since in general $I_m U_{\alpha\beta}(\ell_\mu; \ell'_\mu; \omega^2 - i0)$ is a continuous function of ω . The details are worked out by Maradudin [68] and will not be repeated here.

V. COLOR CENTERS IN AZIDES AS AN EXAMPLE

A. INTRODUCTION

Solid inorganic azides have formed the subject of extensive study both by chemists and physicists. The stability of azides vary over wide limits and many of them can be decomposed readily on exposure to heat, light or ionizing radiations. Most studies by chemists have been aimed at understanding the mechanism of decomposition [70, 71, 72]. The alkali metal azides which form the subject of the present work are relatively stable, while the azides of silver and copper readily decompose.

The azide radical N_3 has been found to play an important role in the damaging of azide crystals - both in the cases of photochemical decomposition and irradiation coloring. In fact, color center formation has been proposed as an intermediate step in decomposition process [73]. The infra-red spectra of irradiated alkali metal azides have been studied [74,75] with a view to understanding the N_3 radical structure. These studies and the electron spin-resonance studies [76,77] have led to the proposal of different models. In the latest of the infra-red studies, Bryant [4] suggests a triangular structure for the azide ion in the irradiated crystal. The structure of the defect N_3 is still a subject of controversy. The earlier experimental and theoretical situation is summarized in the review articles by Gray [78] and Yoffe [79].

The study of Raman spectra of pure and irradiated single crystals of azides was undertaken for several reasons. The color center in the azide system is apparently a simple defect and can be used as an example to study the nature of Raman scattering by defects. This is facilitated by the fact that the Raman spectrum of the pure azide is simple and consists only of a

few lines so that lines arising from the color center modes should be easily discerned. Furthermore, the Raman spectra of irradiated single crystal azides have not been studied and a detailed study of the polarization dependence and frequency of the N_3 vibration may help to establish the nature of the defect conclusively.

1. Color Centers in Azides

Transparent crystals like alkali halides are found to develop color on prolonged exposure to ultra-violet, X or γ -irradiation or when heated in the vapor of a metal or hydrogen. It is to be expected that any defect induced in the crystal by these treatments will alter the charge distribution and change the electronic levels in the vicinity of such defects. This would then bring about changes in the electronic absorption spectra and give rise to new absorption bands. The defects producing a "coloring" of the crystal due to these absorption bands are called "color centers". "A color center is a lattice defect which absorbs visible light", as defined by Kittel [13, p. 572]. Almost all the work on color centers have been done on the alkali halides as these are the simplest diatomic ionic crystals, and are transparent to visible radiation. Hence the classification of centers into F-, M-, R-, V- and U- types of centers is based on the different characteristic types of alkali halide color centers. The F-center which is the simplest prototype, has been studied most extensively. It is well-established that the F-center consists of a negative-ion vacancy in which an electron has been trapped. A V-center, which is the other type of color center with relevance to the azide problem, is poorly understood inspite of extensive study. The usual model for the V-center is that of a "self-trapped" hole. Extensive descriptions

of color centers and their properties are given in a recent book edited by Fowler [80].

In spite of the structural dissimilarities between alkali azides and alkali halides, both NaN_3 and KN_3 show remarkable similarities with the corresponding halides in the formation of color centers. It has thus become common practice to consider azides as being analogous to the alkali halides with the halogen ion replaced by the azide ion and to assign models for the color centers based on the types of centers obtained in the halides.

Considerable variation has been found in the position, half-width and temperature behavior of color center bands in the alkali azides depending on the nature of the irradiation producing these centers. Various detailed investigations have been carried out, mainly of infrared and optical absorption spectra of polycrystalline azides using x-ray [72], ultra-violet [74] and γ [81] radiation. Only color centers produced by ultra-violet radiation are considered in the present study.

A variety of techniques have been used to study the nature of the ground states of color centers. Since most color centers involve an unpaired electron or hole in a bound state, electron spin resonance and electron-nuclear double resonance (ENDOR) form a useful technique for their study [80, Chap. 8]. The centers in ultra-violet irradiated NaN_3 have been studied by King et. al. [82] and those in KN_3 by Horst and co-workers [76] using ESR techniques. The most widely used technique is, of course, the study of optical absorption spectra [83].

However the typical color center absorption lines are broad and structureless. The breadth arises because of the interactions with the phonons or lattice vibrations. These have the effect of producing a random distribution of

local strains in the lattice so that no two centers have quite identical surroundings. This random distribution then gives rise to the typical roughly Gaussian shape of color-center optical spectra. Thus the effect of the lattice vibrations on the color centers are not easily derived from an analysis of the optical spectra.

It is in this context that Raman spectroscopy is likely to become perhaps the most powerful technique of studying color centers. Kleinman [84] proposed that a study of the Raman effect of the F-center in an alkali halide like KCl would yield information about the coupling of the color center to the lattice. He also suggested the possibility of operating advantageously in a resonance Raman region by using an exciting wavelength in the F-band. However, since the F-band is extremely broad and the resonance condition will also imply strong absorption of incident and scattered waves in the sample, there is no likelihood of a great enhancement of the scattered intensity over the non-resonant case. The only measurements of Raman scattering by color centers are that of Warlock and Porto [43] who observed first-order Raman scattering by F-centers in NaCl and KCl and the work of Mitra [85] who observed Raman scattering in additively colored MgO. The spectrum observed by Porto must be due to the vibrations associated with a color center since in a perfect alkali-halide crystal, there is no first-order Raman scattering. However their data is not sufficiently detailed to determine the extent to which the vibrations causing the Raman scattering broaden the F-band. Recently, Henry [86] has shown that Raman scattering gives a direct measurement of the frequency spectrum of the lattice since a given vibrational mode contributes to the total Raman scattering cross-section in direct proportion to its contribution to $\langle E^2 \rangle_{\text{lattice}}$, i.e., the second moment or mean-square energy of a phonon-broadened absorption band. Thus the spectrum of frequencies

measured by Warlock and Porto is just the spectrum of frequencies that broaden the F-band. Though in a complete analysis of the optical absorption spectra, these characteristics of the Raman spectrum would prove useful, the object of the present work is to use Raman spectroscopy to determine the configuration and symmetry of the color centers in the alkali azides. In addition to the features described above, Raman scattering permits one to observe an event in which only one lattice frequency is excited whereas optical absorption generally excites all the lattice frequencies simultaneously.

2. Crystal Growth

Flawless single crystals of alkali azides are not easy to grow! Of the usual methods of crystal growing - from melt, from solution or by black magic - the first method is inapplicable since azides detonate and decompose at their melting point. A combination of the last two methods seem to be the best. The solubility of the azides in water as a function of temperature were studied in order to determine the suitable temperature of growth. The solubility was found to be 50 gms of KN_3 per 100 cc and 42 gms of NaN_3 per 100 cc at a temperature of 20°C . The solubility increased very slowly for KN_3 and RbN_3 near 20°C , but quite radically after approximately $25\text{--}30^\circ\text{C}$ at the rate of about 5 gms/100 cc/ 5°C . In the case of NaN_3 , it was found that the solubility varied with about the same temperature coefficient from about 20°C to 40°C , but had a plateau around 45°C . Thus it seems better to grow KN_3 and RbN_3 crystals around 20°C and NaN_3 crystals around 45°C by a constant temperature evaporation method than by cooling as is usually done in sealed-jar methods.

KN_3 and RbN_3 grow in the form of flat crystals, the fastest rate of growth being parallel to the (001) plane of the tetragonal unit cell if the evaporation

is exceedingly slow and takes place from a large flat surface at a constant temperature. In fast evaporations, however, competing growth of the (101) family of planes tend to give pyramidal crystals. This tendency was a feature in crystals grown by seeding solutions also. As two plane faces at right angles to each other are needed for the Raman experiments, the pyramidal structure was a major disadvantage. This is because none of the growth faces are of the (100) family in this case and two faces will have to be polished then. The crystals are brittle, small, and very difficult to polish. Fast evaporation and seeding a water solution also tended to make the crystals translucent due to inclusion of water. Such trapped water could be observed bubbling out when these crystals were annealed. The technique of diffusion of acetone or ethanol used by Marinkas [87] for growing anhydrous $\text{Ba}(\text{N}_3)_2$ single crystals was tried since it was a constant temperature method but failed to yield clear crystals except for RbN_3 . For this method, a temperature of approximately 15°C was found suitable for RbN_3 . The gel method of Henisch [88] was found to be inapplicable because all the acids usually used for acidifying the gel e.g., tartaric acid, acetic acid, reacted with KN_3 displacing the N_3 radical and giving clear crystals of potassium tartrate acetate etc. The method that finally yielded perfect transparent single crystals of KN_3 was the evaporation of a solution just below saturation (50 gms in 110 cc of distilled water at 20°C) in a dessicator at 20°C . The solution was placed in a glass dish approximately 4" in diameter and the evaporation rate controlled by holes in the lid. The evaporation took place over six months. This yielded numerous good crystals.

NaN_3 crystals grow in film-like layers on the top of the solution and

are fragile and brittle. In this case a small surface area of evaporation was preferred to promote the growth of a single crystal film, since larger surfaces tend to form fragments rather than one single crystal. The best crystals were obtained by evaporating the solution contained in a pyrex test-tube of about 1 cm in diameter placed in a small aluminum furnace whose temperature was maintained constant at 45° by a thermistor temperature controller. Flakes approximately 1 cm in diameter grow over a period of ten days, mostly on the surface of the solution. Sometime, very clear crystals grow in the solution and these should be removed as soon as they reach a sufficient area. Leaving them for a longer period in the solution gives rise to stacks of laminae that were difficult to separate. In spite of these precautions, the NaN_3 crystals appear twinned.

3. Crystal Structure of Azides: [90,91,92]

Potassium, rubidium and cesium azides all possess the tetragonal structure while sodium azides is rhombohedral. Thus the azides with the larger ions (K,Rb,Cs) have eight-fold coordination, while for the smaller cation (Na) the coordination number changes to 6. The azide group N_3 is linear in all the azides. In the ionic azides, it appears as the N_3^- ion. In the perfect crystal it possesses a linear symmetry.

Sodium azide is rhombohedral with the unit cell as illustrated in Fig. 7a and belongs to the space group D_{3d}^5 (R m). [90],[92]. There is a sodium ion at the corners of the unit cell and the azide ion is arranged along the body diagonal (direction $[111]$) of the cell. Each N_3^- ion has six nearest - neighbor sodium ions at a distance 3.28 Å from its center. The layer-growth structure is one in which the sodium ions and the azide ions separate

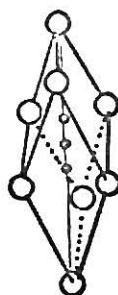
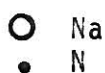
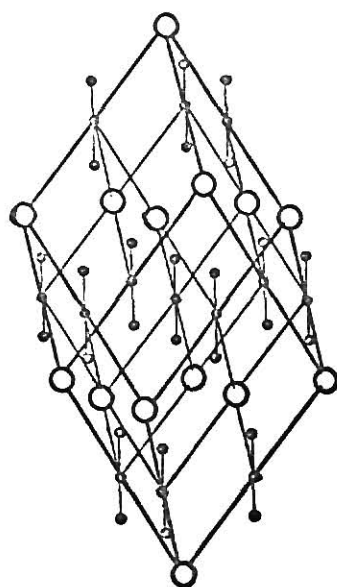
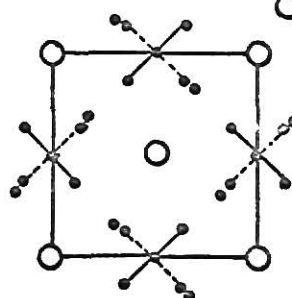
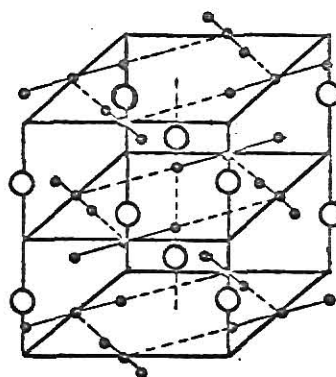


Fig. 7a. Models of the structure and unit of structure of sodium azide single crystals.

Fig. 7b. Model of the structure of CsN_3 crystals.



into parallel planes perpendicular to the (111) direction. Thus the Nye z-axis [50] is perpendicular to the flake. Being a rhombohedral crystal, the Nye x and y axes can be chosen as two arbitrarily perpendicular vectors in the plane of the film.

The structure of Potassium and Rubidium azide is illustrated in Fig. 7. These crystals possess the tetragonal structure with a $\left(\frac{c}{a}\right)$ ratio close to 1, and belong to the space group D_{4h}^{18} (I 4/mcm) [90], [92]. Fig. (7,b) gives the projection on to the (001) plane. The azide groups lie in planes parallel to (001) and inclined at an angle of 45° to the (100) plane. The crystallographic data drawn from Ref.4[90,91,92] are summarized in Table I for easy reference.

The growth habit of KN_3 crystals clearly indicates the four-fold (or C-) axis of the tetragonal structure. This then would be the Nye Z-axis. In the (001) growth face of the crystal however, the Nye axis could be chosen in two ways (x,y) or (x',y') as shown in Fig. (8). It is important to determine which of these are coincident with the x-ray crystallographic conventional axes (x,y) so that the Raman tensors given by Loudon [35c] could be used without ambiguity, especially in trying to classify the

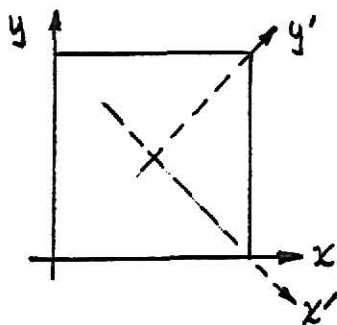


Fig. 8 . Crystal Axes

N_3 internal vibrations. The determination of the orientation of the x-ray crystallographic axes with respect to the growth face was accomplished by means of a Laue back-reflection photograph. The $\left(\frac{c}{a}\right)$ ratio for KN_3 is 1.14 and

Table I

Compound	Crystal Class	Cell Constants	Molecules per unit cell	Co-ordination	N-N distance(A)	M-NIII distance(A)
NaN_3	Body-centered rhombohedral	$a_0 = 5.488\text{\AA}$ $\alpha_0 = 38^\circ 43'$	1	6:6	1.17	2.48
KN_3	Boyd-centered tetragonal	$a_0 = 6.094$ $c_0 = 7.056$	4	8:8	1.16	2.96
RbN_3	"	$a_0 = 6.36$ $c_0 = 7.41$	4	8:8	1.13	3.11
CsN_3	"	$a_0 = 6.72$ $c_0 = 8.04$	4	8:8		3.34

is thus close enough to 1 to enable the orientation to be determined using the cubic stereographic projection once a few Laue spots were indexed. It was thus found that the crystallographic a-b axes coincided with the set (x;y) shown in the figure and not with (x'y'). Nature occasionally smiles down on the investigator.

Note, however, that the crystallographic axes of KN_3 and RbN_3 are at 45° to the azide ion. This is an important point that arises in studying the polarization properties of Raman spectra.

The Raman tensors for the crystal symmetry classes D_{3d} and D_{4h} are reproduced below from Loudon [35] for convenience of reference.

$$\begin{array}{ccc}
 & D_{3d} & \\
 \begin{pmatrix} a & 0 & 0 \\ 0 & a & 0 \\ 0 & 0 & b \end{pmatrix} & \begin{pmatrix} c & 0 & 0 \\ 0 & -c & d \\ 0 & d & 0 \end{pmatrix} & \begin{pmatrix} 0 & -c & -d \\ -c & 0 & 0 \\ -d & 0 & 0 \end{pmatrix} \\
 A_{1g} & E_g & E_g
 \end{array}$$

$$\begin{array}{ccccc}
 & D_{4h} & & & \\
 \begin{pmatrix} a & 0 & 0 \\ 0 & a & 0 \\ 0 & 0 & b \end{pmatrix} & \begin{pmatrix} c & 0 & 0 \\ 0 & -c & 0 \\ 0 & 0 & 0 \end{pmatrix} & \begin{pmatrix} 0 & d & 0 \\ d & 0 & 0 \\ 0 & 0 & 0 \end{pmatrix} & \begin{pmatrix} 0 & 0 & e \\ 0 & 0 & 0 \\ e & 0 & 0 \end{pmatrix} & \begin{pmatrix} 0 & 0 & 0 \\ 0 & 0 & e \\ e & 0 & 0 \end{pmatrix} \\
 A_{1g} & B_{1g} & B_{2g} & E_g & E_g
 \end{array}$$

B. Electronic Spectra of Ultra-violet Irradiated KN_3 and NaN_3 :

The optical absorption spectra of colored KN_3 and NaN_3 were studied in the region 3000-7400 Å to observe the growth of the absorption bands in this region corresponding to different centers as a function of the irradiation time. The behavior of these bands was observed also on warming up the crystal.

The crystal was sandwiched between two copper plates with circular apertures about 2 mm in diameter, and placed in a crystal-holder of a Helium Dewar. This dewar was used at liquid nitrogen temperatures and above. The irradiation was done using a Pen-Ray mercury lamp placed close to the circular quartz window of the Dewar so that radiation from approximately $\frac{3}{4}$ in length of the lamp fell on the crystal. This placed the lamp 1-1/2" from the crystal. The set-up was identical for different irradiations.

A Quartz-iodine standard lamp was used as a continuous source of constant intensity to record the absorption spectra. The light from the lamp was focussed onto the crystal by means of a glass lens. This glass lens also served to filter out any ultra-violet radiation in the standard lamp spectrum which might have continued to damage the crystal while the spectrum was being recorded. Repeated measurements of the spectrum showed that there was no damaging effects due to the standard lamp. The spectrum was scanned using a Bausch & Lomb 1/2-meter monochrometer with an IP-28 photomultiplier, whose output was fed to a Keithley pico-ammeter. A slit width corresponding to a band-pass of $\sim 4\text{Å}$ was used in all experiments. The spectrum was recorded both on a chart recorder and on a digital printer.

The crystal was essentially in a vacuum, the enclosure containing only the exchange gas Helium at a pressure 20-40 μ in all the experiments. The

crystal was cooled to approximately 85° K and the spectrum $I_0(\lambda)$ of the standard lamp as transmitted through the undamaged crystal was first recorded. The crystal was then irradiated for a specific time interval and the spectrum $I(\lambda)$ transmitted by the damaged crystal was recorded. The optical density $\log_{10} \frac{I_0}{I}$ was then plotted as a function of wavelength for different irradiation times. After a total irradiation time of 2-3 hours, the crystal was allowed to warm up in steps of approximately 25° K. The temperatures are maintained steady and the spectra recorded again at each temperature step. The spectra of the crystals taken at these elevated temperatures yields information on the thermal bleaching of the color centers.

The absorption spectrum of the pure crystal taken photographically showed no absorption for wavelengths greater than 2600 Å and complete absorptions below. The absorption spectra at different stages of coloring and thermal bleaching were repeated with different crystals of KN_3 and NaN_3 . At least part of the damage is permanent. Each crystal could be used only once. The irradiation was carried out both with unfiltered radiation from the Hg pen-ray lamp and with a wavelength of 2537 Å, singled out using an interference filter. There was no difference in the absorption spectra in the two cases. The characteristics of the spectra for a given type of crystal could be reproduced very consistently.

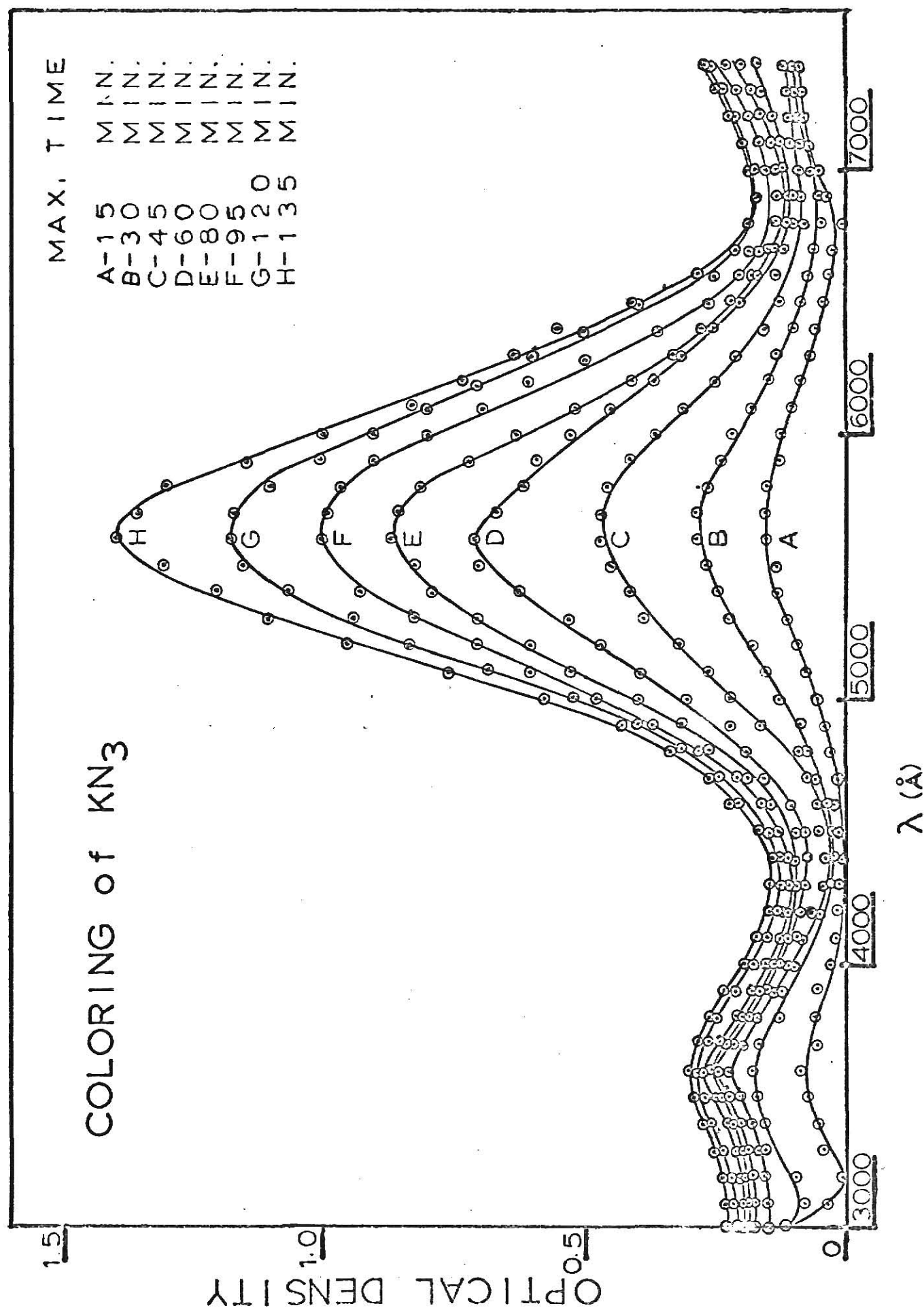
Potassium azide:

A typical spectrum of KN_3 for different times of irradiation is shown in Plate I. Two bands - one centered at 3600 Å and with a half-width of approximately 500 Å and the second centered at 5600 Å and with a half-width 750 Å were found to develop on irradiation. These bands were also found

EXPLANATION OF PLATE I

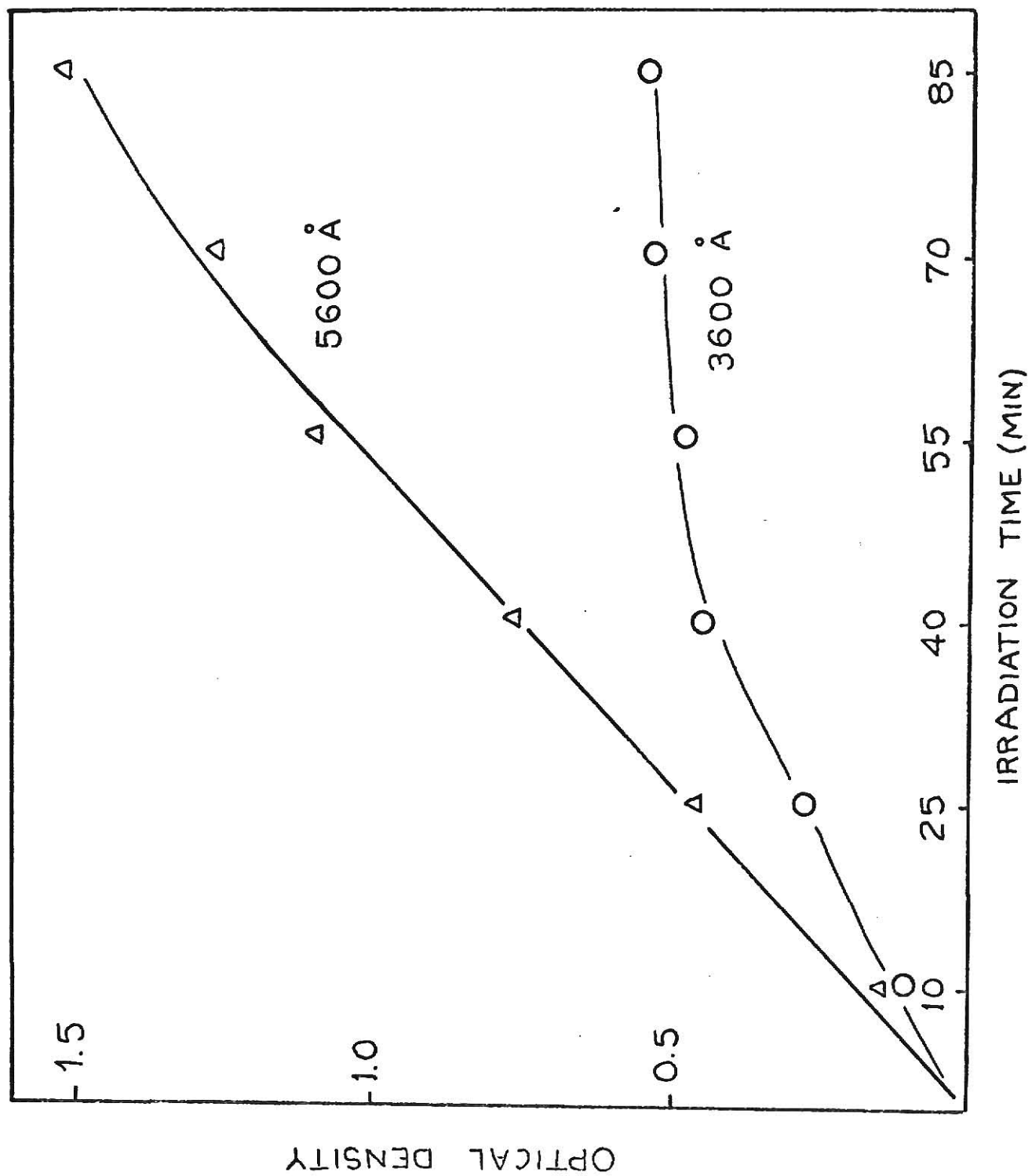
The optical density curves for KN_3 as a function of wavelength and irradiation time.

Plate I



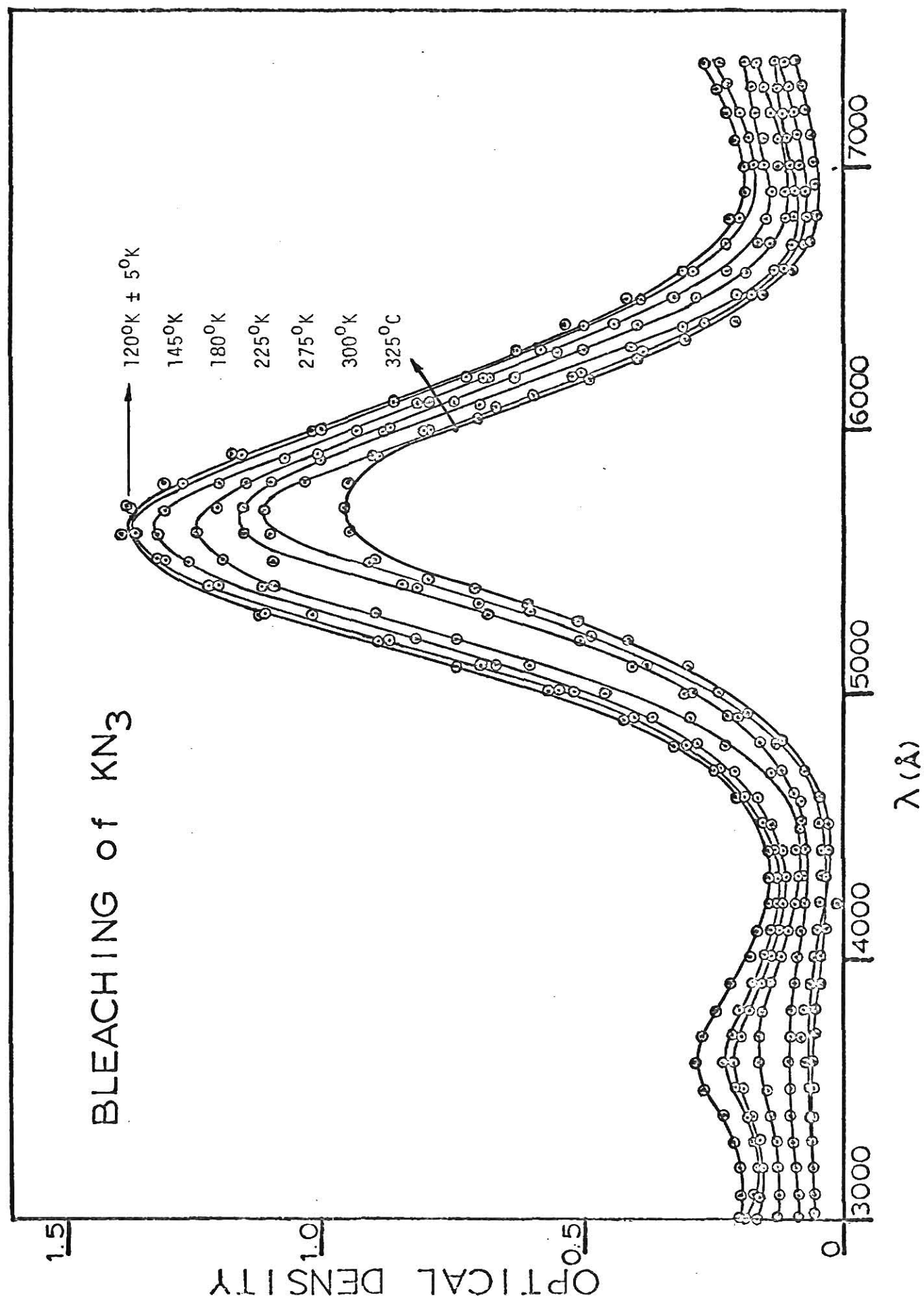
EXPLANATION OF PLATE II

The optical density of the 5600 Å and 3600 Å bands in KN_3 as a function of irradiation time.



EXPLANATION OF PLATE III

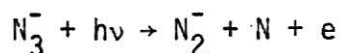
The thermal bleaching of the color bands in KN_3 .



by Papazian [74] and other workers [72], [93].

The 3600 Å band has been called a V-band because of its general behavior. The V-bands in alkali halides have been established to be due to the V-center which consists of a (halogen) $_2^-$ ion on the site of two halogen ions in the lattice and is thus effectively a "self-trapped hole". The V-spectrum of KCl consists of an intense band near 3650 Å and a weak band near 7500 Å. These disappear at higher temperatures.

The 3600 Å band in KN_3 has a remarkably similar behavior as is seen from Plates I, II. It appears on a short irradiation and saturates quickly with continued irradiation. A small rise in optical density was observed at the tail end- above 7000 Å - of the region of measurement but one cannot draw any conclusions regarding this region in the present set-up owing to the limit set by the spectrometer. The bleaching curves show that the V-band also bleaches out quickly at a temperature of 225°K. This behavior has led to the model of this center as being a $\text{N}_3\text{-N}_3^-$ ion in analogy to the halides. Horst et.al., [83], however, proposed a model for the V-centers as N_2^- ion. Their conclusions are drawn from ESR studies that this center consists of N_2^- ions. A mechanism for the formation of N_2^- as conceived by Yoffe [89] in photochemical reactions in azides would be



This mechanism would seem, however, to lead to a permanent damage as the nitrogen could easily diffuse through the lattice and be trapped at vacancies or lost to the crystal. The readiness with which this center bleaches and the crystal reverts to the optical density before irradiation as observed in the present experiments seem to prefer the $\text{N}_3\text{-N}_3^-$ assignment. Such a hole can easily disappear as a result of electron-hole combination, the

crystal then recovering the original state. Also Horst's experiment could have involved a different type of center as γ -rays were used for the irradiation.

The strong band at 6300 Å grows without saturating for a very long time of irradiation and is decreased very little in intensity on warming up. This band has been attributed to an F-type of center by Papazian. According to Papazian, however, the band bleaches at room temperature. This was not the case in the present experiment. The band persisted even at 315°K, and the crystal had acquired a yellowish tinge indicating some type of permanent damage. This behavior resembles that of the analogous centers observed by Horst, who has identified them as a " N_4 center consisting most likely of an unpaired spin associated with a planar configuration of four nitrogen atoms." Shuskus et. al. [95] suggest that this N_4^- ion is formed as a linear tetratomic group along the [110] plane. Bryant in his latest work on the infrared spectrum of damaged KN_3 claims that a cyclic N_3 with a D_{3h} symmetry is the only model entirely consistent with the infrared spectrum. A careful study of polarization behavior of the Raman spectra of the colored crystal as discussed in the last section is needed before any final decision can be made.

Sodium Azide:

Though there are similarities between the absorption spectra of NaN_3 and KN_3 , there are some distinctive differences as seen on comparing Plates I and IV. There is no definite evidence of a V-band and it is difficult to pick out any structure due to the large scatter in the 3000-4000 Å region.

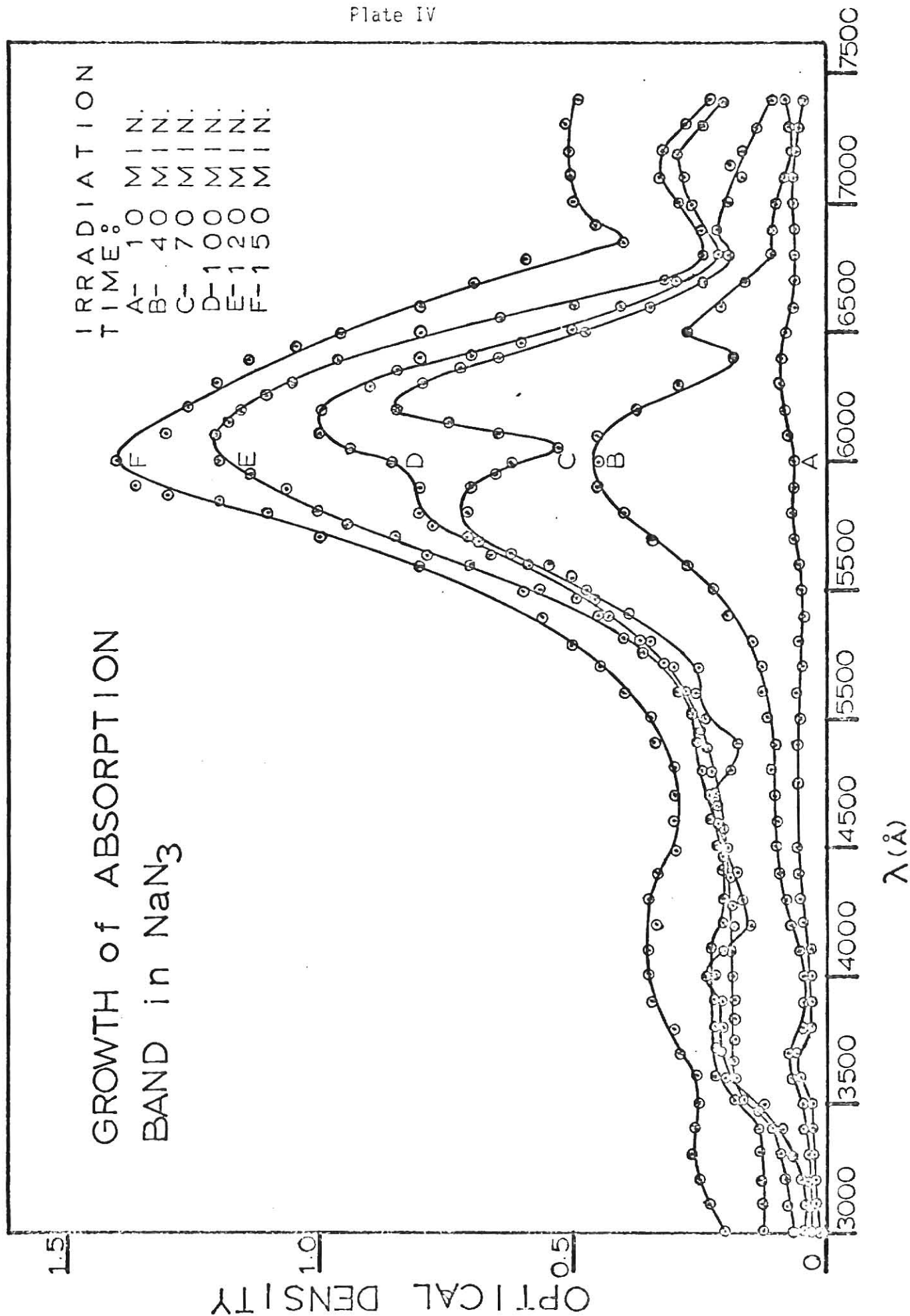
The predominant band is centered around 6000 Å and there seems to be an indication of a band around 7000-7500 Å. Papazian finds bands at 6120 and 7400 Å in NaN_3 . The 6000 Å band in the present experiments consist of two fairly well-resolved bands whose peaks shift with increased irradiation. Very detailed studies would be required before a conclusive explanation of this behavior could be found. It might be relevant to note that considerable change has been observed in the lattice parameter of γ -irradiated NaN_3 [94]. The main effect is a contraction of the structure parallel to the azide ions. There is also evidence of decomposition of x-irradiated NaN_3 [93]. Mechanical strain is also easily induced in these crystals and could arise both as a result of the positioning required in the experiment as well as a result of radiation damage. All these factors have to be considered in detail for a complete description of the color center in NaN_3 .

One distinct and intriguing feature of the NaN_3 band at 6000 Å is that it disappears completely on warming up to room temperature and the crystal appears undamaged and transparent.

Experiments involving very long times of irradiation and an examination of absorption spectra over a broader spectral region should aid in determining the structure of these defects.

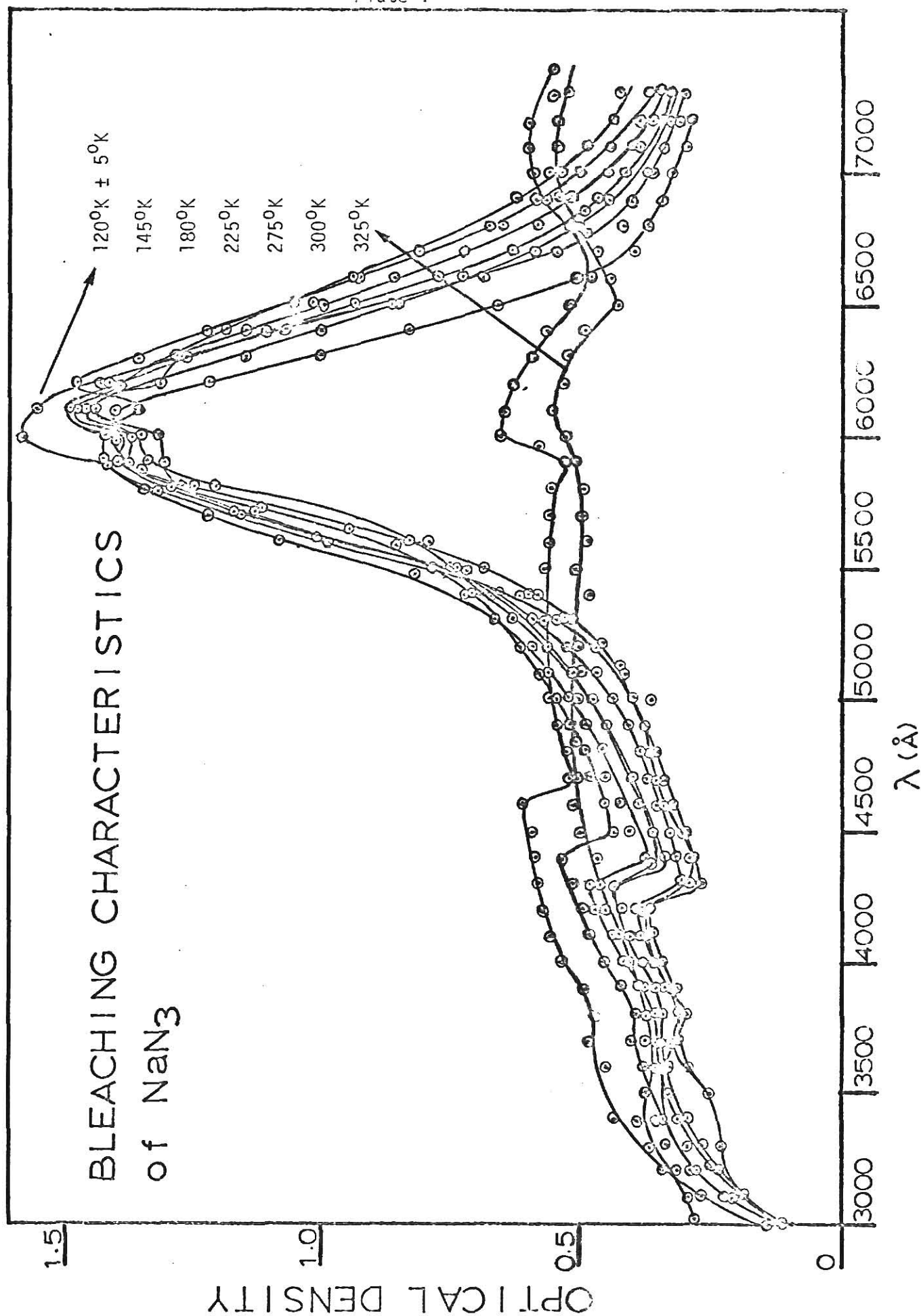
EXPLANATION OF PLATE IV

The optical density curves of NaN_3 as a function of wavelength and irradiation time.



EXPLANATION OF PLATE V

The optical density of the color center in NaN_3 as a function of thermal bleaching.



C. Vibrational Raman Spectra of Pure KN_3 and NaN_3 .

The Raman spectra were recorded using the He-Ne laser as the exciting source. The Raman spectrometer is described in detail by Johnston [96]. As good single crystals were not available at the time the measurements were made, specific crystal orientations could not be chosen. Instead, an optimum crystal setting which gave the best signal-to noise ratio for the Raman spectrum had to be used.

There was a large amount of laser light scattered into the monochromator with these crystals of poor quality. This gave rise to grating ghosts and other instrumental anomalies which could be mistaken for Raman lines. These anomalies were recorded first by scattering a small fraction of the laser light into the monochromator. This problem did not arise with NaN_3 for which clear crystals were available.

The Raman-active vibrations of NaN_3 and KN_3 have been predicted by Bryant [75a] using the "unit-cell" method of Bhagavantam. In the present work, of the three lines predicted for KN_3 and NaN_3 , only the low frequency lattice vibration and the high frequency symmetric stretch of the N_3 ion were observed. These are shown in Fig. (9-10). These data are summarized in Table 2.

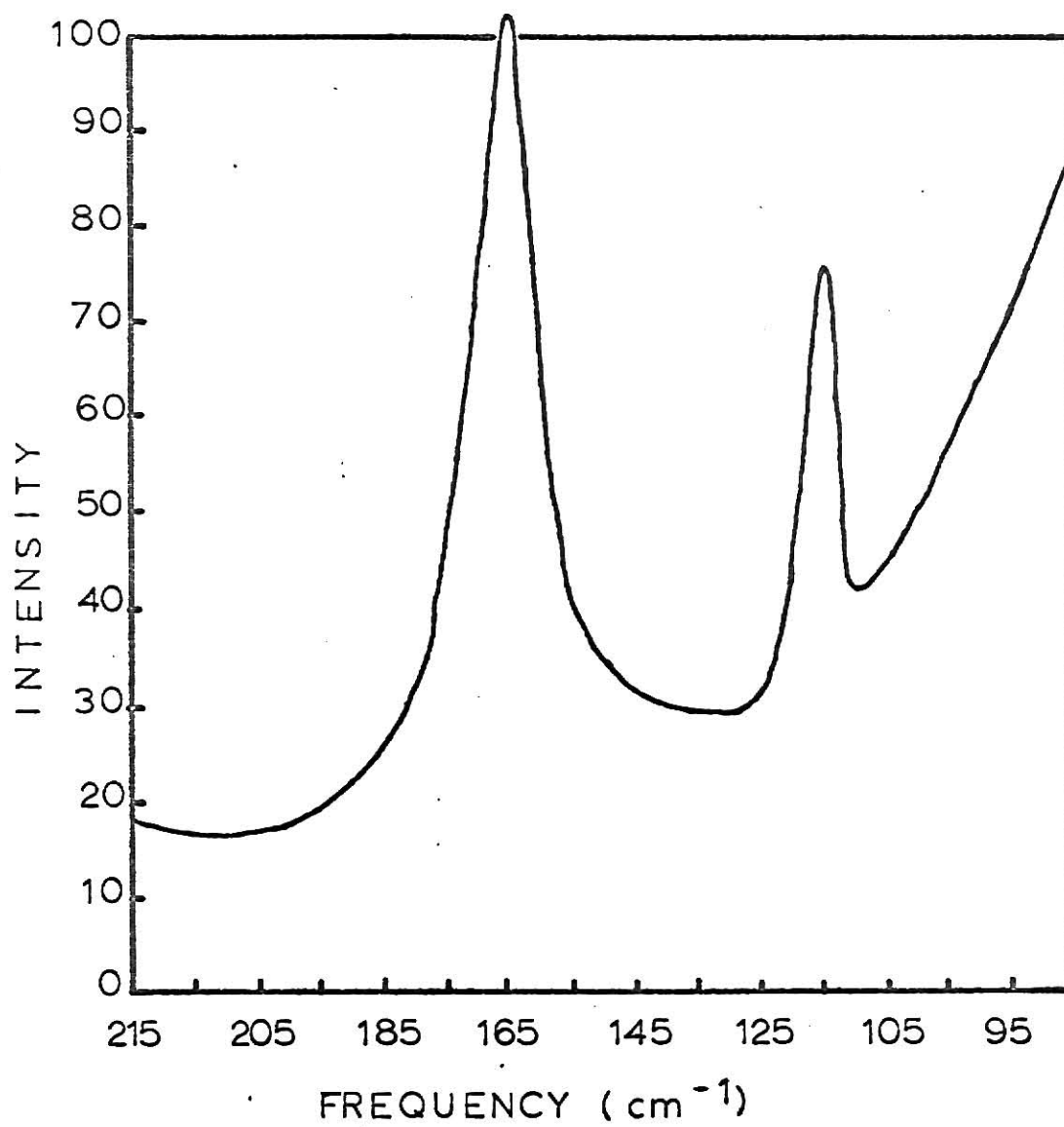


Fig. 9 Raman spectrum of potassium azide.

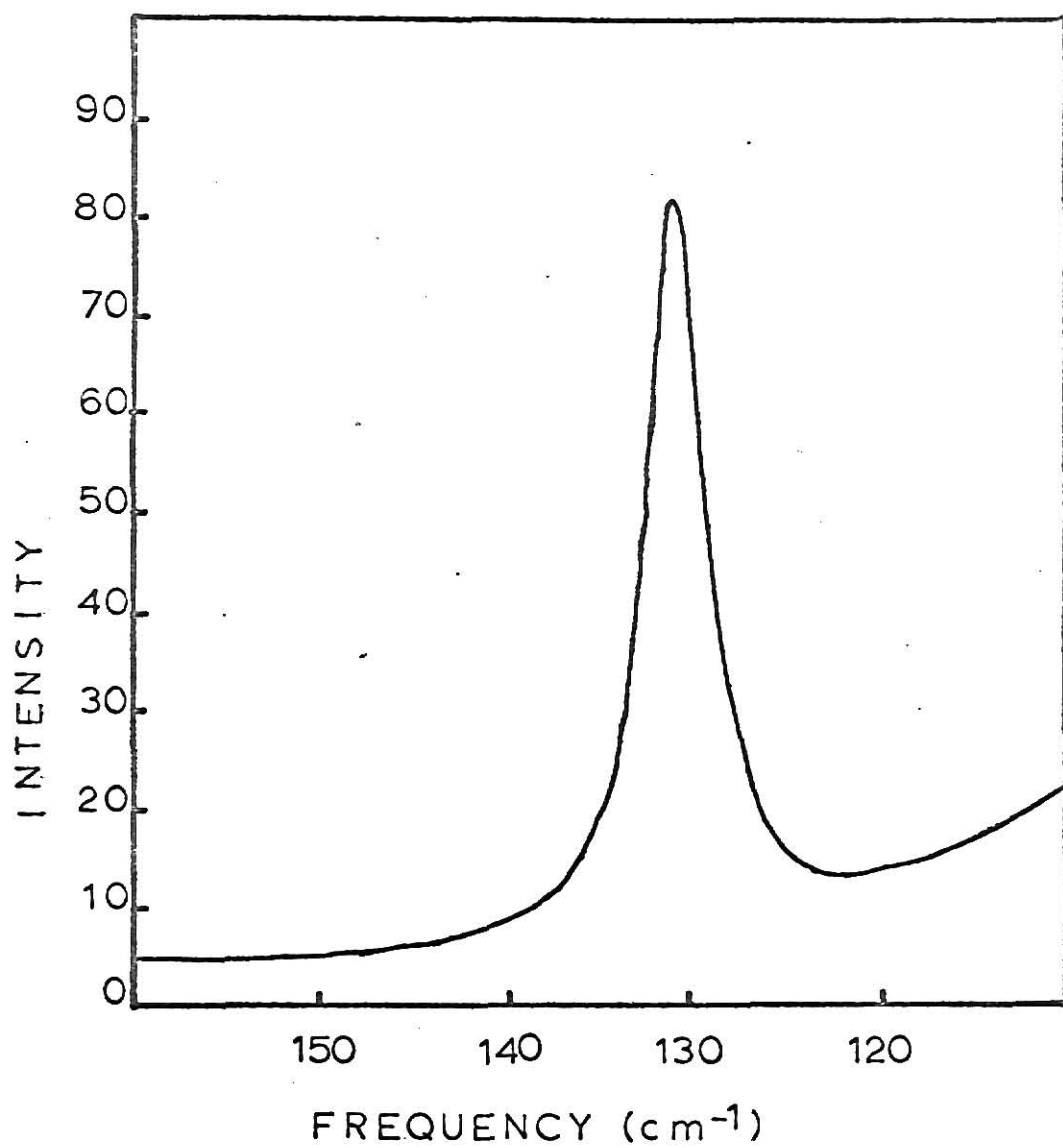


Fig. 10. Raman spectrum of sodium azide.

Table 2

Crystal	Raman shift observed cm^{-1}	Mode responsible	Symmetry	Frequency according to Bryant
NaN_3	130	Rotatory lattice mode	E_g	122 cm^{-1}
	1367	Symmetric stretch of N_3^-	A_1	1358 cm^{-1}
KN_3	115 cm^{-1}	Translational lattice mode	E_g	81 cm^{-1}
	158 cm^{-1}	Rotatory lattice mode	E_g	120 cm^{-1}
	1346	Symmetric stretch of N_3^-	A_1	1343 cm^{-1}

D. Proposed Models for Azide Color Center Structure:

A point group analysis of the color center models proposed by various workers has been carried out. Linear configurations of N_2^- and N_4^- belonging to symmetry $D_{\infty h}$ and square and tetrahedral arrangements of N_4^- suggested as likely by Yoffe [89] were considered. Lastly, the triangular N_3 configuration is described in some detail.

The typical method of analysis is indicated by the D_{3h} point group analysis. It follows the conventional methods used in molecular spectroscopy as described by Herzberg [3]. The results for these various cases are summarized in Table 3.

Point-group analysis of D_{3h} :

Koskr et al., [97] lists the elements of D_{3h} in Table 65, p. 67. Thus

$$D_{3h}: E, 2C_3, 2S_3, \sigma_h, 3C_2, 3\sigma_v$$

The operations are

E (identity)

$2C_3: (132): (123)$

$3C_2: (1) (23)$

$(2) (31)$

$(3) (12)$

$\sigma_h: (1) (2) (3)$

$2S_3: (132): (123)$

$3\sigma_v: (1) (23)$

$(2) (31)$

$(3) (12)$

$$\chi^{\Gamma}(E) = 9$$

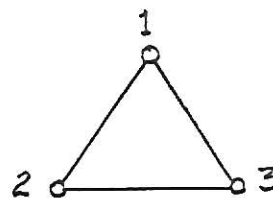
$$\chi^{\Gamma}(C_3) = 0$$

$$\chi^{\Gamma}(C_2) = (1-2) = -1$$

$$\chi^{\Gamma}(\sigma_h) = 3(-1+2) = 3$$

$$\chi^{\Gamma}(S_3) = 0$$

$$\chi^{\Gamma}(\sigma_v) = 1(-1+2) = 1$$



D_{3h}	E	$2C_3$	$3C_2$	σ_h	$2S_3$	$3\sigma_v$
Γ	9	0	-1	3	0	1

Using the character table for D_{3h} and the equation

$$n_i(R) = \frac{1}{g^0} \sum_R \chi^{\Gamma}(r) \chi^i(R)$$

give the symmetry of genuine vibrations as

$$A_1' + E'.$$

Both these vibrations are Raman-active while E' is infra-red active.

To obtain the frequency of these vibrations the secular equation must be set up and solved. The relevant analysis is in progress at the present.

Table 3 shows that if the defect is planar as in the case of a square or a triangle, and could be assumed to lie in the (001) plane, there should be a strong Raman line corresponding to the A_1 type of vibration. This line will then have large values of the diagonal elements of the corresponding Raman tensor and zero (or at least small values) off-diagonal elements. Careful polarization studies of the Raman lines and the effect of polarizing the damaging light on the electronic spectra together with complete ESR data are needed for a final determination of the geometry of the defect and its positioning in the lattice.

Table 3

Ion	Configuration	Point group symmetry	No. of Raman-active vibration	Symmetry of Raman-active vibrations	Corresponding polarizability components
N_2^-	linear	D_h	one (symmetric stretch)	Σ_g^+	
N_4^-	linear	D_h	three (symmetric stretch bending)	Σ_g^+ π_g	
N_4^-	square	D_{4h}	3	A_{1g} B_{1g} B_{2g}	x^2+y^2, z^2 x^2-y^2 xy
N_4^-	tetrahedral	T_d	3	A_1 E T_2	$x^2+y^2+z^2$ x^2-y^2 xy, xz, yz
N_3^-	triangular	D_{3h}	2	A_1 E	x^2+y^2, z^2 xz, yz
N_3^-	linear	D_h	one	Σ_g^+	

E. Summary and Conclusions

The attempt in this thesis has been to provide an introduction to the literature on the Raman Effect in Crystals and to present the results of the preliminary studies on the alkali azide system.

The alkali azides form an ideal crystal system in which to undertake Raman scattering studies of defects. The Raman spectrum of the perfect crystals consists at most of three lines and it should be easy to observe any new vibration frequencies the defects may give rise to.

High quality crystals of NaN_3 , KN_3 and RbN_3 have been grown. The production of color centers by ultra-violet irradiation of NaN_3 and KN_3 and their thermal bleaching properties have been studied. Models for the possible structures of these color centers have been analyzed by point group theoretical methods to determine Raman activities.

A single frequency obtained from infra-red studies on colored KN_3 is available from the work of Bryant. If as is claimed in that work, the defect is triangular N_3 ion of D_{3h} symmetry, the present analysis shows that the vibration observed by Bryant should be an E' vibration. This should then be also Raman-active. From Bryant's data then using a central force model with a single force constant one could make an estimate of the frequency of the A_1' vibration which would be Raman active. This analysis is being done.

The Raman spectrum of the defect in an azide has not been recorded yet. This has been a problem because of the lack of proper experimental equipment. However the experimental situation is being remedied presently and the studies will be undertaken.

These studies will serve as a starting point on the understanding of both the Raman scattering from defects and the structure of the defect in

the azides. Certainly further analysis will be needed once such data is obtained. The present analysis is based on imbedding the defect in an "isotropic" medium. The crystal host, of course, will lower the site symmetry of the defect and deviations from the predicted Raman activities are to be expected. Furthermore, there is a possibility of different orientations of the defects with respect to the crystal axes. Not only will careful Raman polarization data be needed but the manner in which the color center is produced should be refined. The critical wavelength at which the damage begins to occur should be determined. Polarizing the ultraviolet radiation used in irradiating may prove useful in orienting the defects to a certain degree.

ACKNOWLEDGEMENTS

The author wishes to express her deep sense of gratitude to her major professor, Dr. C. E. Hathaway for his guidance, constructive criticism, kindness and the interest he has taken during the course of the work and the preparation of this thesis. She is deeply indebted to Dr. J. D. Spangler for guiding her through many difficult points in the theory and for the use of his equipment, and to Nelson Kilmer for suggesting the measurements on electronic spectra and helping in the experiments. Thanks are also due to Dr. R. B. Dragsdorf for the help in x-ray analysis and to Dr. B. Curnutte, Jr. and Dr. N.O. Folland for helpful discussions. The assistance of George Simonis and Harvey Johnston is much appreciated.

Appendix I

The Hermitean Nature of the Polarizability

The work done per second by the radiation field on the molecule is

$$\begin{aligned}
 \omega &= \frac{1}{2} (\dot{\vec{p}} + \dot{\vec{p}}^*) \cdot \frac{1}{2} (\vec{E} + \vec{E}^*) \quad (I-1) \\
 &= \frac{1}{4} \sum_i \sum_j (a_{ij} E_j + a_{ij}^* E_j^*) (E_i + E_i^*) \quad i, j = 1, 2, 3. \\
 &= \frac{1}{4} \sum_i \sum_j (a_{ij} E_j E_i + a_{ij}^* E_j^* E_i^* + a_{ij} E_j E_i^* + a_{ij}^* E_j^* E_i^*). \quad (I-2)
 \end{aligned}$$

If the field is harmonic, of frequency ω ,

$$\begin{aligned}
 \dot{E}_i &= i\omega E_i, \quad \dot{E}_j^* = -i\omega E_j^*, \quad \text{etc. and} \\
 \omega &= \frac{1}{4} \sum_i \sum_j \left\{ \frac{1}{2} a_{ij} \frac{d}{dt} (E_i E_j) + \frac{1}{2} a_{ij}^* \frac{d}{dt} (E_i^* E_j^*) \right. \\
 &\quad \left. + a_{ij} E_i^* i\omega E_j - a_{ij}^* i\omega E_j^* E_i \right\}. \quad (I-3)
 \end{aligned}$$

Since i, j are dummy indices they can be interchanged in the last term. Hence

$$\omega = \frac{d}{dt} \left\{ \frac{1}{8} \sum_i \sum_j (a_{ij} E_i E_j + a_{ij}^* E_i^* E_j^*) \right\} + \frac{i\omega}{4} \sum_i \sum_j (a_{ij} - a_{ji}^*) E_i^* E_j. \quad (I-4)$$

The second double sum cannot be written as the time derivative of a function of the components of the field. It therefore represents the work done by the frictional or damping forces. If one assumes that there is no damping, then $a_{ij} = a_{ji}^*$, i.e., the polarizability tensor must be Hermitean for this case.

Appendix II

Expression for the Average of the Square of the Fluctuation in the Dipole Moment.

The fluctuations in $\sum_k \vec{p}^k$ are caused in part by fluctuations $\Delta n = n - \bar{n}$ in the number of molecules within V and partly by fluctuation $\Delta \vec{p}^k = \vec{p}^k - \bar{\vec{p}}^k$ in the dipole moments of the individual molecules. If second order terms are neglected,

$$\begin{aligned} \Delta \sum_k \vec{p}^k &= \bar{\vec{p}}^k \Delta n + \sum_{k=1}^{\bar{n}} \Delta \vec{p}_k, \text{ therefore} \\ \overline{|\Delta \sum_k \vec{p}^k \cdot \mathbf{e}|^2} &= \overline{(\bar{\vec{p}}^k \cdot \mathbf{e} \Delta n + \sum_{k=1}^{\bar{n}} \Delta \vec{p}_k \cdot \mathbf{e})(\bar{\vec{p}}^k \cdot \mathbf{e} \Delta n + \sum_{k=1}^{\bar{n}} \Delta \vec{p}_k \cdot \mathbf{e})^*} \\ &= |\bar{\vec{p}}^k \cdot \mathbf{e}|^2 \overline{(\Delta n)^2} + \overline{|\sum_{k=1}^{\bar{n}} \Delta \vec{p}_k \cdot \mathbf{e}|^2}, \quad (\text{II-1}) \end{aligned}$$

since the factors containing $\overline{\Delta n} = 0$ vanish.

From statistical mechanics it can be shown for ideal gases that $\overline{(\Delta n)^2} = n = NV$ where N is the average number of molecules per unit volume.

For ideal gases, the fluctuations of the electric moments of the individual molecules will be independent of one another.

The second term reduces to $\bar{n} |\Delta \vec{p} \cdot \mathbf{e}|^2$, where $\Delta \vec{p}$ is the fluctuation of the induced moment of an arbitrary molecule, since all the quadratic terms on the average will be equal. Thus

$$\overline{|\Delta \sum_k \vec{p}^k \cdot \mathbf{e}|^2} = \bar{n} [|\bar{\vec{p}} \cdot \mathbf{e}|^2 + |\Delta \vec{p} \cdot \mathbf{e}|^2]. \quad (\text{II-2})$$

The first term arises from the fluctuation in n and the second term due to fluctuation in p_k .

Using the relation

$$\begin{aligned}
 \overline{|\Delta \vec{p} \cdot \vec{e}|^2} &= \overline{|(\vec{p} - \bar{\vec{p}}) \cdot \vec{e}|^2} \\
 &= \overline{(\vec{p} - \bar{\vec{p}}) \cdot \vec{e} (\vec{p}^* - \bar{\vec{p}}^*) \cdot \vec{e}} \\
 &= \overline{|\vec{p} \cdot \vec{e}|^2} - \overline{|\bar{\vec{p}} \cdot \vec{e}|^2} - \overline{|\bar{\vec{p}} \cdot \vec{e}|^2} + \overline{|\bar{\vec{p}} \cdot \vec{e}|^2} \\
 &= \overline{|\vec{p} \cdot \vec{e}|^2} - \overline{|\bar{\vec{p}} \cdot \vec{e}|^2} ,
 \end{aligned}$$

it follows that

$$\overline{|\Delta \sum_k \vec{p}_k \cdot \vec{e}|^2} = \bar{n} \overline{|\vec{p} \cdot \vec{e}|^2} .$$

Appendix III

Average of the Polarizability Over All Possible Directions

The scalar product of the induced moment \vec{p} with an arbitrary unit vector e is given by

$$\vec{p} \cdot e = \sum_x \sum_y a_{xy} E_y e_x \quad (\text{III-1})$$

$$= \sum_X \sum_Y a_{XY} E_Y e_X, \quad (\text{III-2})$$

where the second expression is referred to a coordinate system fixed with respect to the molecule. The tensor a_{xy} must be averaged over all possible orientations since the orientation of the molecule is arbitrary. An equivalent procedure for performing such an average involves using the second expression and averaging over all possible directions of \vec{E} and \hat{e} . This procedure is more convenient.

Let \hat{e}_1 denote a unit vector in the direction of the electric field of the incident light, and \hat{e}_2 another unit vector, coplanar with \vec{E} and \hat{e} and perpendicular to \hat{e}_1 . Then,

$$\vec{E} = \hat{e}_1 E, \quad \hat{e} = \hat{e}_1 \cos \psi + \hat{e}_2 \sin \psi, \quad \text{and}$$

$$|\vec{p} \cdot e|^2 = E^2 \sum_x \sum_y \sum_{x'} \sum_{y'} (\cos \psi x_1 + \sin \psi x_2)(\cos \psi x'_1 + \sin \psi x'_2) y_1 y'_1 a_{xy} a_{x'y'}^*, \quad (\text{III-3})$$

where $x_1 y_1 z_1$ and $x_2 y_2 z_2$ are components of \hat{e}_1 and \hat{e}_2 , respectively. That is, they are the directional cosines of \hat{e}_1 and \hat{e}_2 in the coordinate system rotating with the molecule.

To evaluate the right hand side, average values of a number of products of directional cosines of two orthogonal vectors are needed. They may be

divided in groups and the required results are as follows:

$$\begin{aligned}
 (a) \quad \overline{X_1^4} &= \overline{Y_1^4} \dots\dots\dots = \overline{Z_2^4} = \frac{1}{5} \\
 (b) \quad \overline{X_1^2 Y_1^2} &= \overline{X_1^2 Z_2^2} \dots\dots = \overline{Y_2^2 Z_2^2} = \frac{1}{15} \\
 (c) \quad \overline{X_1^2 Y_2^2} &= \overline{X_1^2 Z_2^2} \dots\dots = \overline{Z_1^2 Y_2^2} = \frac{2}{15} \\
 (d) \quad \overline{X_1 Y_1 X_2 Y_2} &= \dots\dots = \overline{Y_1 Z_1 Y_2 Z_2} = -\frac{1}{30} \\
 (e) \quad \overline{X_1 Y_2^2 X_2} &= \overline{X_1 Y_1 Z_1 X_2} = \dots\dots = 0
 \end{aligned} \tag{III-4}$$

Expanding the sum (III-3), substituting the averages from Eqs. (III-4), and assuming that a_{xy} is Hermitean, yields, after considerable reduction,

$$|\vec{p} \cdot \vec{e}|^2 = R_0 E^2 \cos \psi + RE^2 \left(1 + \frac{1}{3} \cos^2 \psi\right), \tag{III-5}$$

where

$$\begin{aligned}
 R_0 &= \frac{1}{9} (a_{xx} + a_{yy} + a_{zz})^2 \\
 R &= \frac{1}{30} \left\{ (a_{yy} - a_{zz})^2 + (a_{xx} - a_{yy})^2 \right. \\
 &\quad \left. + 6 (|a_{yz}|^2 + |a_{zx}|^2 + |a_{xy}|^2) \right\}
 \end{aligned} \tag{III-6}$$

Appendix IV

Proof:

$$\frac{\partial}{\partial E_\alpha} \epsilon_l(\vec{E}) = - \int \psi_l^*(\vec{E}) M_\alpha \psi_l(\vec{E}) d\tau \quad \dots \quad (I.29)$$

The result above is an extension of the following theorem: Given a Hamiltonian $H(\xi)$ which depends on a parameter ξ , then

$$\frac{\partial}{\partial \xi} \epsilon_l(\xi) = \int \psi_l^*(\xi) \frac{\partial H(\xi)}{\partial \xi} \psi_l(\xi) d\tau, \quad (IV-1)$$

where ϵ_l is an eigenvalue of the system considered and ψ_l the corresponding wave function, both being functions of ξ . The integration is over all coordinates of the system, which are independent of ξ .

$$\epsilon_l(\xi) = \int \psi_l^*(\xi) H(\xi) \psi_l(\xi) d\tau. \quad (IV-2)$$

Therefore,

$$\begin{aligned} \frac{\partial}{\partial \xi} \epsilon_l(\xi) = \lim_{\delta \xi \rightarrow 0} \frac{1}{\delta \xi} \left\{ \int \left(\psi_l(\xi) + \frac{\partial \psi_l(\xi)}{\partial \xi} \delta \xi + \dots \right)^* \left(H(\xi) + \frac{\partial H(\xi)}{\partial \xi} \delta \xi + \dots \right) \times \right. \\ \left. \times \left(\psi_l(\xi) + \frac{\partial \psi_l(\xi)}{\partial \xi} \delta \xi + \dots \right) d\tau - \int \psi_l^*(\xi) H(\xi) \psi_l(\xi) d\tau \right\}. \end{aligned} \quad (IV-3)$$

Neglecting terms of second and higher orders in the first integral,

$$\begin{aligned} \frac{\partial}{\partial \xi} \epsilon_l(\xi) = \lim_{\delta \xi \rightarrow 0} \frac{1}{\delta \xi} \left\{ \delta \xi \int \psi_l^*(\xi) \frac{\partial H(\xi)}{\partial \xi} \psi_l(\xi) d\tau \right. \\ \left. + \left[\left(\psi_l(\xi) + \frac{\partial \psi_l(\xi)}{\partial \xi} \delta \xi \right)^* H(\xi) \left(\psi_l(\xi) + \frac{\partial \psi_l(\xi)}{\partial \xi} \delta \xi \right) d\tau \right. \right. \\ \left. \left. - \int \psi_l^*(\xi) H(\xi) \psi_l(\xi) d\tau \right] \right\} \quad \dots \quad (IV-4) \end{aligned}$$

The expression given in the square bracket is the change in the expectation value of the Hamiltonian H due to a small variation $\delta\xi(\frac{\partial\psi_l}{\partial\xi})$ in the wave function. According to the variational principle (9), this variation must vanish to the first order.

Hence,

$$\frac{\partial}{\partial\xi} \epsilon_l(\xi) = \int \psi_l^*(\xi) \frac{\partial H(\xi)}{\partial\xi} \psi_l(\xi) d\tau \dots \quad (\text{IV-1})$$

which completes the proof of the theorem.

In a static electric field \vec{E} , the Hamiltonian, eigenfunctions and eigenvalues of a molecular system contain \vec{E} as a parameter. According to Eq. (25),

$$H(\vec{E}) = H(0) - \vec{M} \cdot \vec{E} = H(0) - \sum_{\alpha} M_{\alpha} E_{\alpha},$$

so that $\frac{\partial H(E_{\alpha})}{\partial E_{\alpha}} = -M_{\alpha}$.

The application of (IV-1) then gives

$$\frac{\partial}{\partial E_{\alpha}} \epsilon_l(\vec{E}) = - \int \psi_l^*(\xi) M_{\alpha} \psi_l(\xi) d\tau ,$$

which is Eq. (27) of the text.

Appendix V

Total Rate of Radiation

From the expression (I.4b) for \overline{S}_1 the total rate of radiation is

$$R^2 \overline{S} \, d\Omega = \frac{\omega^4}{2\pi c^3} \int \left\{ \sum_i \sum_{\alpha\beta} e_{\alpha}^i e_{\beta}^i m_{\alpha}^+ m_{\beta}^- \right\} d\Omega .$$

Using polar coordinates the unit vectors e^1 and e^2 can be chosen as follows:

$$\begin{aligned} e_1^1 &= \cos \theta \cos \phi & e_2^1 &= \cos \theta \sin \phi & e_3^1 &= -\sin \theta \\ e_1^2 &= -\sin \phi & e_2^2 &= \cos \phi & e_3^2 &= 0. \end{aligned}$$

Substituting these in Eq.(I.4b) recalling $d\Omega = \sin \theta \, d\theta \, d\phi$ and integrating, one arrives at the result

$$R^2 \overline{S} \, d\Omega = \frac{4\omega^4}{3c^3} \sum_{\alpha} m_{\alpha}^+ m_{\alpha}^- .$$

Appendix VI

Adiabatic Approximation

The general form of the Hamiltonian for a system of nuclei and electrons can be written as

$$H = T_N + T_E + V_{NN} + V_{EE} + V_{NE} + V, \quad (\text{VI-1})$$

where

$$T_N + \sum_A \frac{-\hbar^2}{2M_A} \nabla_A^2 \quad \text{is the kinetic energy of the nuclei,}$$

$$T_E + \sum_i \frac{-\hbar^2}{2m_i} \nabla_i^2 \quad \text{is the kinetic energy of the electrons,}$$

$$V_{NN} + \frac{1}{2} \sum_B' \sum_A \frac{Z_B Z_A e^2}{R_{AB}} \quad \text{is the coulomb energy of the nuclei; a function of nuclear coordinates only,}$$

$$V_{EE} = \frac{1}{2} \sum_i' \sum_j \frac{e^2}{r_{ij}} \quad \text{is the coulomb energy of the electrons; a function of electronic coordinates only,}$$

$$V_{NE} = - \sum_i \sum_A \frac{Z_A e^2}{r_{iA}} \quad \text{is the mutual coulomb energy of electrons and nuclei; a function of both nuclear and electronic coordinates, and}$$

$$V = V(r, R, \dot{r}, \dot{R}) \quad \text{is, in general, an external potential.}$$

Consider the problem of a free molecular system so that $V = 0$. The corresponding time-independent Schrodinger equation is

$$H\psi(\vec{R}_i, \vec{r}_i) = E\psi(\vec{R}_i, \vec{r}_i) \quad (2)$$

In general, then, ψ is a nonseparable function of both electronic and nuclear coordinates. However, the problem is insoluble at this stage, unless one resorts to approximation methods.

The most widely used approximation in molecular and solid-state problems is the Born-Oppenheimer or adiabatic approximation which is based on physical considerations. Since the atomic nuclei are much heavier than the electrons, they move much more slowly, and it is therefore reasonable to start with the approximation in which they are taken to be at rest, though not necessarily in their equilibrium positions. Then if $\{\vec{R}\} \equiv \vec{R}_1, \dots, \vec{R}_N$ denote the nuclei positions, one can attempt to solve the Schrodinger equation for the motion of n electrons, with coordinate vectors $\{\vec{r}\} \equiv \vec{r}_1, \dots, \vec{r}_n$, in the field of the nuclei in the configuration \vec{R} . The resulting wave function will be a function of the $3n$ variables $\{\vec{r}\}$ and contain \vec{R} as a parameter. The energy eigenvalue ϵ_{en} will also contain \vec{R} as a parameter. The lowest electronic eigen function $\phi_0(\vec{r}, \vec{R})$ and eigenvalue $\epsilon_{e0}(\vec{r}, \vec{R})$ are then defined. If the real problem now is considered in which the nuclei are not fixed, the assumption might be made that at any time the state of the electrons is described by the same wave function, inserting for \vec{R} , the positions of the nuclei at that time. Then the state of motion of the nuclei is represented merely by a function $\chi(\vec{R})$ and therefore the wave function of the whole system appears in the form

$$\psi(\vec{r}, \vec{R}) = \chi(\vec{R}) \phi_0(\vec{r}, \vec{R}). \quad (3)$$

This is known as the adiabatic approximation, since the function $\phi_0(\vec{r}, \vec{R})$ represents the variation of the electronic state upon adiabatic changes of the parameters.

Substitution of Eq. (3) into the Schrodinger Eq. (2), the electronic and nuclear Schrödinger equations can be separately written as

$$(T_E + V_{EE} + V_{NE}) \phi_n(\vec{r}, \vec{R}) = \epsilon_{en}(\vec{R}) \phi_n(\vec{r}, \vec{R})$$

$$(T_N + V_{VV}) \chi_n(\vec{R}) = \epsilon_{nv} \chi_{nv}(\vec{R})$$

provided a cross term

$$\frac{-\hbar^2}{2M_A} (\chi \nabla_A^2 \phi + 2 \vec{\nabla}_A \phi \cdot \vec{\nabla}_A \chi)$$

can be neglected. Thus the next step in the Born-Oppenheimer approximation is writing $\nabla_A \phi \cong 0$. This is physically equivalent to saying that the frequency of electronic transition is much larger than the frequency with which a change in the electronic potential is brought about by the nuclear motion and may be written as

$$\frac{U}{\lambda} < \frac{\Delta E}{\hbar} \quad \text{or} \quad \frac{U\hbar}{\lambda} < \Delta E,$$

where U is the velocity of the nuclei, λ is the distance by which the nuclei must move to produce an appreciable change in $\phi_0(\vec{r}, \vec{R})$ and E is the difference of the first excited electronic level, at fixed \vec{R} , from the ground state.

In a molecular solid which is usually built from chemically saturated units this is generally true. The energy of excitation ΔE is several electron volts, while $\frac{U\hbar}{\lambda}$ is much less. Another typical case is that of an ionic solid like NaCl in which each of the ions again has a closed-shell configuration. In a homopolar lattice, e.g. diamond, one can regard the

electronic state as saturated, but because of their high delocalization cannot look upon the lattice as made up of small saturated sub-units.

One example in which the adiabatic approximation cannot be justified is in the case of a metal. There are many almost degenerate levels in a partially occupied conduction band and ΔE is thus almost zero and the inequality cannot hold. Even in a non-metallic crystal, the adiabatic approximation will be valid only for the electronic state of lowest energy. This is because, if one visualizes an excited state simply as the excitation of one atom, there will be N such states of very similar energy, since any one of the N atoms may be excited and the inequality is again bound to fail.

REFERENCES

1. C. V. Raman and K. S. Krishnan, *Nature* 121, 501 (1928); *Proc. Roy. Soc. (London)* 122 A, 23 (1928); *Ind. J. Phys.* 2, 387 (1928).
2. G. Landsberg and L. Mandelstam, *Naturwiss.* 16, 557, 772 (1928).
3. G. Herzberg, *Infrared and Raman Spectra*, Van Nostrand, New York (1945).
4. J. I. Bryant, *Spectrochimica Acta* 22, 1475 (1966).
5. L. D. Landau and E. M. Lifshitz, *Classical Theory of Fields*, Addison-Wesley, Reading (1951).
6. J. B. Marion, *Classical Electromagnetic Radiation*, Academic Press (1965), p. 224.
7. M. Born and K. Huang, *Dynamical Theory of Crystal Lattices*, Oxford University Press, Oxford (1956).
8. M. Born and E. Wolf, *Principles of Optics*, Pergamon Press, Macmillan Co., New York (1964).
9. San-ichiro Mizushima, *Handbuch der Physik*, Vol. XXVI, Part 11, pg. 171, Springer-Verlag, Berlin (1955).
10. H. Goldstein, *Classical Mechanics*, Addison-Wesley, Reading (1965).
11. W. Heitler, *Quantum Theory of Radiation*, Oxford University Press, Oxford (1954).
12. L. I. Schiff, *Quantum Mechanics*, 3rd edition, McGraw-Hill, New York (1968).
13. C. Kittel, *Introduction to Solid State Physics*, 3rd edition, John Wiley, New York (1967).
14. G. Placzek, *Handbuch der Radiologie*, Akademische Verlage gesellschaft, Vol. 6, Part 2, pg. 205 (1934).

15. K. Huang, Proc. Roy. Soc. A208, 352 (1951).
16. a. P. P. Shorygin, Dokl. Akad. Nauk. SSSR 78, 469 (1951).
b. J. Behringer and J. Brandmüller, Z. Elektrochem. 60, 643 (1956).
17. R. D. Mattuck, A Guide To Feynman Diagrams in the Many-Body Problem, McGraw-Hill, New York (1967).
18. D. R. Bates, Quantum Theory, Vol. 10-I, II, III, Academic Press, New York (1961-62).
19. J. M. Ziman, Principles of the Theory of Solids, Cambridge University Press, Cambridge (1964).
20. M. Born and M. Bradburn, Proc. Roy. Soc. A 188, 161 (1947).
21. C. V. Raman Proc. Ind. Acad. Sci. A 18, 237 (1948).
22. A. A. Maradudin, E. M. Montroll and G. H. Weiss, Theory of Lattice Dynamics in the Harmonic Approximation, Academic Press, New York (1963).
23. G. Koster, Space Groups and Their Representations, Academic Press (1967).
24. G. H. Begbie and M. Born, Proc. Roy. Soc. A 188, 179 (1947).
25. F. Seitz, Modern Theory of Solids, McGraw-Hill, New York (1940).
26. D. Pines, Lectures on the Many-Body Problem, W. A. Benjamin, New York (1961).
27. L. Brillouin, Wave Propagation in Periodic Structures, Dover Publishing Co., New York (1953).
28. L. van Hove, Phys. Rev. 59, 1189 (1953).
29. J. C. Phillips, Phys. Rev. 194, 1263 (1956).
30. C. Kittel, Quantum Theory of Solids, John Wiley, New York (1962).
31. M. Morse, Trans. Am. Math. Soc. 27, 345 (1925).

32. R. S. Krishnan and N. Krishnamurthy, J. de Phys. 26, 630 (1965).
33. R. H. Lyddane, R. E. Sachs and E. Teller, Phys. Rev. 59, 673 (1941).
34. R. Loudon, Proc. Phys. Soc. A 82, 393 (1963).
35. R. Loudon, Adv. Phys. 13, 423 (1964).
36. J. L. Birman, Phys. Rev. 162, 806 (1967).
37. G. D. Whitfield, Phys. Rev. 121, 720 (1961).
38. R. Peierls, Quantum Theory of Solids, Oxford University Press, Oxford (1955).
39. E. J. Woodbury, Phys. Rev. Let. 9, 455 (1962).
40. N. Bloembergen, Non-linear Optics, Benjamin, New York (1965).
41. R. Loudon, J. de Phys. 26, 677 (1965).
42. a. J. T. Hongen and S. Singh, Proc. Roy. Soc. 277A, 193 (1964).
b. J. A. Koningstein, J. Chem. Phys. 46, 2811 (1967).
43. J. M. Worlock and S. P. S. Porto, Phys. Rev. Let. 15, 697 (1965).
44. J. P. Russell, J. de Phys. 26, 620 (1965).
45. L. Brillouin, Ann. de Phys. Paris 17, 88 (1922).
46. E. B. Wilson, J. C. Decins and P. C. Cross, Molecular Vibrations, McGraw-Hill, New York (1955).
47. V. Heine, Group Theory in Quantum Mechanics, Pergamon Press, New York (1960).
48. J. P. Mathiew, Spectres de Vibration et Symétrie des Molécules et des Cristaux, Hermann, Paris (1951).
49. S. Bhagavantam and T. Venkatarayudu, Group Theory and Its Application to Physical Problems, Andhra University Press, Andhra (1952).
50. J. F. Nye, Physical Properties of Crystals, Oxford University Press, Oxford (1957).

51. A. A. Maradudin, "Phonons and Phonon Interactions", W. A. Benjamin, New York (1964), p. 424.
52. A. A. Maradudin, Rep. Prog. Phys. 28, p. 331 (1965).
53. A. A. Maradudin, Solid State Physics, Vols. 18 and 19, Academic Press (1967).
54. I. M. Lifshitz, J. Phys. USSR 1, 8 (1944); Nuovo Cimento Suppl [10] 3, 716 (1956).
55. E. W. Montroll and R. B. Potts, Phys. Rev. 102, 72 (1956).
56. R. F. Wallis, Phys. Rev. 116, 302 (1959).
57. W. M. Visscher, Ann. Phys. 9, 194 (1960).
58. G. Schaefer, Phys. Chem. Solids 12, 233 (1960).
59. B. Mozer, K. Otnes and V. W. Myers, Phys. Rev. Let. 8, 278 (1962).
60. M. Balkanski and M. Nusimovici, Phys. Stat. Sol. 5, 635 (1964).
61. J. A. Krumhansl, Jour. App. Phys. Suppl. 33, 307 (1962).
62. G. E. Stedman, Contemp. Phys. 9, 46 (1968).
63. P. Dennerly and A. Krzywicki, Mathematics for Physicists, Harper and Row, New York (1967).
64. A. A. Maradudin, "Astrophysics and the Many Body Problem", W. A. Benjamin, New York (1963), pg. 110.
65. J. D. Jackson, Electrodynamics, John Wiley, New York (1966).
66. C. T. Walker and R. O. Pohl, Phys. Rev. 131, 1433 (1963).
67. Wagner, Phys. Rev. 131, 1443 (1963).
68. Nguyen Xan Xinh, R. A. Coldwell-Horsfall and A. A. Maradudin, J. de Phys. 26, 717 (1965).
69. A. I. Stekhanov and M. Eliashberg, Fiz. Tverd. Tela 5, 2985 (1963) [English Transl. Societ Phys. - Solid State 5, 2185 (1964)]; 6, 3397 (1964) [English Transl. Societ Phys. - Solid State 6, 2718 (1965)].

70. R. W. Dreyfus and P. W. Levy, Proc. Roy. Soc. (London) A246, 233 (1958).
71. E. A. Secco, Cand. J. Chem. 40, 2191 (1962).
72. H. G. Heal and J. P. S. **Pringle**, J. Phys. Chem. Solids 15, 261 (1960).
73. P. W. M. Jacobs and F. C. Tompkins, Proc. Roy. Soc. (London) A 215, 254, 265 (1962).
74. H. A. Papazian, a. J. Chem. Phys. 32, 456 (1960).
b. J. Chem. Phys. 34, 1614 (1961).
c. J. Phys. Chem. Solids, 21, 81 (1961).
75. J. I. Bryant, a. J. Chem. Phys. 38, 2845 (1963).
b. J. Chem. Phys. 42, 2270 (1965).
c. J. Chem. Phys. 45, 689 (1966).
76. R. B. Hurst, J. H. Anderson and D. E. Milligan, J. Phys. Chem. Solids 23, 157 (1967).
77. E. Gelerinter, Ph.D. Thesis, Cornell University, Material Science Report No. 414 (1966).
78. P. Gray and A. D. Yoffe, Chem. Rev. 55, 1069 (1955).
79. A. D. Yoffe, Developments in Inorganic Nitrogen Chemistry, Ed. by C. B. Colburn, Elsevier Publishing Co., New York (1966), p. 72.
80. W. B. Fowler, Physics of Color Centers, Academic Press, New York (1968).
81. H. Rosenwasser, R. W. Dreyfus and P. W. Levy, J. Chem. Phys. 24, 184 (1956).
82. G. J. King, B. S. Miller, F. F. Carlson and R. C. Macmillan, J. Chem. Phys. 35, 1442 (1961); 34, 1499 (1961).
83. J. J. Markham, F. Centers in Alkali Halides, Suppl. 6, Solid State Physics, Academic Press, New York (1966).

84. D. A. Kleinman, Phys. Rev. 134A, 423 (1964).
85. S. S. Mitra, Raman Newsletter (1969).
86. C. H. Henry, Phys. Rev. 152, 699 (1966).
87. P. L. Marinkas, Nature 211, 1288 (1966).
88. H. K. Henisch, private communication.
89. H. K. Henisch, J. Phys. Chem. Solids 26, 493 (1964).
90. S. B. Hendricks and L. Panling, J. Am. Chem. Soc. 47, 2904 (1925).
91. L. K. Frevel, J. Am. Chem. Soc. 58, 779 (1936).
92. R. G. Wyckoff, Crystal Structures, Vol. II, Interscience, New York (1964).
93. J. Cunningham and F. C. Tompkins, Proc. Roy. Soc. (London) A 251, 27 (1959).
94. D. T. Keating and S. J. Krasner, J. Phys. Chem. Solids 20, 150 (1961).
95. A. J. Shuskus, C. G. Young, O. R. Gillam, and P. W. Levy, J. Chem. Phys. 33, 622 (1960).
96. H. L. Johnston Jr., M. S. Thesis, Kansas State University (1969).
97. G. Koster, Properties of the Thirty-two Point Groups, MIT Press, Cambridge (1963).

SCATTERING OF ELECTROMAGNETIC RADIATION
BY DEFECTS IN CRYSTALS

by

INDIRA RADHAKRISHNAN NAIR

M.Sc., Bombay University, 1962

AN ABSTRACT OF A MASTER'S THESIS

submitted in partial fulfillment of the
requirements for the degree

MASTER OF SCIENCE

Department of Physics

KANSAS STATE UNIVERSITY

Manhattan, Kansas

1970

A review of the theory of the Raman effect in crystals including an extensive synthesis of the current literature is presented. A brief review of the dynamics of a perfect lattice and a lattice with defects with particular attention given to the analysis of the Raman spectra is included. A study of the electronic and Raman spectra of pure and ultraviolet irradiated potassium azide and sodium azide is reported. The measurement of the electronic spectra of the damaged crystals are described and discussed. The Raman spectra of the pure alkali azide crystals are described and discussed. The unit analysis of the undamaged azides is followed by proposed models for the defects formed by u.v. irradiation.